UNCLASSIFIED

AD NUMBER
AD342328
CLASSIFICATION CHANGES
TO: **UNCLASSIFIED**
FROM: ~~**CONFIDENTIAL**~~
AUTHORITY
31 Jul 1975 DoDD 5200.10

THIS PAGE IS UNCLASSIFIED

UNCLASSIFIED

AD NUMBER
AD342328
CLASSIFICATION CHANGES
TO: **CONFIDENTIAL**
FROM: **SECRET**
LIMITATION CHANGES
TO: **Distribution authorized to U.S. Gov't. agencies and their contractors; Specific Authority; APR 1964. Other requests shall be referred to Air Force Weapons Lab., Kirtland AFB, NM.**
FROM: **Distribution: Further dissemination only as directed by Air Force Weapons Lab., Kirtland AFB, NM, JUL 1963, or higher DoD authority.**
AUTHORITY
31 Jul 1966, DoDD 5200.10 ; AFWL ltr 7 Apr 1964

THIS PAGE IS UNCLASSIFIED

GENERAL DECLASSIFICATION SCHEDULE

IN ACCORDANCE WITH

DOD 5200.1-R & EXECUTIVE ORDER 11652

UNCLASSIFIED

[redacted]

AD 342328

DEFENSE DOCUMENTATION CENTER
FOR
SCIENTIFIC AND TECHNICAL INFORMATION
CAMERON STATION, ALEXANDRIA, VIRGINIA

CLASSIFICATION CHANGED
TO SECRET
FROM SECRET "L"
PER AUTHORITY

64-16 15 AUG. 64

DOWNGRADED AT 3 YEAR INTERVALS:
DECLASSIFIED AFTER 12 YEARS
DOD DIR 5200.10

[redacted]

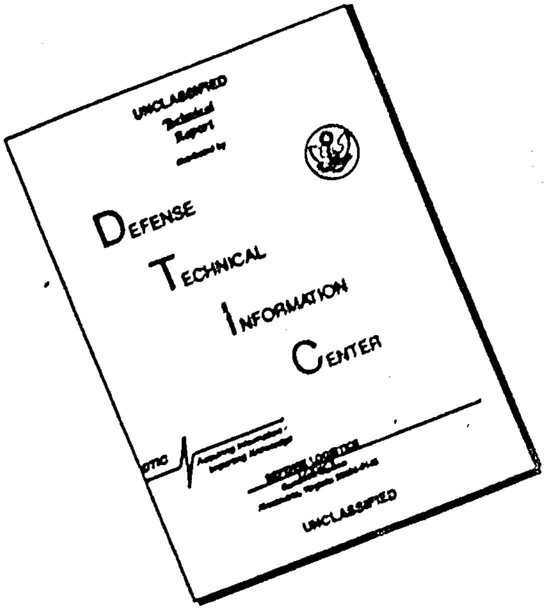

~~SECRET~~

(1) RTD TDR 63-3006 V[illegible] 4

(19)

(20)

RTD
TDR
63-3006
Vol IV

(5) 350 350

(Unclassified Title)

(9) TECHNICAL SUMMARY REP[illegible]T,
(6) NUCLEAR PULSE PROPULSION PROJECT.

Vol IV, Experimental Structural Response (U).

(11) Jul~~y 19~~63,

AD No. 342328

COPY

TECHNICAL DOCUMENTARY REPORT NO. RTD TDR-63-3006, Vol IV

Research and Technology Division
AIR FORCE WEAPONS LABORATORY
Air Force Systems Command
Kirtland Air Force Base
New Mexico

(16) Proj~~ect No~~. 3775, (17) Task ~~No~~. 377501

GROUP-4
Downgraded at 3 year intervals;
Declassified after 12 years.

DDC
SEP 30 1963
TISIA

(18)
~~(Prepared under~~ Contract AF 29(601)-2207,
(10) by J. C. Nance, ~~et al.~~, General Atomic
Division, General Dynamics Corporation,
San Diego, California)

Copy No. 76

342328

~~SECRET~~

Research and Technology Division
Air Force Systems Command
AIR FORCE WEAPONS LABORATORY
Kirtland Air Force Base
New Mexico

This report is classified SECRET because it reveals the results of research on an advanced nuclear space propulsion concept.

WARNINGS

This material contains information affecting the national defense of the United States within the meaning of the Espionage Laws, Title 18, USC, sections 793 and 794, the transmission or revelation of which in any manner to an unauthorized person is prohibited by law.

SPECIAL HANDLING REQUIRED---NOT RELEASABLE TO FOREIGN NATIONALS.

This report is made available for study upon the understanding that the Government's proprietary interests in and relating thereto shall not be impaired. In case of apparent conflict between the Government's proprietary interests and those of others, notify the Staff Judge Advocate, Air Force Systems Command, Andrews AF Base, Washington 25, DC.

This report is published for the exchange and stimulation of ideas; it does not necessarily express the intent or policy of any higher headquarters.

Copies of this report have not been placed in the DDC collection. Address all requests for copies to AFWL (WLL), Kirtland AFB, N Mex.

FOREWORD

The technical summary report on the Nuclear Pulse Propulsion Project (Project ORION) is being published in four volumes. Each volume will cover a specific portion of the research; the volume titles are: Volume I. Reference Vehicle Design Study; Volume II. Interaction Effects; Volume III. Pulse System; and Volume IV. Experimental Structural Response. This report has been prepared by the General Atomic Division, General Dynamics Corporation, under Contract AF 29(601)-2207. Mr. J.M. Wild is Project Manager and Dr. T.B. Taylor is Technical Associate Director. (U)

The effort on experimental structural response summarized in this volume was under the direction of Mr. J.C. Nance, Assistant Director of the Project, Mr. E.A. Day, and Mr. C.V. David. Other General Atomic staff members contributing to the research were: L.O. Lavigne, W.H. Mandleco, R.D. Morton, C.H. Richards, S.J. Sand, R.A. Skeehan, and E.L. Wasser. The General Atomic report number is GA-4205. (U)

Tentative publication dates for the remaining volumes in this series are: Volume I, July 1963; Volume II, August 1963; and Volume III, September 1963. (U)

(This abstract is classified Confidential)

ABSTRACT

Exploration of the response of the ORION pusher and attached structures requires the development of a simulation technique for producing a controllable pressure pulse on plates of various sizes. An arrangement using sheet high explosive and foam attenuators has been investigated and seems to fulfill the requirement for this simulation technique over a wide range of the important variables. The experimental results have been used to determine the peak pressures, radial distribution of the pressures on the plate, pulse duration, pulse shape, and total impulse produced as functions of the amount of HE used, the depth and density of the foam attenuator, and partial confinement of the HE. Promising though not definitive results have been obtained from initial experiments on the structural response of scaled pusher plates. Edge-buckling modes of such plates have been tested statically. A technique for recovering small samples after exposure to the severe environment of a nuclear explosion was investigated. (C)

PUBLICATION REVIEW

This report has been reviewed and is approved.

An unclassified abstract can be found on the catalog cards in the back of this report.

Ronald F Prater
RONALD F. PRATER
Lt USAF
Project Officer

JOHN O. BERGA
Capt USAF
Project Officer

DAVID R. JONES
Col USAF
Chief, Physics Branch

Perry L Huie
PERRY L. HUIE
Col USAF
Chief, Research Division

CONTENTS

Figures

1. (U) INTRODUCTION

1.1. (U) DESCRIPTION OF TEST PROGRAM

(C) The work discussed in this report has been directed toward two primary objectives. The first objective is to develop methods for producing a family of impulses using chemical high explosives, comparable to the impulses predicted for the ORION pulse system. This includes producing impulses equal to that prescribed for ORION, producing scaled impulses, developing techniques for applying impulses over large areas, and varying the radial distribution of the impulse in a prescribed manner. The second objective of the program involves subjecting various scaled ORION components and subsystems to these impulses and studying their behavioral patterns to verify and supplement the predicted analytical results.

(U) The technique developed for providing the required impulses incorporates commercial sheet high explosive[*] (HE) and a low-density plastic material (foam) as an attenuator. By varying the geometry of the experimental setup, as described in Section 2 of this report, a large spectrum of impulse shapes can be obtained. This work is, in part, a continuation of earlier experimental efforts.(1).

(U) The preliminary component testing that has been performed is presented in Sections 3, 4, and 5. Dynamic testing using HE is discussed in Sections 3 and 5, and a simple static test that was performed to obtain preliminary data on the buckling characteristics of circular plates prior to proceeding with the dynamic response testing of scaled pusher plates is described in Section 4.

1.2. (U) TECHNICAL BACKGROUND

(S) A major portion of the ORION Project staff effort during the preceding year has been directed toward analyzing a typical ORION vehicle model. The size chosen for this analysis was the 4,000-ton reference vehicle. The latest iteration of the pulse-system data compatible with this vehicle size provides certain impulse parameters at the pusher and these,

---

[*] The HE used was Du Pont 506A series, which is approximately 85% PETN mixed with rubber binder. In this report reference is made to this material as follows: A-1 is 506A-1, A-2 is 506A-2, etc.; A-1 is 1 $g/in.^2$, A-2 is 2 $g/in.^2$, etc.

in turn, provide a means for estimating the loads imposed on various upper sections of the vehicle. The current pulse system specifies a peak pressure of 4.3 kbar at the pusher center, the pressure gradient tapering off to about 1/3 of that value at the pusher edge. The interaction time of the impulse and pusher is on the order of 400 μsec. This results in the pusher being subjected to approximately 20,000 g's. The primary shock absorber attenuates this loading so that the platform between the primary and secondary shock absorbers is subjected to about 80 g's.

(S) This set of force conditions on the pusher are considered conservative,based on the best available analytical and experimental studies of the response of a steel pusher.

(S) The design of the pusher and, in particular, the choice of materials to be used depend essentially on the modes of failure which may be encountered. A documentation, by means of tests, of the possible modes of failure and the corresponding loads is a necessary premise to a final analysis. The following modes of failure can be foreseen at present:

1. Yield due to maximum bending and membrane stresses, depending on the deformation caused by the misfit between the impulse and mass distributions. Axially symmetric and nonsymmetric impulse misfits have to be considered.

2. Shear, depending on the local misfits between the impulse and the mass distributions due to irregularities in the impulse distribution and to local discontinuities in the mass caused by fittings.

3. Failure at the shock-absorber attachments, depending primarily on the outstanding length of the attachments compared to the length of the strain pulse induced and local damping.

4. Buckling of the edge in the presence of large hoop compressive stresses, especially in the thin pusher (steel contruction). Hoop stresses appear only during maximum deflection and last only a few milliseconds. Under certain conditions of pusher flexibility and primary shock-absorber reactions, considerable reinforcement is provided by the shock absorbers.

5. Bending into a developable surface or general instability into almost plane lobes separated by narrow regions with large plastic deformation.

6. Fragmentation due to the radial expansion induced by Poisson's effect. In general, brittle failure should be avoided with a margin in favor of ductile failure.

7. Spalling is not expected to result from the pressure pulse because the pulse is long compared to the thickness of the pusher plate. Recent pulse-system designs indicate essentially no X-ray-induced vaporization pulse.

[redacted] 8. Thermal stresses induced by neutron radiation and by mechanical damping following ringing will be fairly well distributed throughout a one-material pusher. Heat conducted into the pusher from the propellant and removed on the upper surface will produce a temperature gradient and thermal stresses,which must be considered.

(S) For testing full-thickness pusher-plate sections under pulse conditions,all the characteristics of the simulated impulse should match those expected from the propellant-pusher interaction. The method discussed here considers only the pressure-time history. Simulation of the thermal characteristics as well as pressure are discussed in Vol. II, Interaction Effects. It is logical to separate the hydrodynamic response from the other effects because each pulse is a separate entity and the conditions of the pusher just prior to any given pulse should be predictable. Also, the pressure pulse is the most critical condition of pusher loading, and, of course,considerable structural and mechanical proof-testing can be done without nuclear explosions. For equal stress in scaled pushers or sections of scaled pushers the pulse pressure remains the same, whereas the pulse time varies with the linear scale factors. Therefore, in developing pulse generators one strives to match the shape of the propellant-pusher interaction pulse. The sheet HE—foam combination produces an impulse envelope quite similar in shape to that predicted for the reference vehicle (see Vol. I, Reference Vehicle Design Study), except that the HE pressure pulse is somewhat narrower in time. The rise and "tail" are good approximations. Therefore, to transmit the same momentum, the HE impulse requires either a somewhat higher peak pressure or longer pulse length.

(S) The analytical studies have been limited by the over-simplified boundary conditions required in a low-cost study. The experimental studies have been limited to a relatively small number of probing-type tests. There is considerable latitude in the design of the pulse system which varies the force conditions on the pusher. In general, specific impulse is improved with higher pulse pressures acting for shorter periods and higher center-to-edge pressure ratios (see Vol. I of this report). Under a development program for an optimum vehicle design, sets of limiting load conditions for various pusher designs would be established. These conditions could then be weighed against the design restraints of the pulse system and its depolyment and detonating systems. The approach followed here has been to establish a degree of reliability of a given set of design conditions. This being done in parallel with the design study of an ORION engine with iterations in pusher loading conditions warranted the development of several HE-generated impulses for loading test elements. Adding to this the necessity for scaled tests indicates the need for a considerable range of desired impulses. Hence, impulse development over a considerable range was undertaken. This does not imply that a thorough parametric study has been accomplished. However, with these data as a starting point and with a minimum of development at any set of impulse conditions within the range covered, reproducible impulses can be made available.

(C) It was expected that once pulse-generating systems and recovery techniques were available, some response tests on scaled pusher elements would provide data on some of the modes of failure, and general and quantitative data have been collected on several. Considerable data on special-purpose attachments for the toroidal shock absorber have been taken and are discussed in Section 3. During the development of the recovery system, much information was gathered on fittings (related to shock-absorber attachments), shear effects, bending, lack of fragmentation, and lack of spalling.

2. (U) DEVELOPMENT OF IMPULSE-PRODUCING TECHNIQUES

2.1. (U) SINGLE-IMPULSE-SHAPING TEST

(U) Several approaches could be taken toward developing impulses to perform the tasks specified in Section 1.2 of this report. In early tests, bulk and shaped charges were tried. The experimental setups with these types of charges worked well with small test samples. However, as the frontal area of the test specimen is increased, the separation (standoff) distance between the specimen and the explosive charge must be increased proportionately to obtain a relatively uniform impulse over the test area. Hence, excessively large bulk charges would be required. Later tests have confirmed that placing sheet high explosives (HE) parallel and closely adjacent to the test specimen provides the desired spectrum of impulses with acceptable efficiencies.

(U) An impulse-test setup is portrayed in Fig. 2.1, in which it can be noted that several approaches are available for varying the impulse received by the test plate. The thickness and/or the density of the attenuator may be varied, and, in turn, the energy transferred to the test plate will vary. The sheet HE is available in various thicknesses (weight per unit . area), providing another variable for obtaining different impulse shapes. Figure 2.1 also shows the position of the backup material that was used in some of the tests. Ideally, an infinite backup would increase the impulse by a factor of two over that resulting when no backup is used. Varying the backup mass provides another variable which can be used to modify the impulse curve. Center-detonated and edge-detonated tests were tried to determine if the detonation location changed the pressure-pulse characteristics. Pipe containment of the test setup was used on some of the small-diameter-plate test shots to minimize the edge losses, thereby simulating the conditions that would be encountered in the center portions of large-diameter plates. Figure 2.2 is a photograph of a typical test setup. The long tube-shaped device in the foreground is the piezoelectric pressure probe.(2) The interaction (pressure) at the test-plate surface results in a piezoelectric crystal voltage output that is proportional to the pressure change. The resulting signal is displayed on an oscilloscope and recorded photographically. Figure 2.3 shows a typical oscilloscope trace of an impulse test.

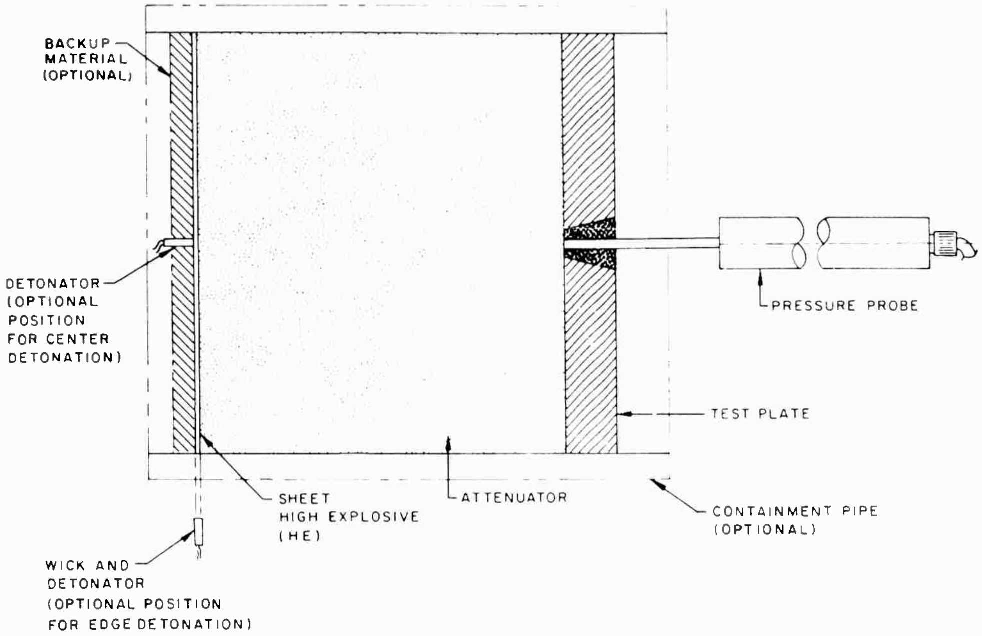
BACKUP MATERIAL (OPTIONAL)
DETONATOR (OPTIONAL POSITION FOR CENTER DETONATION)
PRESSURE PROBE
TEST PLATE
SHEET HIGH EXPLOSIVE (HE)
ATTENUATOR
CONTAINMENT PIPE (OPTIONAL)
WICK AND DETONATOR (OPTIONAL POSITION FOR EDGE DETONATION)

Fig. 2.1--Typical impulse-test setup

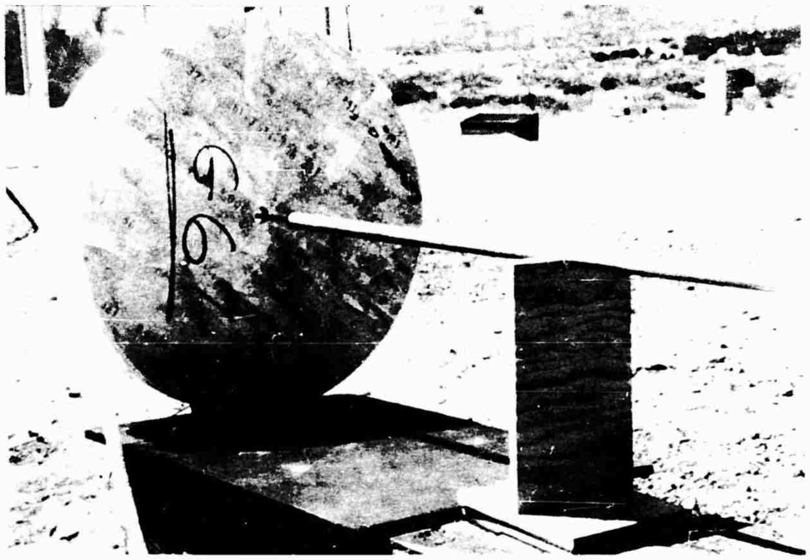

Fig. 2.2--Pressure-probe—test-plate experimental setup

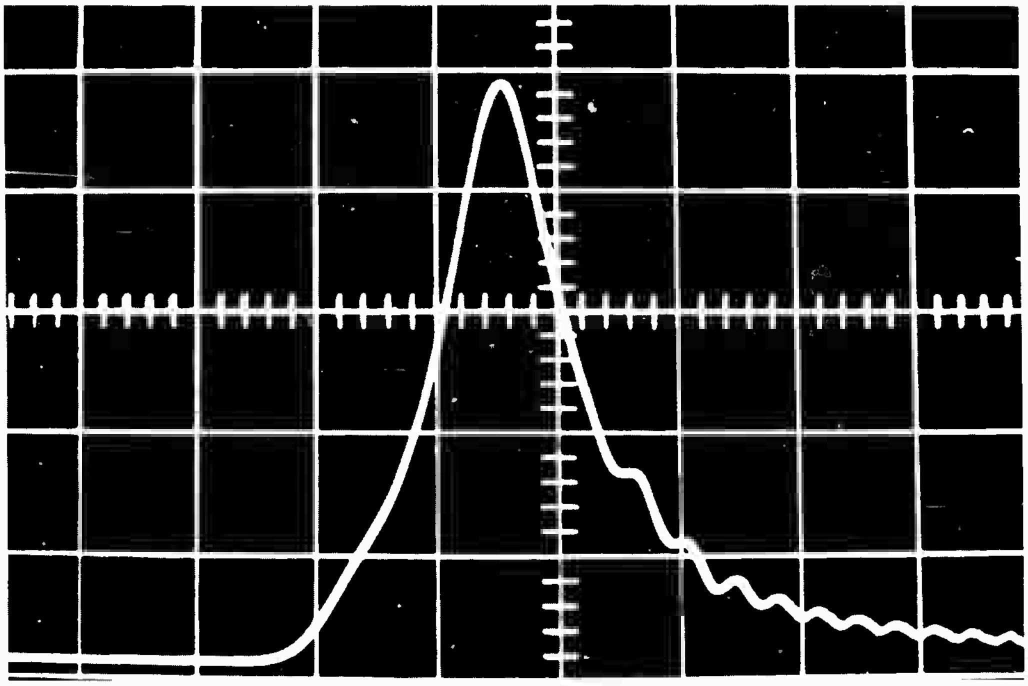

Fig. 2.3--(U)Typical pressure-probe oscilloscope trace (9,100 psi per square, vertical; 10 μsec per square, horizontal)

2.1.1. (U) Effect of HE Weight

(C) Although the effect of varying the attenuator geometry on pulse-shaping was of primary interest in these tests, a small amount of data was obtained by varying the HE configuration. Although the data is not conclusive, it does imply certain trends; some of those noted are:

1. With other parameters held constant, an increase in the thickness (weight per unit area) of the HE produced a directly proportional increase in peak pressure.

2. The impulse per unit area varies in direct proportion with HE weight per unit area when scatter in the experimental data is averaged.

3. The pulse duration and its general shape are not strongly dependent on the weight of the HE.

4. The rate of rise of the pressure tends to be increased with HE weight when other conditions are held constant. The experimental data collected are insufficient to quantitatively establish this parameter. Additional data should be collected on this parameter before accurate predictions of the results of more than a few test setups can be made. The effect of rate of rise of the pressure on the ORION pusher will depend on the properties of the pusher and pusher-attachment materials. Tough, or ductile, materials are more resistant to rise rates than are more brittle materials. In the current ORION design where weldable low-alloy steel is used the rise rate should not be a dominant parameter.

(U) Essentially identical test setups produced a considerable variation in peak pressure and impulse measurements. These variations appeared even when more than one pressure probe was used in a single test. This scatter was investigated in more detail and the results are discussed in Section 2.5.

2.1.2. (U) Effect of Attenuator Density

(C) The use of foam plastics to attenuate the HE impulse yielded impulse shapes similar to those expected from the ORION pulse system. Therefore, in most tests of this series, various densities of foam were used to modify the impulse received from the HE.

(U) Styrofoam[*] of about 2 lb/ft^3 and 4 lb/ft^3 density was readily available and was used in the test series when a low-density foam was required. Styrofoam of higher density presented a procurement problem, so urethane[†] foam was used for the various tests incorporating the high-density foams. The test-plate diameters were 8 in. in the first tests and 20 in. in later tests. The ratios of peak pressure to weight per unit area of explosive as functions of attenuator (plastic foam) density and depth are shown in Figs. 2.4 and 2.5, respectively. Summaries of the effects of foam density on pulse peak pressure and pulse duration are plotted in Figs. 2.4, 2.6, and 2.7. Peak pressures were highest when the 4-lb/ft^3 foam was used. Total impulse increased with foam density and so did the pulse duration. Rate of rise of the pressure pulse generally decreased with increased foam density. It should be noted that Figs. 2.4, 2.5, 2.6, and 2.7 are plots of data points; the lines connect averages of the data which were taken from similar tests, or indicate trends. There is no established significance to the peak pressures being highest when 4-lb/ft^3 foam density is used. A conjectured explanation of the maximum in the peak pressure is that the peak pressure at the test plate for any value of attenuator density which is less than the density that corresponds to the maximum peak pressure results from the pile-up of vaporized attenuator material at the plate. Under this condition the pressure is expected to increase with added mass between the HE and the plate. However, at some value of increased attenuator density, vaporization and melting of the foam are not complete and the pile-up of vaporous material is then against the unmelted foam, which acts as a true pressure attenuator, and results in lower peak pressures at the test plate. This occurs when higher density foams are used. There is experimental evidence to support this latter theory: With low-density or thin foam, only a carbon dust residue is evident. With higher-density foam or very thick layers of light foam, granulated or compressed blocks of the attenuator of the original white color were recovered.

(U) Some additional testing of foam in the 3-, 6-, and 8-lb/ft^3 density range is needed to examine the full range of attenuator-density effects. Except for peak pressure at 2 lb/ft^3 density (see Section 2.1.3), Styrofoam and urethane foams behave differently when subjected to the HE impulse (see Section 2.5.). It might be advisable, therefore, to make comparative tests of these two foam types in the 2- and 4-lb/ft^3 density range.

(U) The pressure-pulse durations shown in Fig. 2.7 were measured as the period from the time of onset of the pressure signal to the time that the pressure had dropped to 10 per cent of its peak value. The total impulse values shown in Fig. 2.6 were determined by integrating the total area under the pressure-time curve (on the oscilloscope traces).

---

[*] A foam polystyrene plastic made by Dow Chemical Company.

[†] Urethane is the CPR International Corp. No. 704 polyurethane base plastic.

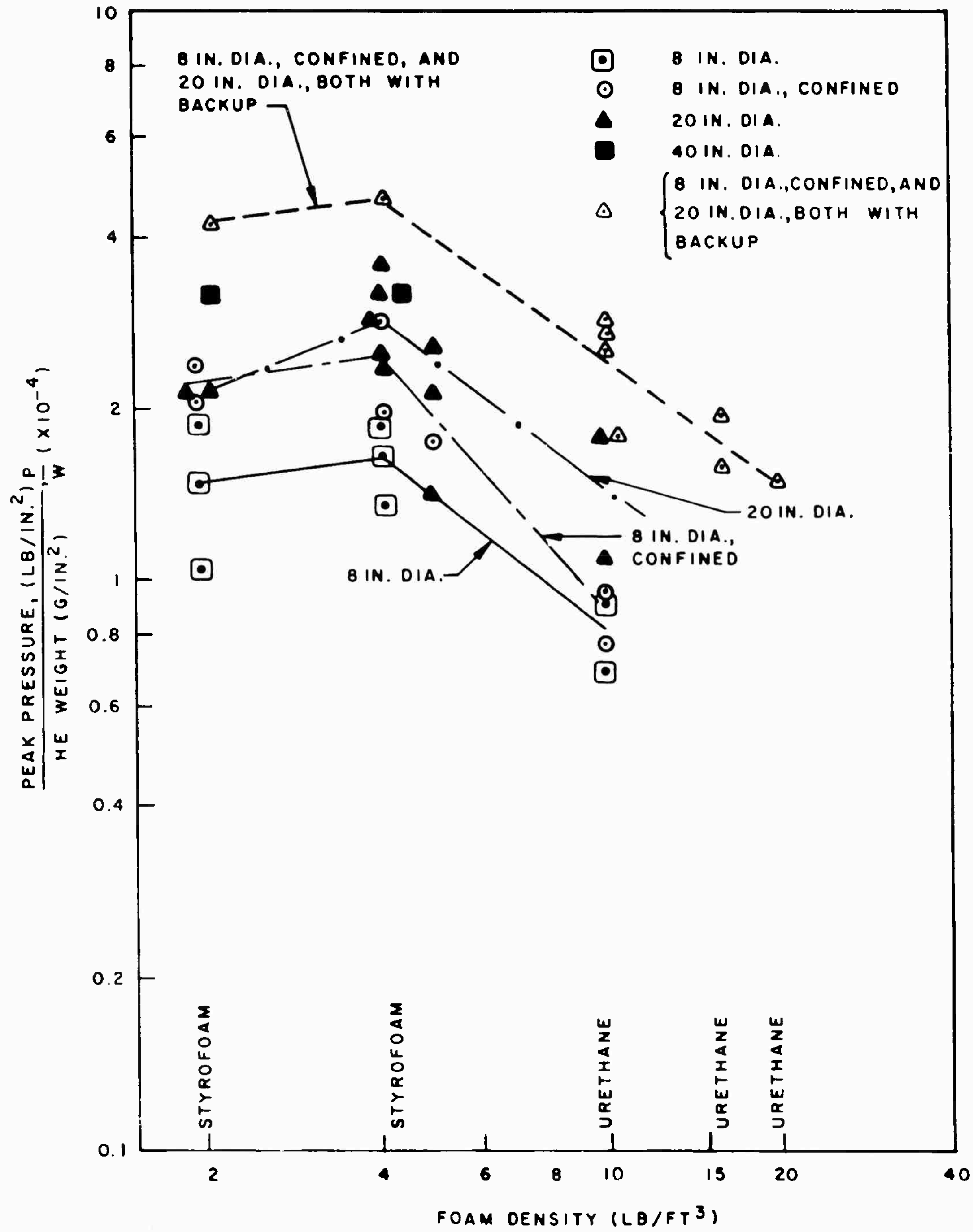

Fig. 2.4--Effect of foam attenuator density on peak pressures (all tests were made with 8 in. foam depth)

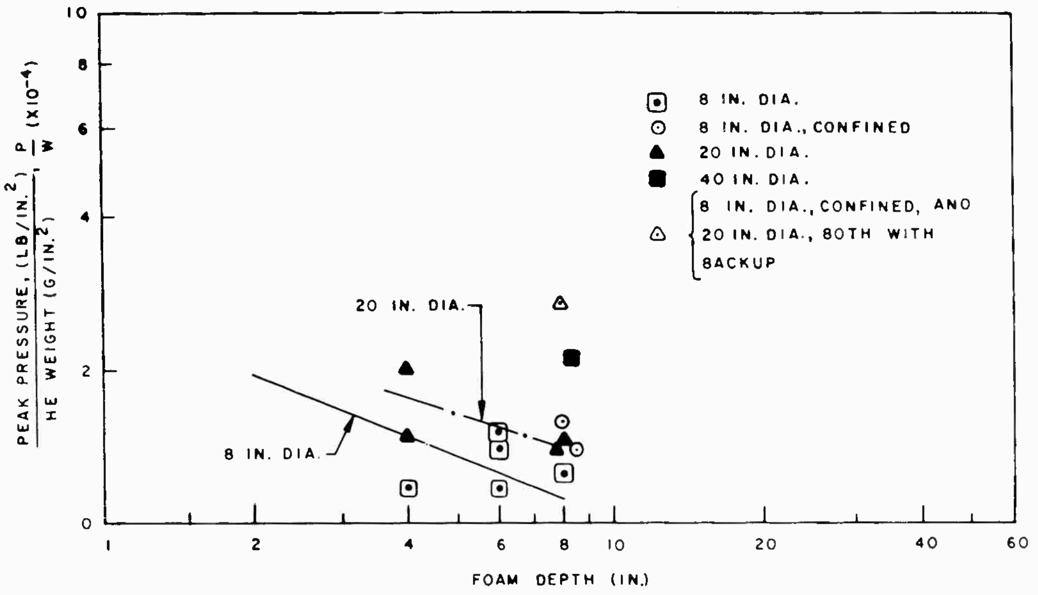

(a) 2-lb/ft^3-density foam

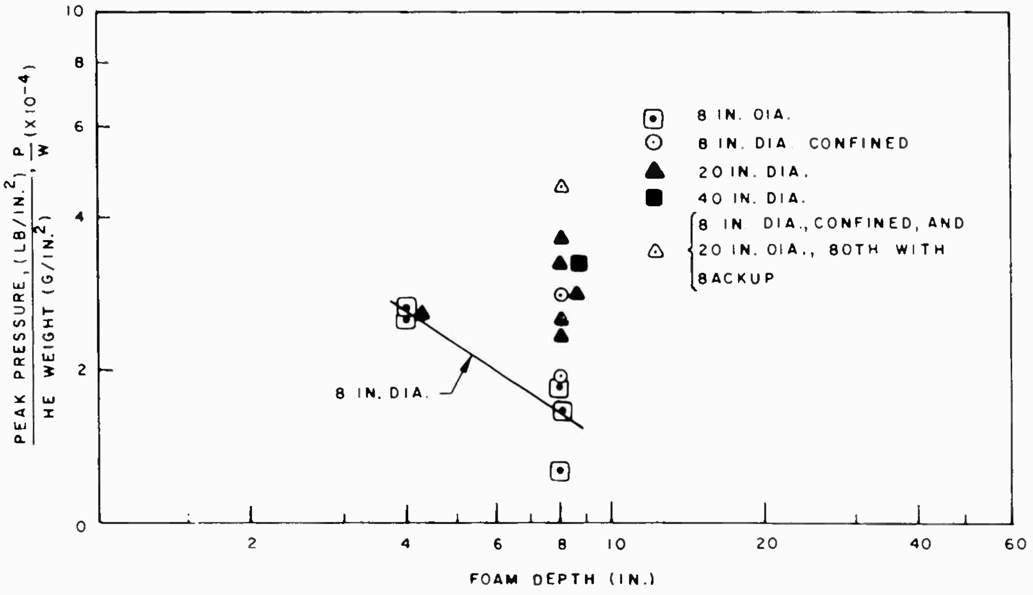

(b) 4-lb/ft^3-density foam

Fig. 2. 5--Effect of foam attenuator depth on peak pressures

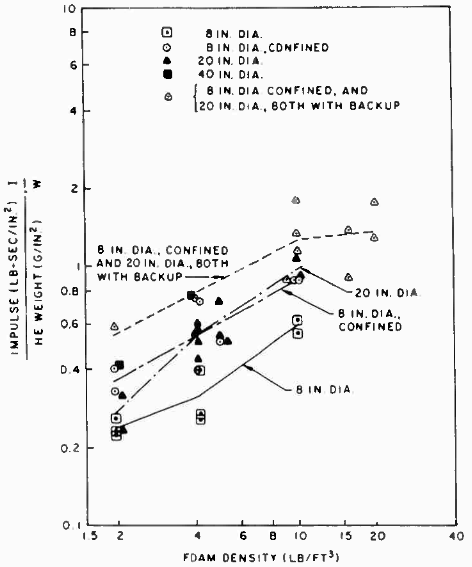

Fig. 2.6--Effect of foam attenuator density on impulse (all tests were made with 8-in. foam depth)

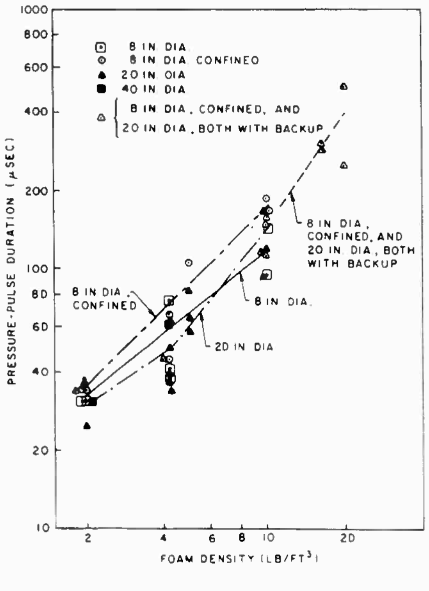

Fig. 2.7--Effect of foam attenuator density on pulse duration (all tests were made with 8-in. foam depth)

2.1.3. (U) Effect of Attenuator Depth

(U) Styrofoam of 2 lb/ft^3 density was available early in the test period, and several tests were made in which the depth of this foam was varied. The data plotted in Fig. 2.5a for experiments using 8-in.-diam test samples and Styrofoam correlate well with similar data taken earlier when urethane foam of approximately the same density was used. Fig. 2.5b gives the data for 4-lb/ft^3-density foam. The data taken for higher-density foams were insufficient for developing trends.

2.1.4. (U) Effect of Side Confinement of HE and Attenuator

(U) Producing pulses over small areas is desirable for impulse-loading of small test structures and for conserving materials. When the diameter of the test plate is not large compared to the attenuator depth, one-dimensional conditions do not exist. It is important, therefore, to know the impulse resulting from experiments where edge effects (rarefaction waves converging over the test plate) are significant. Such edge effects were apparent in some of the experiments conducted with 8-in.-diam plates and no confinement of the attenuator and HE; the results of these tests are also plotted in Figs. 2.4, 2.5, 2.6, and 2.7.

(U) For purposes of comparison, experiments were conducted with a reflector placed around the explosive and attenuator (i.e., the experiment was fired in a heavy-walled containment pipe). This configuration, which reduces edge effects, yielded fairly close correlation of data with those obtained from the larger-diameter unconfined shots using the same attenuator depth and HE weight. (See Figs. 2.4 through 2.7.)

2.1.5. (U) Effect of Mass Backup Behind HE

(U) A series of experiments was performed to determine the increase in total impulse on the test sample when the high explosive was partially confined. Confinement was achieved by placing a sheet of plywood on the back side (see Fig. 2.1) of the sheet HE. Figures 2.4 and 2.6 indicate the magnitude of the peak pressures and impulses obtained and also show that increased peak pressures and total impulses occur when the HE is backed up.

2.1.6. (U) Effect of Foam Plus Air Attenuator

(U) Two confined tests using an attenuator composed of foam urethane and an air gap were fired in an 8-in.-diam pipe. A 1-in. air gap next to the test plate plus 7 in. of foam provided an 8-in. separation between the A-2 sheet HE and the test plate. Urethane foam of 10 lb/ft^3 and 6 lb/ft^3 density was used in the tests.

(U) The result of the test using the 10-lb/ft^3 foam is shown in Fig. 2. 8. The slow initial rise in pressure, to about 4, 000 psi in 100 μsec, is attributed to the compression of the 1-in. air gap. The sharper rate of rise of pressure from 4, 000 psi is attributed to the pile-up of foam on the test plate. The peak pressure reached was approximately 18, 000 psi. The test with the 6-lb/ft^3 foam produced a higher peak pressure of shorter duration, which is consistent with data from tests of uniform foam with no air gap. The rise time was extended by the air gap, but was less pronounced than in the test with 10-lb/ft^3 foam.

(U) These tests indicate that a large variety of pulse shapes can be obtained by varying the distribution and composition of the attenuating material.

2. 2. (U) AN APPROACH TO DOUBLE-PEAK IMPULSES

(C) One version of the ORION pulse system is expected to produce a double-peaked pressure pulse at the pusher. To simulate this condition and to stretch out the duration of the impulse to about 400 μsec, the use of more than one sheet of high explosive separated by varying depths and densities of foam was considered. The use of strips of HE as timer wicks to detonate the sheets of HE at precise intervals was investigated as a preliminary part of the study of multiple-HE shots. Coaxial switches were tested and various techniques for incorporating these switches into the test geometry were investigated.

(U) Two tests were conducted to determine whether any significant variations existed in the detonation-wave propagation rate in HE wicks which were placed flat against wood, steel, aluminum, dense foam, light foam, and in air. The wicks were made of 1/2-in. -wide, 20-in. -long A-2 sheet HE. The measured rate of propagation for all the wicks was 3. 4 ±0. 1 μsec/in. (~0. 3 in. /μsec). The proximity effect of the six materials is probably insignificant as this small rate variation (±0. 1 μsec/in.) could have existed in the test circuitry. These test results have shown that the 1/2-in. A-2 HE wick is a sufficiently accurate delay timing device for use in the multiple-peak impulse test.

(U) Two tests of the coaxial switch reliability and gap geometry were made to determine whether placing the switches at various distances from the edge and the face of exploding A-2 sheet HE or wick would influence the timing or closing characteristics of the 50-ohm subminax cable switches.

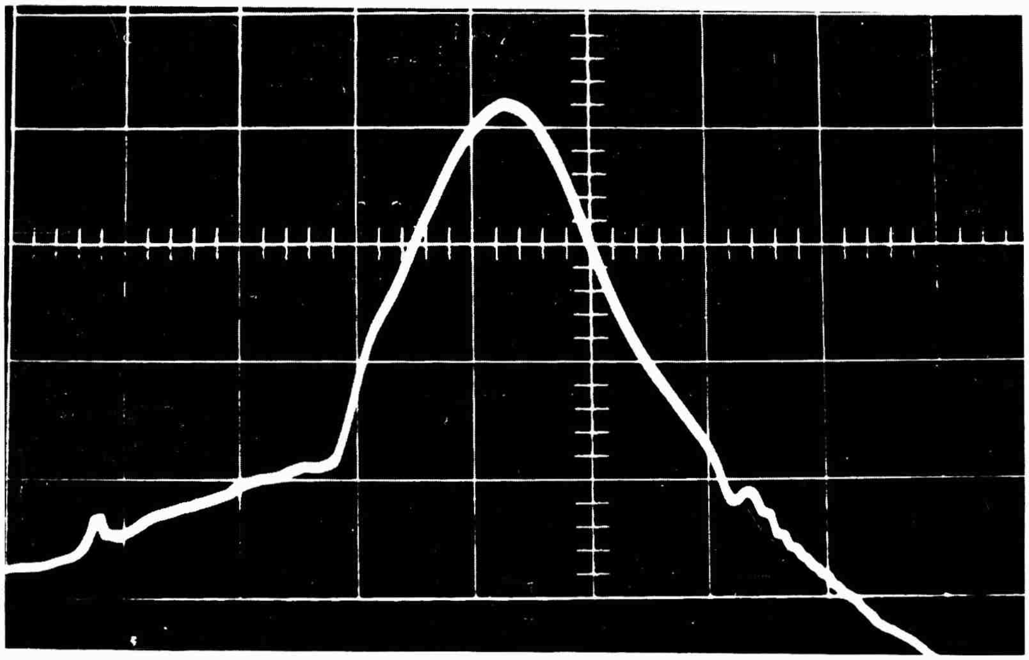

Fig. 2.8--(U)Pressure-probe oscilloscope trace made with 7 in. of 10 lb/ft^3 foam plus 1 in. of air attenuator and A-2 HE (4,550 psi per square, vertical; 50 μsec per square, horizontal)

These switches (fabricated by the normal shearing of the cable) were imbedded 1/32 in. in the HE sheet, placed flush with the surface of the HE sheet, or mounted with 0.010-in., 0.25-in., and 0.050-in. gap clearances between the sheared face of the cable and the HE sheet. No significant difference in closing times (the shorting of the ends of the butt-sheared coaxial cable) could be observed when the switches were mounted on or within 0.050 in. of the face of the HE sheet. But a significant delay, about 10 μsec, was observed when the switch was mounted 0.050-in. away from the edge of the HE sheet. These tests indicated that the switches made of sheared 50-ohm subminax cable operate dependably when placed on or within 0.025 in. of the surface, or edge, of the A-2 sheet HE.

(U) Only one multiple-HE shot (separated by foam) was fired; the two HE discs were detonated simultaneously. The test sample was a 20-in.-diam aluminum test plate with one centrally located piezoelectric pressure probe. Six-inch-thick urethane foam of 10 lb/ft^3 density was placed between the plate and the first sheet of HE, and 2-in.-thick, 4-lb/ft^3-density urethane foam was placed between the two A-2 HE sheets. Although several configurations were considered, this initial test configuration was simplified as much as possible to aid in interpretation of the results. With this test geometry and simultaneous detonation of the two HE sheets, the shock wave from the outer HE sheet would take 100 μsec to travel through the 2 in. of 4-lb/ft^3 foam to reach the plane of the inner HE sheet. If this shock wave continued inward, a second impulse peak should follow the primary (inner HE sheet) impulse by 100 μsec. On the resulting oscilloscope traces, only a slight variation in the trace was noted at the point 100 μsec behind the initial pulse. The peak pressure of the primary pulse more closely resembled that of another series of tests where a 1-in. plywood backup mass was used to partially contain the energy from the HE. These results indicate that either a mass backup of the outer HE sheet or a delayed detonation of one of the HE sheets might produce the desired double-peaked pressure pulse.

2.3. (U) IMPULSE VARIATION ACROSS PLATES

(C) One of the goals of the ORION experimental effort is the generation of data which will assist in the understanding of the response of large plate-like structures to impulse loads. The first major step in such a program was to acquire an understanding of the applied impulse and to develop experimental techniques for simulating this impulse in a controlled manner. Using these techniques, impulse data have been obtained at or near the center of relatively small diameter plates. However, edge effects and radial distribution patterns had not previously been studied. Local discontinuities which have only been passively observed are discussed in Section 2.5.

(U) Three tests were conducted to study the radial distribution of the impulse. The tests were made using 8-in. -thick foam and 40-in. -diam test plates of 1-in. -thick aluminum alloy. In two of the tests, 6-lb/ft^3-density urethane foam was used, and in the third, 4-lb/ft^3-density urethane foam was used. Type A-2 sheet HE was used for all three tests. The piezoelectric pressure probes used in this series were positioned along a radius or diameter of the test plate. Figure 2.9 shows an eleven-probe test configuration.

(U) Five pressure probes were used in the first test; the results are shown in Fig. 2.10. The variation in the data obtained is similar to the variation in previous data taken at or near the center of 20-in. -diam test plates. There is no obvious trend of impulse change with radius in this 40-in. -diam test. The second test configuration was essentially the same as the first except that a sixth pressure probe was placed 1/2 in. in from the periphery of the test plate. The results of this test are shown in Fig. 2.11. In the third test, eleven probes were located along a diameter of the 40-in. -diam plate and were spaced 4 in. apart, except the outer probe on each end was spaced 3-1/4 in. from its adjacent probe. This experimental setup is shown in Fig. 2.9. Two probe circuits failed during the test. The data received from the remaining probes are plotted in Fig. 2.12. The results from Probes No. 1 and No. 11, which were 3/4 in. from the periphery, and Probe No. 10, which was 4 in. from the periphery, show considerable variation from the average, both in peak pressure and total impulse. These variations may be the result of localized turbulence, which has been observed in some tests with lead-faced test plates.

(C) The multiprobe tests indicated that strong turbulence or a multisource wave front resulted from this impulse-loading technique. Evidence exists (see Section 2.5) showing that these pulse conditions produce a pressure pattern of relatively small dimensional cell-like structure at the test plate. The formation of this structure is largely dependent on the details of the attenuator material utilized; the size of the cells ranges from a very small fraction of an inch up to approximately 1 in. across on the test plates used thus far. Although these pulse conditions are not desirable, it is believed that this experimental technique is valuable for studying large-diameter structural plates and attachments if the intensity of the peak pressures of shock-wave interactions at the surface of the plate is below the yield strength of the structural materials. These turbulent conditions are quite localized, resulting in the high-pressure peaks acting as point sources. No large area asymmetric loading conditions are apparent; therefore, this type of impulse-producing technique should not cause erroneous indications when structural testing pusher-plate samples and secondary structures, such as shock absorbers.

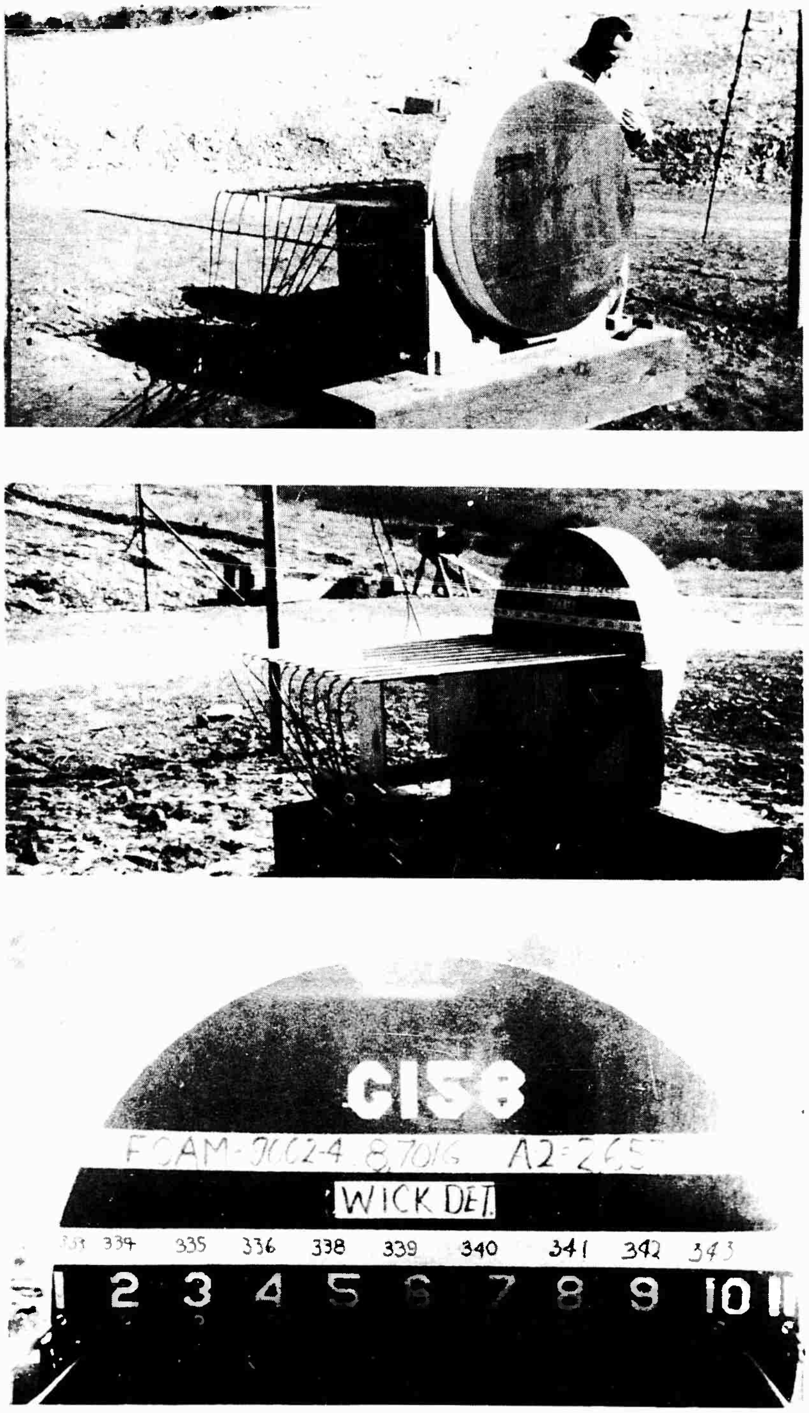

Fig. 2.9--(U) Test setup using eleven pressure probes

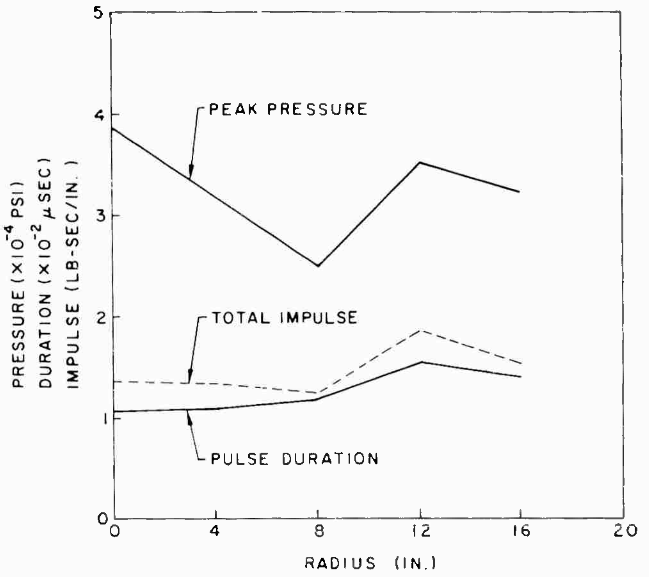

Fig. 2.10--(U)Plot of impulse-distribution test using five pressure probes

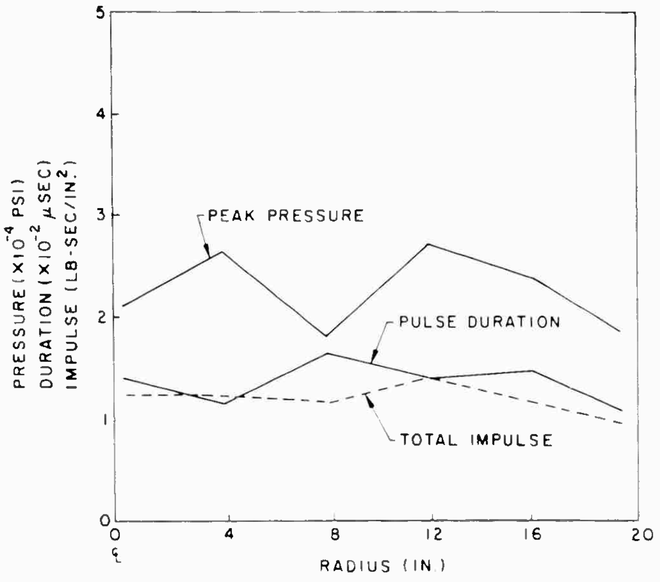

Fig. 2.11--(U)Plot of impulse-distribution test using six pressure probes

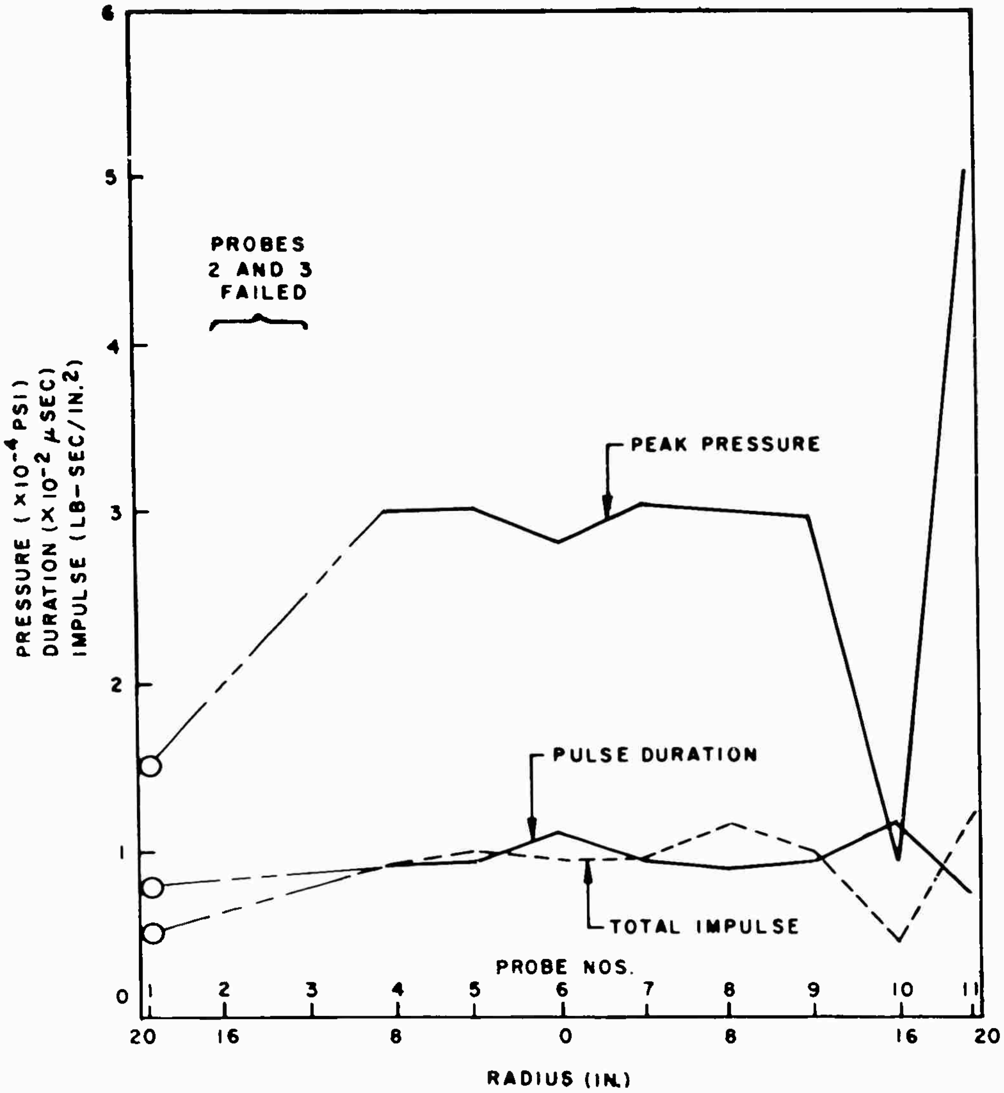

Fig. 2.12--(U)Plot of impulse-distribution test using eleven pressure probes

2.4. (U) SHOCK VELOCITIES THROUGH ATTENUATOR

2.4.1. (U) Transit Time for Plastic Wave

(U) The proper time delay between the detonation of the HE and the onset of the pressure signal at the oscilloscope must be predicted if the pressure pulse is to be properly recorded. The elements of this delay time include initial trigger delay time, detonation traverse time (from detonation point to the point normal to probe position) in the sheet explosive, transit time through the foam attenuator, and transit time through the tungsten bar of the pressure probe. All of these delay times, except the transit time through the foam attenuator, are constant or vary only a small amount with different test conditions. A summary of the transit times through various foams of 4 in. and 8 in. depths under various conditions of loading are plotted against foam depth in Fig. 2.13. The points shown are averages when more than one test of a kind was made.

2.4.2. (U) Technique for Transit-time Measurements

(C) One criterion for properly simulating the time history of the ORION impulse is that the pulse must strike the test plate first at the center and then progress radially outward at a controlled rate. The first step in fulfilling this criterion was to develop a method of measuring the pulse arrival times.

(U) An experiment was set up to measure pulse arrival times at several points located radially across a 20-in.-diam test plate. These arrival times were measured by using wafer-type switches of 1-mil-thick brass shim stock placed over a 1/4-in.-diam recessed hole drilled in a piece of plexiglass. The other switch contact was a pointed screw located perpendicular to and directly below the shim stock; a gap of approximately 0.005 in. was left between the shim stock and screw point. The thin shim stock was used to minimize the moving mass in the switch and to reduce the reaction time. The first test showed that the weak early arrival elastic, or shock, wave triggered the switches rather than the later primary pressure pulse. These early arrival waves were observed in other tests when dense foam was used as the attenuating medium and the pressure-probe signals were highly amplified. The transient time of this early wave through 8 in. of 10-lb/ft^3-density foam is on the order of 250 μsec, which compares to a transient time of roughly 500 μsec for the main plastic wave. Further testing indicated that the elastic-wave arrival time is not radically affected by adding a backup mass behind the HE and varies linearly with foam thickness.

(U) A second set of wafer switches fabricated of 1/32-in.-thick brass

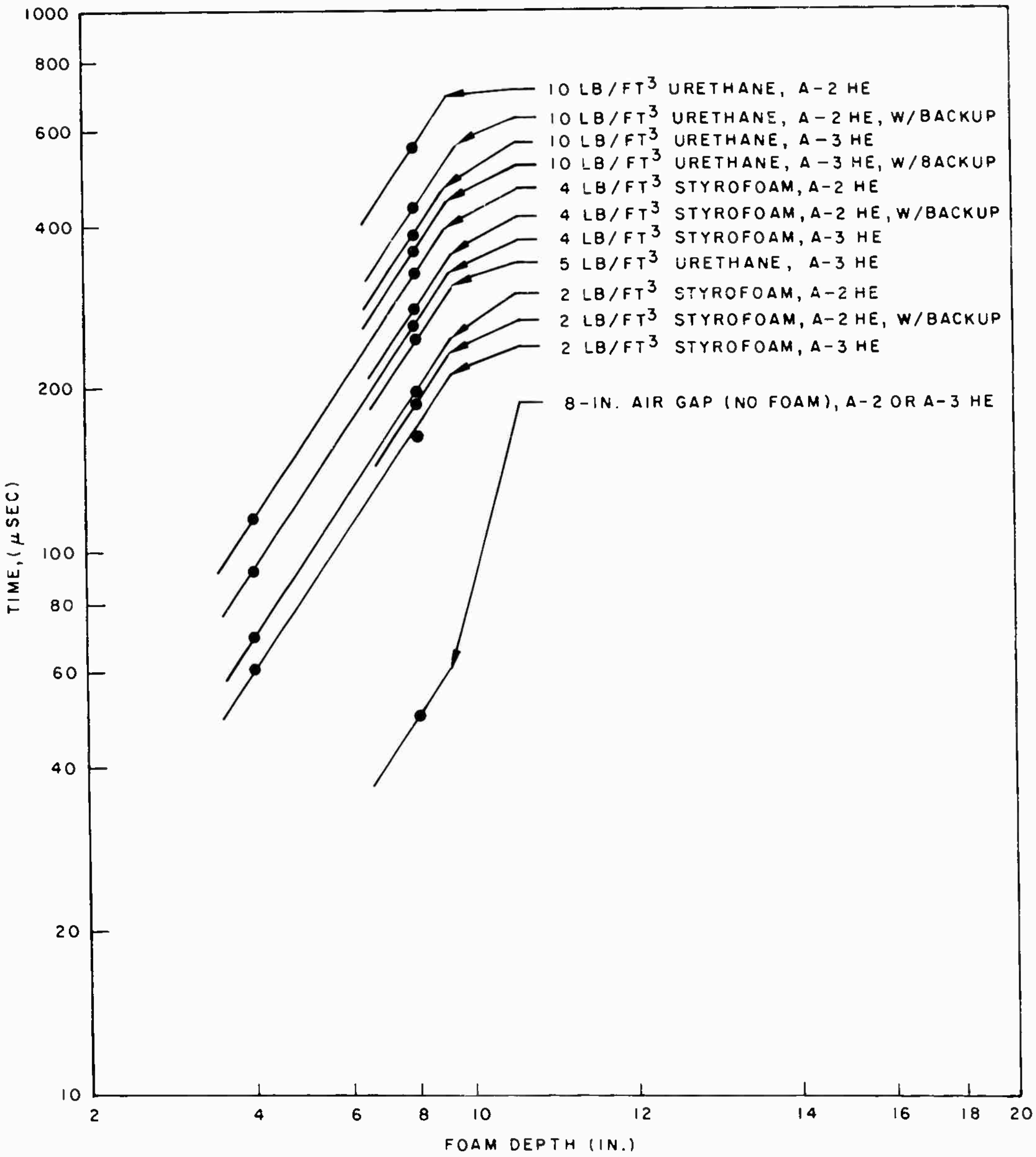

Fig. 2.13--(U) Transit time for plastic wave through foam attenuators; all tests used 20-in.-diam test plates

shim stock were supported over a 1/2-in.-diam recess. Again the switches were closed by the early shock wave. The third set was fabricated from 1/16-in.-thick brass stock supported over a 1/4-in.-diam recess. These switches were not actuated by the early pulse but were closed by the plastic wave, indicating that they might be acceptable for future impulse-arrival-time experiments. The delay induced by these heavier switches should be measured before impulse-arrival experiments can be performed.

2.5. (U) LOCAL VARIATIONS OF IMPULSE INTENSITIES

(U) Early in the development program of experimental impulse-simulating techniques it was noted that similar test setups gave large variations in the pulse parameters impinging on the test sample, or at least this condition was indicated by the pressure-probe data.

(U) To check whether or not the pressure probes were contributing to the variations in the increased impulse, three pressure probes were set up in a water tank opposite a hemisphere of C-4 (plastic type) high explosive. A 6-in. water gap was left between the explosive and the pressure probes. The hemisphere of HE was placed on a steel plate and center-detonated by a C-4 train through a small hole in the plate. The data received from this test showed an impulse spread of less than 10 per cent between the three probes, indicating that the instrumentation contributed very little to the data scatter observed on the previous shots.

(U) Subsequently, one of the tests on an aluminum plate exhibited a surface condition which might correspond to the large pressure variations observed in previous tests of this nature. In this test, Styrofoam of 4 lb/ft^3 density was used to attenuate the HE impulse. The markings on the surface of the test plate were in a cell-like pattern outlined by narrow grooves (see Fig. 2.14), a pattern which one might expect from the interaction of strong shock waves on a metal surface. When adjacent bumps of the turbulent, or mottled, front of a shock wave interact at the plate's surface, a pressure amplification results which, under this set of conditions, is above the dynamic elastic compressive limit of the metal surface and an indented groove results. Should such an interaction occur over the 1/4-in.-diam face of the pressure probe, the result would be a higher pressure reading than would be received from a probe not subjected to this localized interaction. This phenomenon was observed on the aluminum test plate only when the 4-lb/ft^3-density Styrofoam was used as the attenuating material and did not occur when 4-lb/ft^3-density urethane foam was used in a similar test. In some of the tests, large pieces of distorted Styrofoam were recovered after the test, and a mottled pattern matching that of the test plate was observed on the surface of the Styrofoam that had been adjacent to the plate during the test.

(U) A series of tests were performed to study these turbulent effects. The test plates were made from steel, 8 in. in diameter and 5/8 in. thick, with a 1/8-in.-thick layer of lead bonded to one face. The lead facing was machined to a fine finish. A typical test plate is shown in Fig. 2.15. The tests used 8-in.-thick foam and A-3 sheet HE. The parameters varied were: foam type, foam density, center- or edge-detonated, and confined or unconfined.

(U) Figure 2.16 shows a typical unconfined test setup. The confined test setup is mounted in a steel pipe of 1/2-in. wall thickness. The nylon lines, which are used for test-plate recovery, were attached to an overhead support cable and a drag chain.

(U) Figures 2.17 through 2.28 show the results of the test shots made with varied parameters. The results indicate that

1. Confinement induces considerable turbulence at the periphery of the test plate.
2. In unconfined tests, when either center-detonated or edge-detonated and 2-lb/ft^3-density Styrofoam or 4-lb/ft^3-density urethane foam is used, a peripheral ring of ~1/2 in. width of unperturbed surface and an adjacent ring of slightly smaller diameter of more than average surface damage result.
3. Center detonation produces a 3- to 4-in.-diam concentric ring, or surface wave, both in the unconfined or confined test setups.
4. Wick detonation from the edge of the HE produces a more uniform distribution of surface effects than the center-detonated shots.

2.6. (U) IMPULSE DETERMINATION BY VELOCITY MEASUREMENTS

(U) During the effort to develop pulse-shaping techniques, a wide spread in peak pressures was observed from supposedly identical setups. Furthermore, significant pressure gradients were measured when multiple pressure probes were located adjacent to each other diametrically across the face of the test plate. This condition was further verified with lead-covered test plates which showed the pock-marked patterns resulting from the pulse variations (see Section 2.5). These variations reduce the accuracy of determining the total impulse from measurements of the impulse at one point. It was therefore decided to supplement the pressure-probe data by making an independent determination of total impulse. This was accomplished by accurately measuring the velocity of the test plates and calibrating the total impulse from the velocity data. These velocity measurements were taken with a Fastax framing camera operating at speeds of 1,000 to 3,000 frames/sec, depending on lighting conditions. An electronic

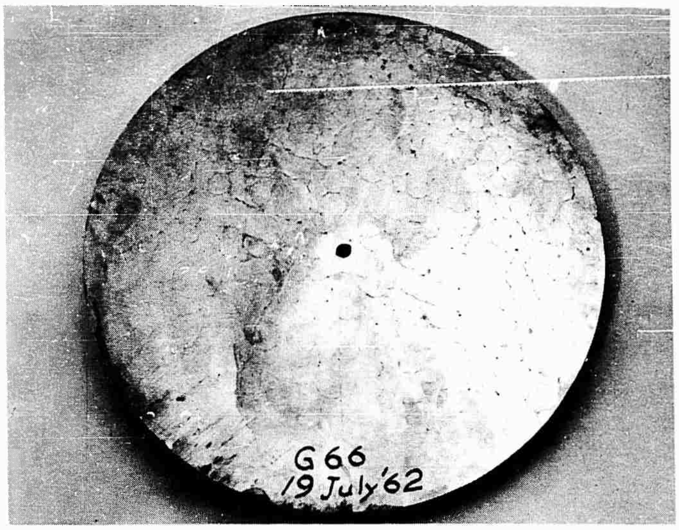

Fig. 2.14--Surface pattern of indentations from nonuniform pulse; the test plate is aluminum alloy, 20 in. in diameter by 1 in. thick; the attenuator was 4.2 lb/ft^3 Styrofoam; and the HE was A-3, bottom-wick-detonated

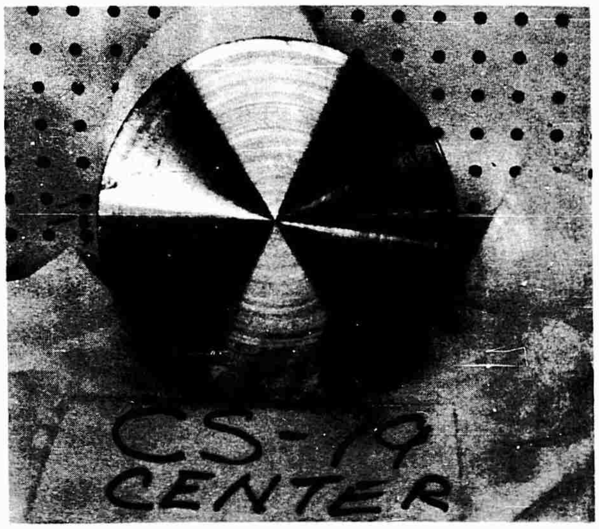

Fig. 2.15--Typical 8-in.-diam test plate of 5/8-in. hot-rolled steel with 1/8-in.-thick lead face, showing the machined lead face

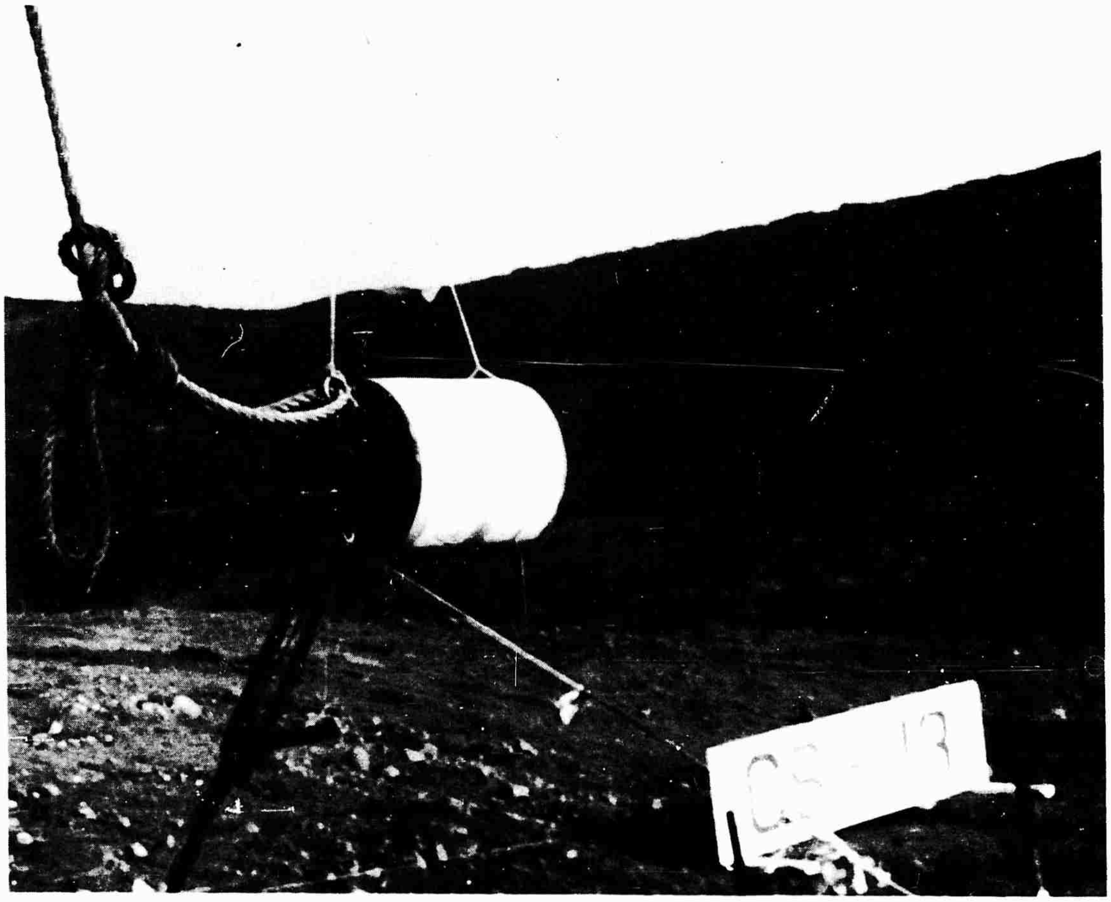

Fig. 2.16--Typical string-suspended assembly with 8-in.-thick foam attenuation (note wick hanging from sheet HE at bottom right of assembly)

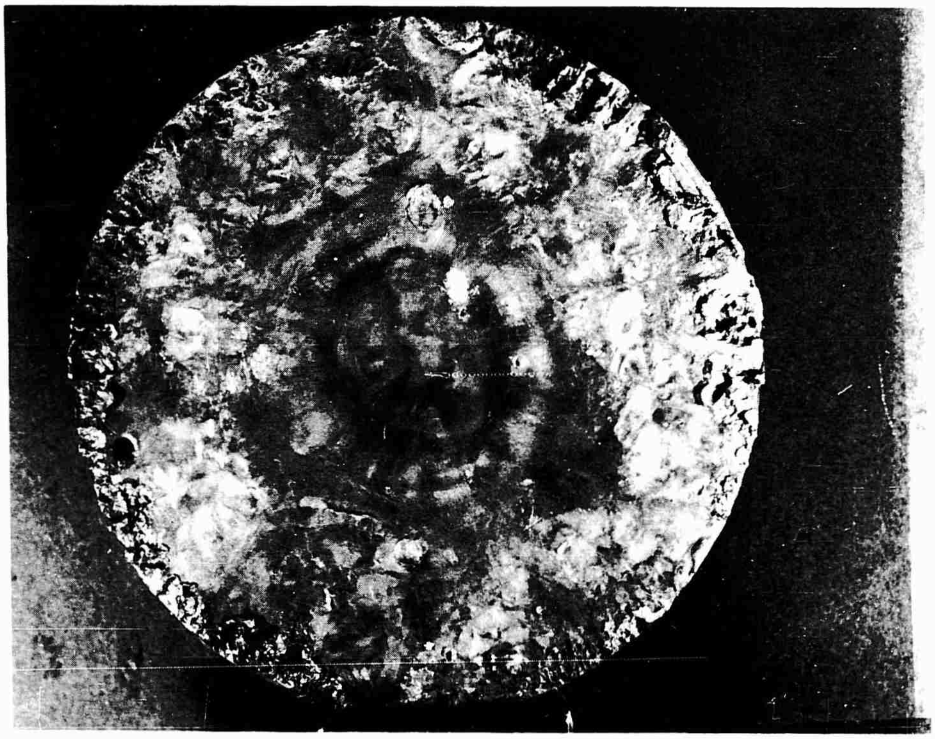

Fig. 2.17--Result of center-detonated, 4-lb/ft^3-urethane-attenuated, pipe-contained test

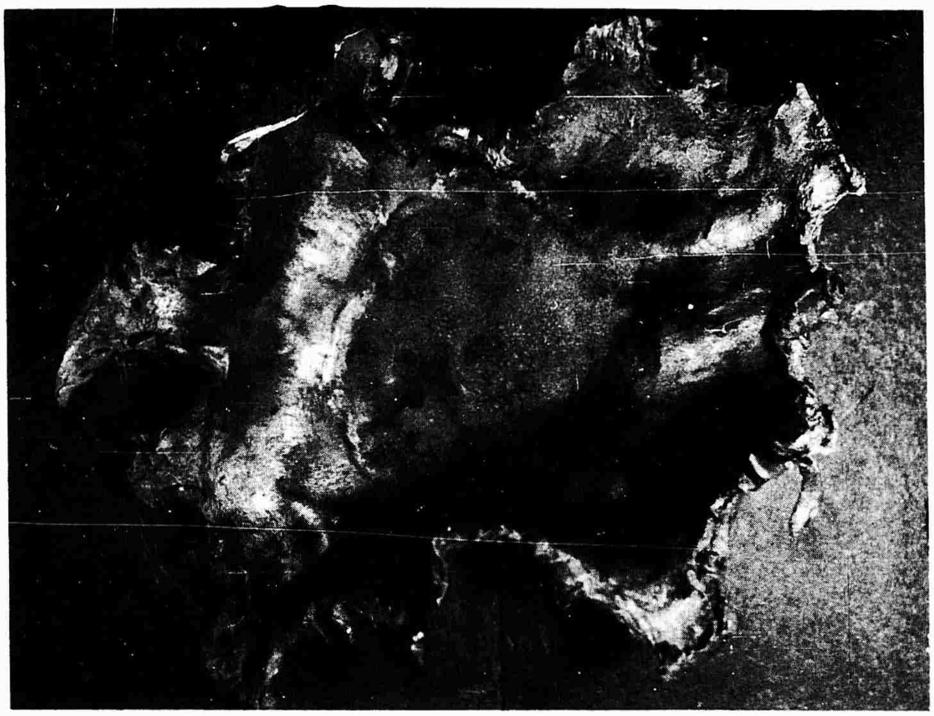

Fig. 2.18--Result of center-detonated, 6-lb/ft^3-urethane-attenuated, pipe-contained test

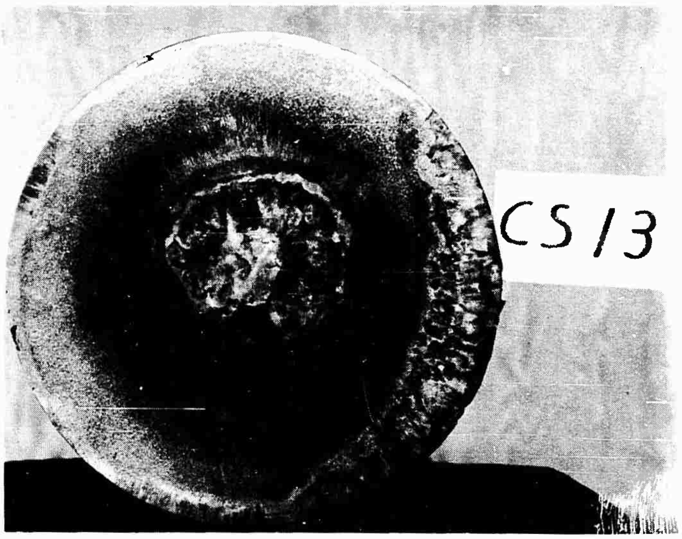

Fig. 2.19--Result of center-detonated, 4-lb/ft^3-urethane-attenuated, platform-supported test (bottom of the plate rested on the plywood support)

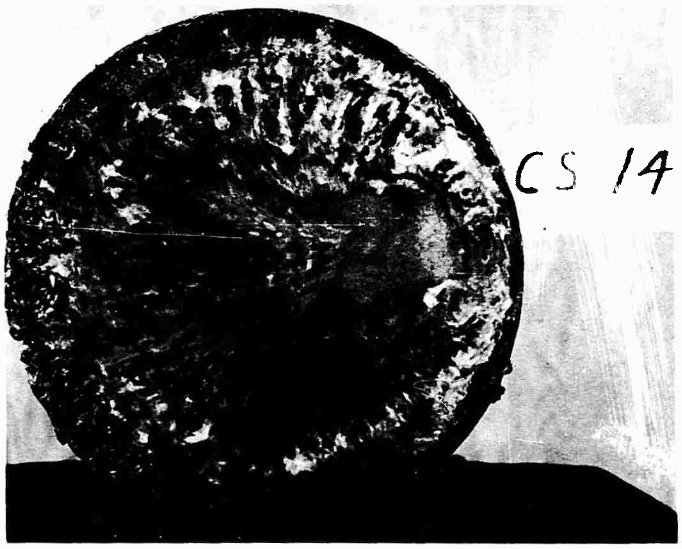

Fig. 2.20--Result of bottom-wick-detonated, 4-lb/ft^3-urethane-attenuated, pipe-contained test

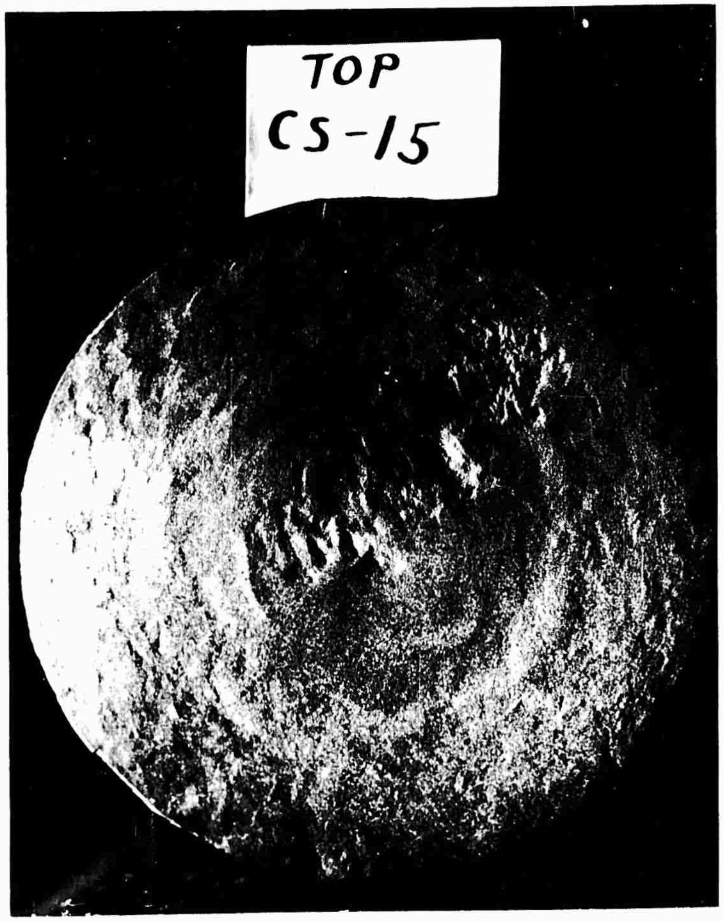

Fig. 2.21--Result of center-detonated, 6-lb/ft^3-urethane-attenuated, string-suspended test

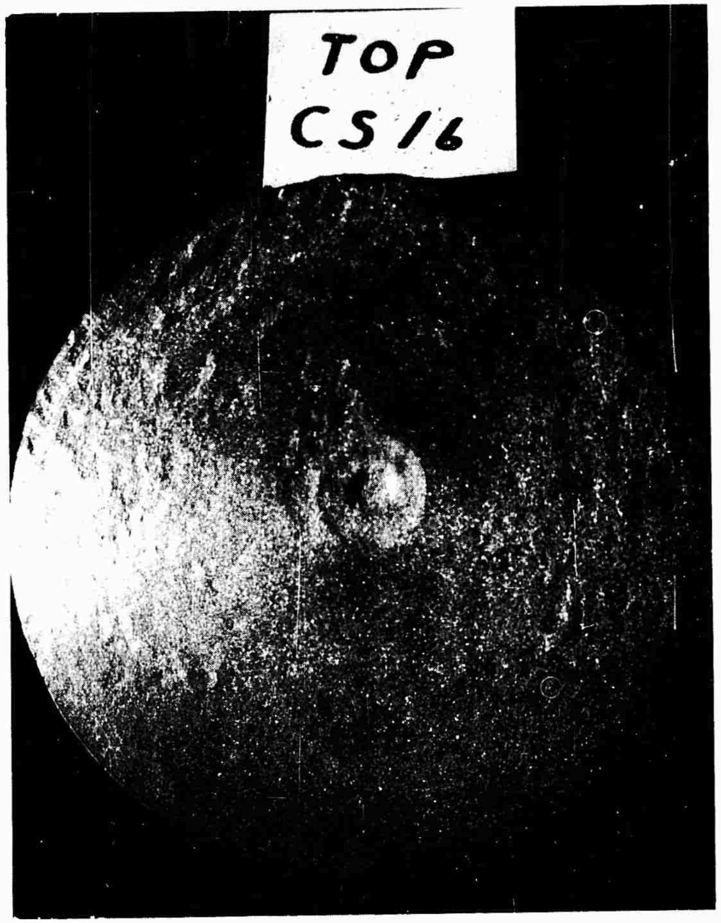

Fig. 2.22--Result of bottom-wick-detonated, 6-lb/ft^3-urethane-attenuated, string-suspended test

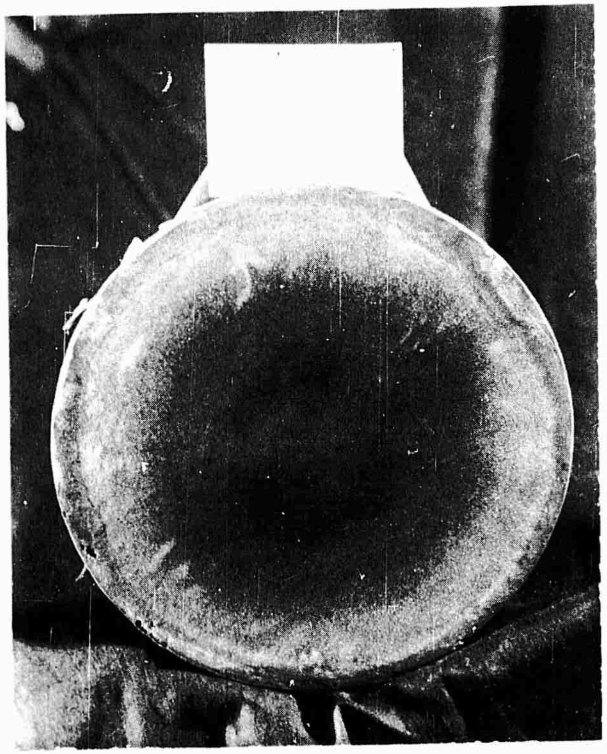

Fig. 2.23--Result of center-detonated, 4-lb/ft^3-urethane-attenuated, string-suspended test

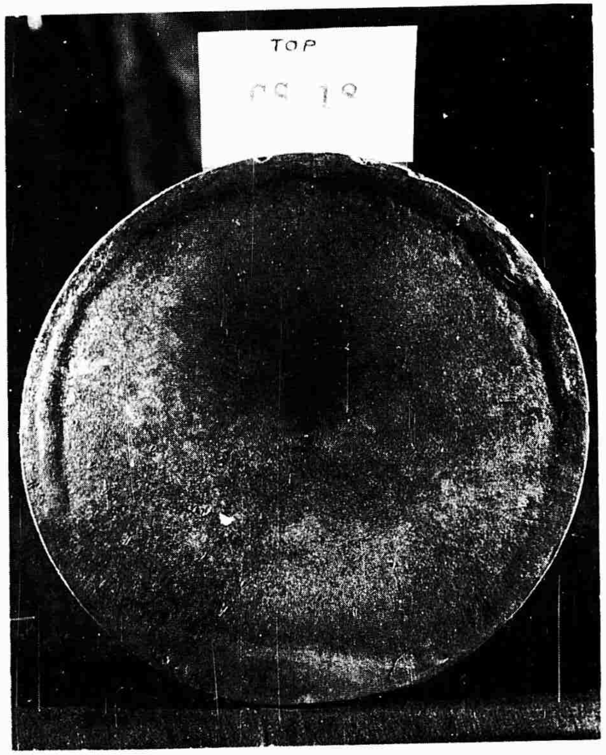

Fig. 2.24--Result of bottom-wick-detonated, 4-lb/ft^3-urethane-attenuated, string-suspended test

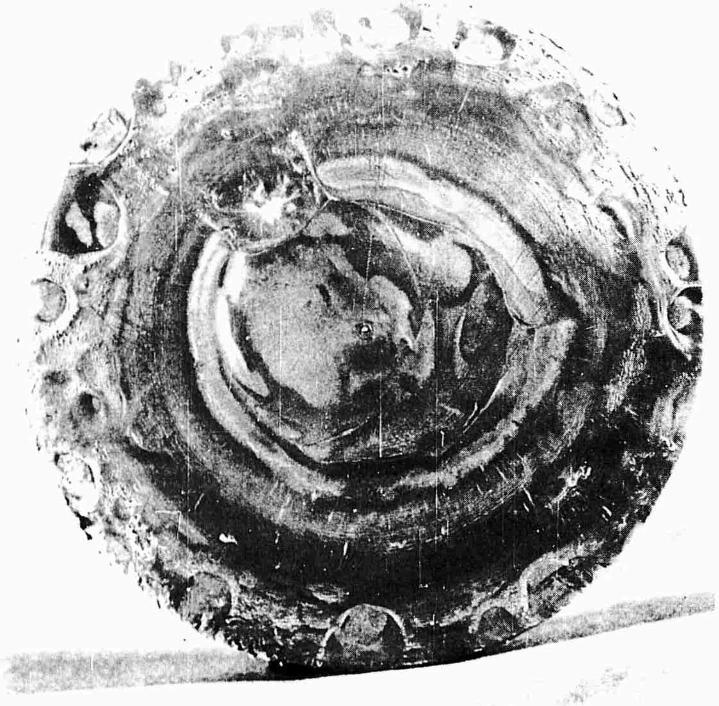

Fig. 2.25--Result of center-detonated, 4-lb/ft^3-Styrofoam-attenuated, string-suspended test

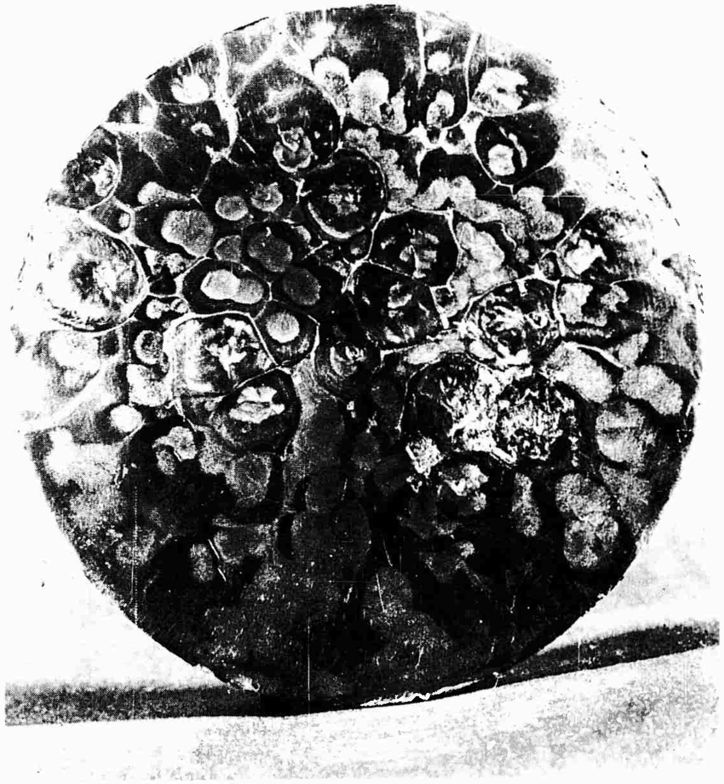

Fig. 2.26--Result of bottom-wick-detonated, 4-lb/ft^3-Styrofoam-attenuated, string-suspended test

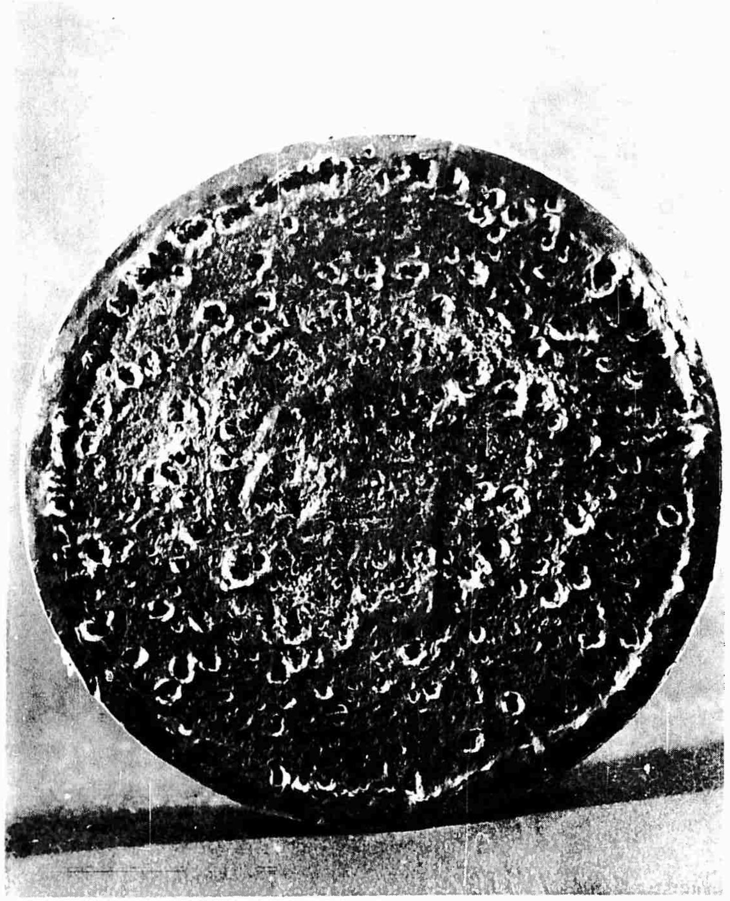

Fig. 2.27--Result of center-detonated, 2-lb/ft^3-Styrofoam-attenuated, string-suspended test

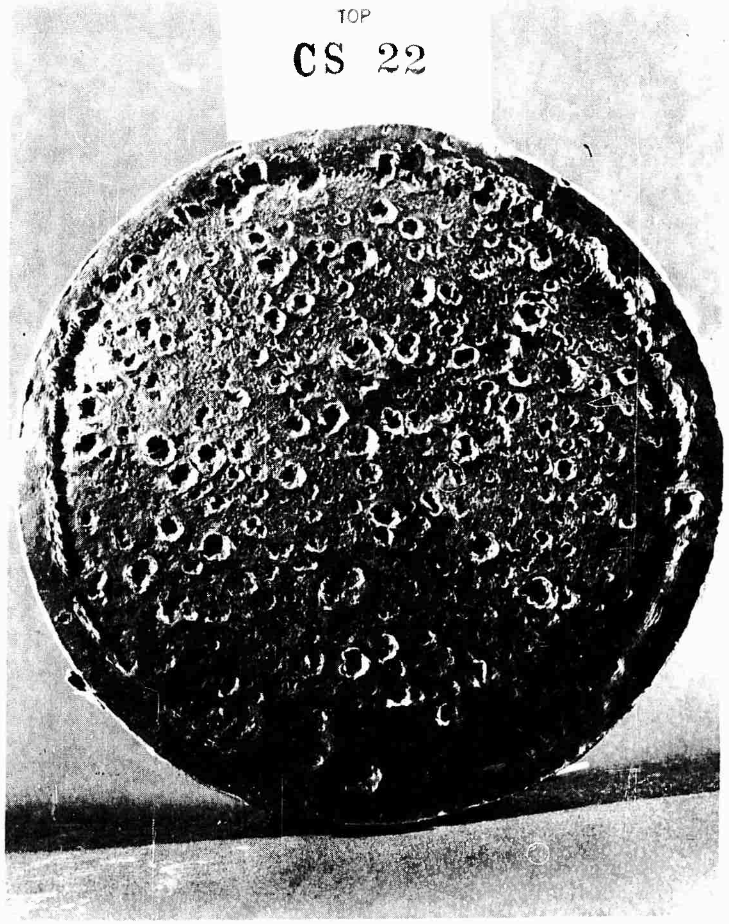

Fig. 2.28--Result of bottom-wick-detonated, 2-lb/ft^3-Styrofoam-attenuated, string-suspended test

timer very accurately marked the film at preset time intervals.

(U) The most desirable approach for obtaining reliable impulse data would have been to make both pressure-probe measurements and velocity measurements on each test plate. Since the very tight test schedule at the instrumented test bunker precluded this, the velocity-impulse tests were performed at the cable stand. The test setups at the cable stand were made to duplicate the setups at the test bunker so that correlation could be made with the previous pressure-probe test shots. The majority of experiments to date have been made with 8-in. -diam, 5/8-in. -thick steel plates. The plates were confined in an 8-in. -ID pipe, and 8-in. -diam, 8-in. -thick foam of varying densities was used for the attenuator. The sheet HE was then attached to the foam. The tests were confined in the pipe to minimize the edge effects and thus to simulate the results that would be expected with a larger-diameter test plate.

(U) Velocity measurements were taken on twelve 8-in. -diam test plates and on four 40-in. -diam test plates. The 8-in. -diam tests were confined, the 40-in. -diam tests were unconfined. A majority of the test setups that supplied the velocity data were made primarily for other purposes; however, most of the setups were compatible with the velocity-impulse requirements and provided an inexpensive and expeditious means for obtaining preliminary data. A summary of this preliminary data is shown in Fig. 2.29. Note that the velocity impulses and the pressure-probe impulses agree rather well for the lower density foam, but that there is quite a difference for the denser foam. The significance of this is not fully understood. However, the difference in total impulse measurements is not surprising since previous multiple pressure-probe tests have recorded impulse variations of comparable magnitude from probes located just inches apart on a test plate. In fact, the large variation in pressure-impulse measurements was the primary reason for initiating the velocity-impulse studies.

(U) Quite recently, provisions for the instrumentation required to obtain pressure-probe data have been completed at the cable stand so velocity data and pressure-probe data can be taken concurrently on each impulse-measurement test. Future experiments at this facility can thus be covered with both optical (for velocity measurements) and electronic (for pressure measurements) instrumentation.

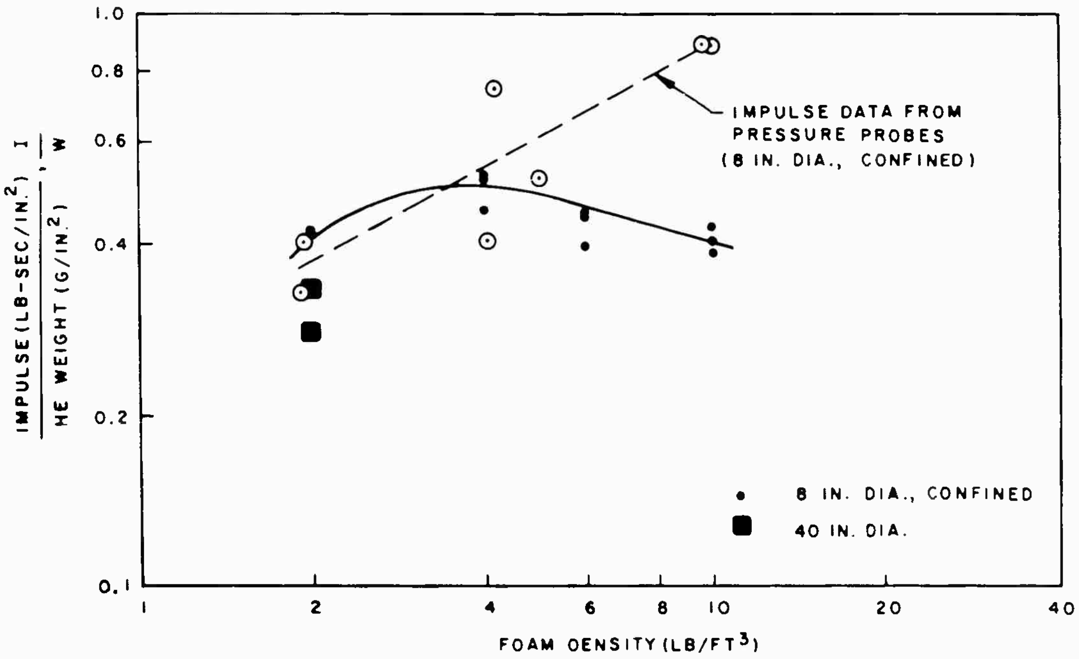

Fig. 2.29--Average impulse determined from velocity data

3. (U) HE RESPONSE TESTS

3.1. (U) RECOVERY-TECHNIQUE DEVELOPMENT

(U) Structural characteristics of various test specimens will be evaluated by dynamic loading (using sheet HE) during the succeeding phases of the response testing program It is important that recovery techniques which produce minimum extraneous effects be developed. The efforts to develop acceptable test-plate recovery techniques are described in this section.

(U) The cable stand shown in Fig. 3.1 was constructed at the Green Farm Test Site for use with specific tests requiring test-specimen recovery. This cable stand consists of a 3/4-in.-diam steel cable, ~500 ft long, that is supported at both ends by pipe structures to provide a mean cable height of ~12 ft above the ground. The cable stand was constructed on a 10 per cent grade to aid in decelerating the test specimens.

(U) A series of experiments was conducted to evaluate various methods of attaching test specimens to the cable stand. In these experiments, an 18-in.-diam, 1/4-in.-thick steel plate was subjected to a pulse of about 60,000 psi for 40 μsec, producing a plate velocity of about 400 ft/sec. The pulse was obtained with A-3 sheet HE and was attenuated through 2 in. of 2-lb/ft^3-density urethane foam in contact with the test plate.

(U) In conjunction with the primary experiments, type T-1 steel* was used in making a preliminary evaluation of welding techniques. In addition, the T-1 plate material was subjected to a small number of impulse loads and was then analyzed to determine if the structural characteristics were significantly affected.

(U) In the first test, integral eyes were machined on the periphery of the test plate, as shown in Fig. 3.2 A single steel cable, 3/16 in. in diameter, was spliced to one of the top eyes on the plate. The other end of the cable was attached to a piece of 1/2-in.-diam nylon line and the line was attached to the cable stand using a clevis as a slide. To decelerate the plate, one end of a 3/16-in.-diam steel cable was attached to a bottom eye on the plate and the other end to a piece of 1/2-in. nylon line which was

---

*Produced by the U.S. Steel Corporation.

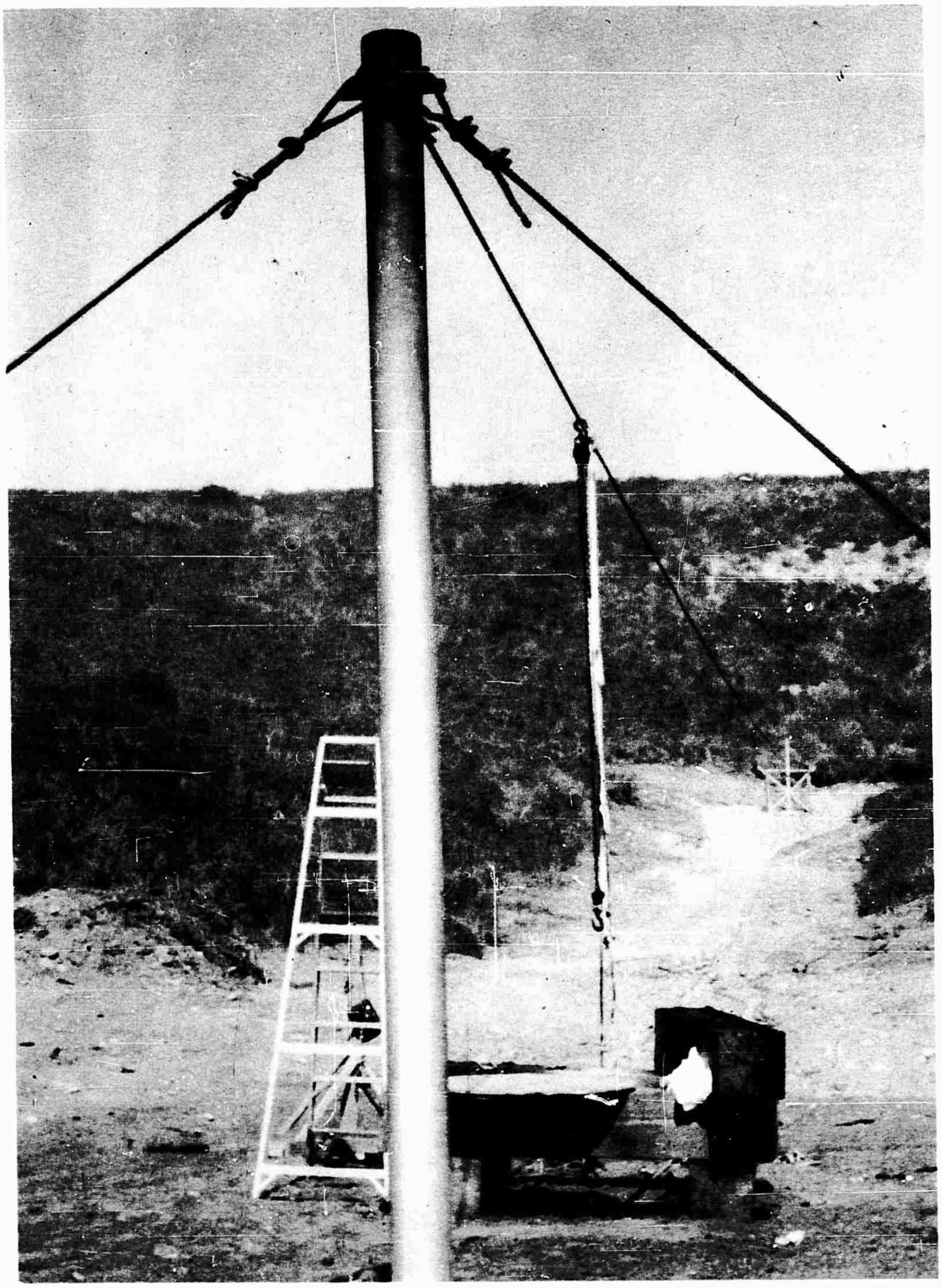

Fig. 3.1--Cable test stand

attached to a pair of drag chains. Two 100-ft sections of 1/2-in. chain, backed up by two 100-ft sections of doubled 1/2-in. chain, were used for the drag.

(U) The support assembly (cable harness assembly) failed during the test. Examination showed that the top cable-splice failed. Slight bending of the test plate occurred, but this was attributed to the plate's impacting a large rock upon ground contact.

(U) The second test setup used three 3/16-in.-diam steel cables attached to the top eyes of the test plate. These three cables were then attached to three 1/2-in. nylon lines that were attached to the cable clevis slide. Three eyes, fabricated from 1/4-in. T-1 plate stock, were welded to the bottom front face of the test plate and a 3/16-in.-diam steel cable was attached to each eye. The other end of each cable was attached to a 1/2-in.-diam nylon rope and the three ropes were attached to the drag chains. Again the support assembly failed, and again the failure occurred at the cable splices. It was noted that the welded eyes on the bottom of the plate remained intact.

(U) On the third test, the steel cables were replaced by three 1/2-in.-diam nylon lines which were attached with shackles to the three eyes on the top and to the three eyes on the bottom of the plate (see Fig. 3.3). These lines were then attached to the cable clevis slide and drag chain as for the previous tests.

(U) The shackles attaching the nylon line to the test plate failed during the test. The welded-on eyes were examined quite closely and all were found to be in good shape except one, which closer examination revealed that that particular weld exhibited poor penetration.

(U) On the fourth test, sets of paired eyes were welded to the front face of the test plate approximately 3/4 in. apart. Three pairs were welded to the top of the plate and three pairs to the bottom, as shown in Fig. 3.4. A 1/2-in.-diam stainless-steel bolt was used through each pair of eyes to provide large pick-up points for the harness of 1/2-in. nylon line. These lines were attached to the cable-stand slide and to the drag chains as in previous tests.

(U) On this test the bolts failed. The exact results of this test were not well defined because attachment parts were scattered over a large area of rough terrain, making it impossible to find all the parts. However, enough parts were collected to disclose two interesting facts. It was apparent that some of the bolts failed upon initial impulse from the test shot because of the large inertial loads resulting in part from large tolerance holes in the plate eyes. These failures occurred at the nut end of the bolt

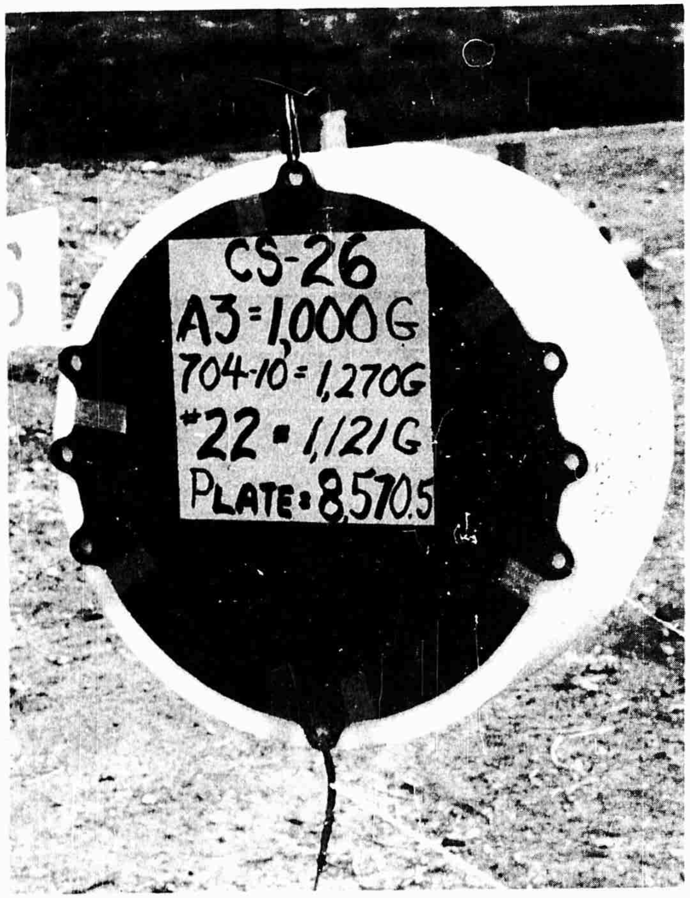

Fig. 3.2--Recovery test plate with machined eyes

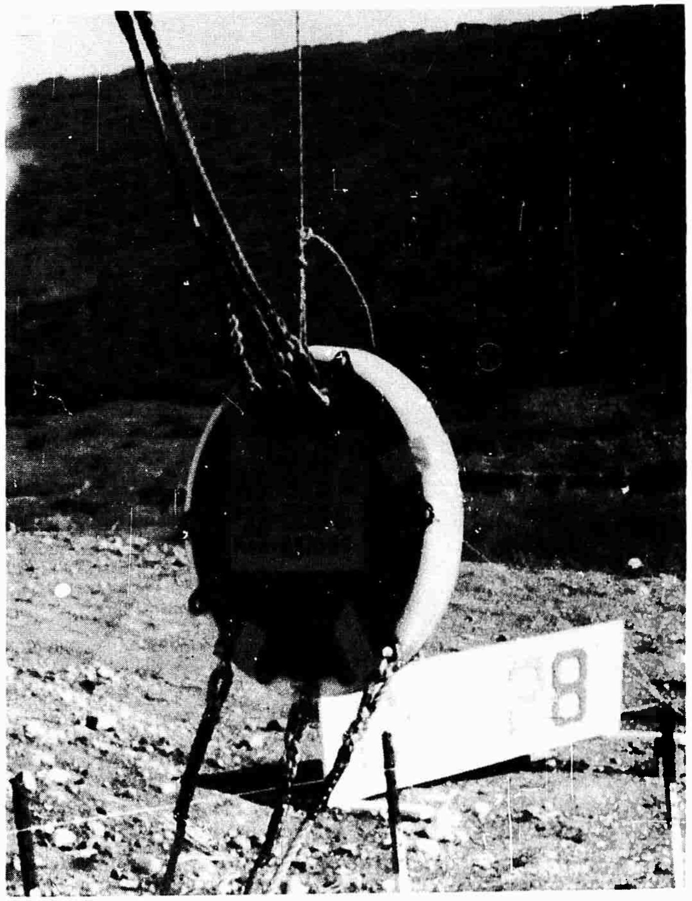

Fig. 3.3--Recovery test plate with welded eyes

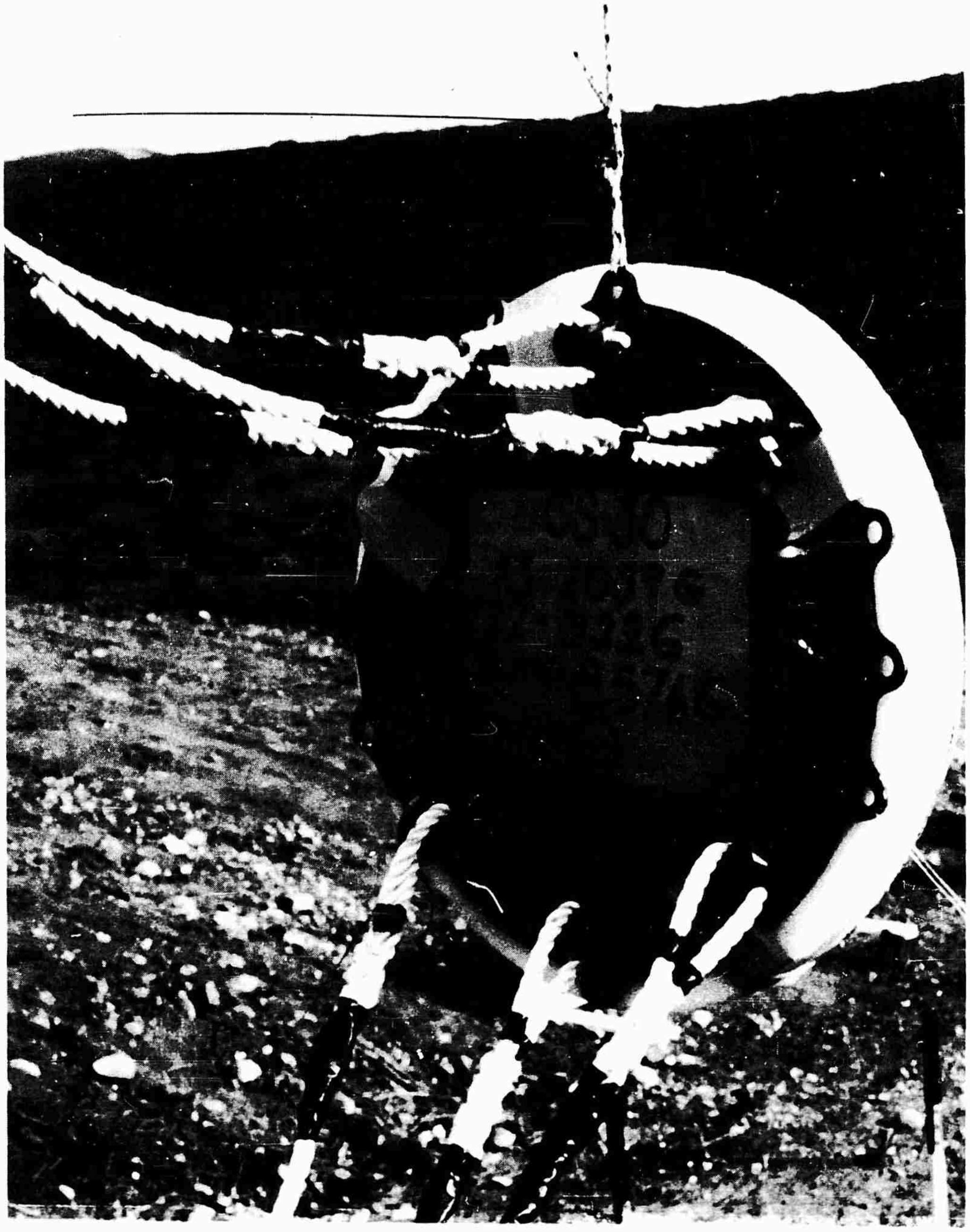

Fig. 3.4--Recovery test plate with doubled eyes

and were attributed to the mass of the nut. The bolts failed before they had an opportunity to contribute to the attachment scheme. It was also noted that the nuts were missing from some of the bolts that were still intact. A simple check verified that when the slack was taken out of the nylon attachment lines, and during their period of stretching, a spinning action was imparted to the bolts, causing the loss of some of the nuts.

(U) The same basic setup was used on the fifth test to verify some of the results obtained from the fourth test. During the previous four tests, it was noted that the clevis used for the cable slide was showing appreciable wear, indicating that considerable drag was being encountered. This caused concern over the possibility of damaging the main support cable on the cable stand. To alleviate this problem, a more complex cable slide was constructed. This slide, shown in Fig. 3.5, consists of a stainless-steel tube split down the middle and held together with stainless-steel strap clamps. A boxlike fitting was welded to the top of the slide tube to provide an attachment for the nylon line.

(U) On all previous tests, a double drag chain had been employed to slow the test plate after the shot. It was apparent that a double chain was not required, so a single drag chain was used for this fifth test to reduce the load on the plate attachments.

(U) The attachment bolts failed as on the previous test. A thorough inspection verified that the eye welds had survived with no noticeable effects as in all the previous tests. The new cable slide tube performed satisfactorily.

(U) The test-plate deformation throughout this test series became progressively worse from the repeated impact of the plate with the ground. It was therefore decided to retire this test plate and to cut a 1-in. strip from its center to study material physical characteristic changes.

(U) The sample strip was compared with a virgin piece of T-1 steel and the samples were tested for Rockwell hardness in the laboratory. Readings were taken at 1-in. spacings from the center of the test sample to its periphery, corresponding to the radius of the test plate. Three readings were taken at each location, with all readings agreeing quite closely. No detectable differences were noted in the hardness of the test sample compared to the control sample. Although definitely not conclusive, this simple test does indicate that no appreciable physical change occurred in the T-1 test plate after being subjected to five HE impulses.

(U) A new test plate was fabricated for the sixth test. Eyes were made for the plate by bending 1/2-in.-diam steel rod into U shapes. Slots were cut in the plate so that the bent rods could be inset ~3/4 in. in from

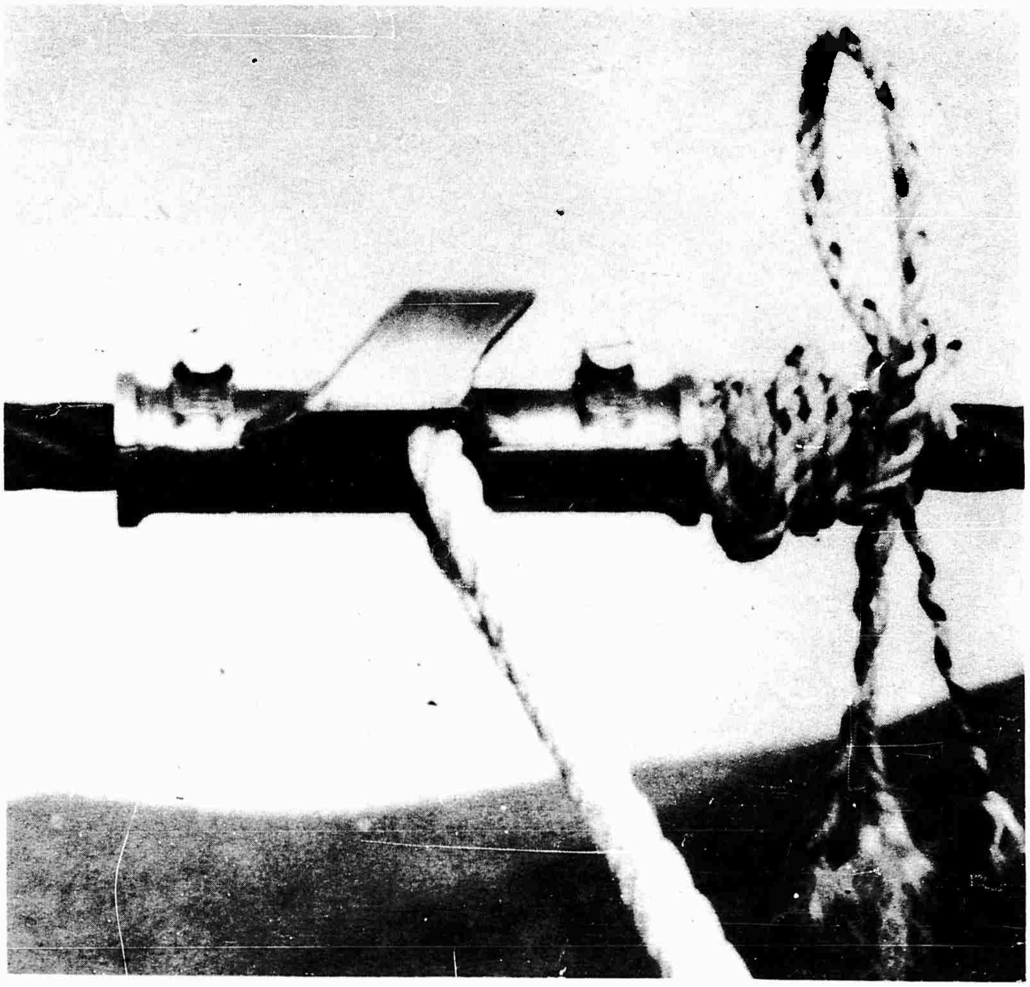

Fig. 3.5--(U) Cable slide for specimen recovery at cable stand

the periphery of the plate and welded in place. The eyes were located 30° apart; three on top and three on the bottom. A 1/2-in.-diam nylon line was used to assemble the harnesses. The top harness consisted of a line from each eye terminating in a double line connected to the cable-slide tube. The bottom harness was identical and connected to the drag chain. This attachment system, shown in Fig. 3.6, functioned quite well during the test. All components remained intact when the test plate traveled 190 ft down the cable.

(U) The four tests of the plate with welded-on eyes indicated that welds on T-1 steel demonstrate high structural capabilities for shock loading if the procedures recommended by the manufacturer are followed quite closely. The basic physical characteristics of T-1 steel are not noticeably changed after being subjected to a small number of high-magnitude, short-duration impulses.

(U) A satisfactory method has been found for recovering scaled test plates of sizes up to the physical limits of the cable test stand. This recovery scheme minimizes the outside physical perturbation on the test sample and permits an accurate assessment of the physical changes caused by the test shot.

3.2. (U) SCALED-PLATE TEST

(S) The majority of the engineering tests using high explosives at the Green Farm Test Site have been to develop techniques for obtaining impulse shapes compatible with the requirements for testing ORION engine components. This work has progressed to the point where it is believed that a representative impulse could be given to a scaled pusher plate (up to 1/17 scale of the pusher for the 4000-ton vehicle) with sufficient accuracy to observe the structural behavior of the plate. The test described in this section is the first of a series which will be conducted to determine the structural characteristics of a scaled pusher plate and to evaluate methods for plate fabrication and for attaching various items to the pusher plate. Some of these tests will be conducted on a repetitive basis to determine the multiple-impulse load effects on the pusher plate.

(S) In the first test of the series, a 5-ft-diam, 1/4-in.-thick test plate was used. The dimensions of the plate correspond closely to 1/17-scale pusher plate, neglecting the taper. The 1/4-in. thickness corresponds to the average scaled thickness of the tapered pusher. This test plate was constructed from Type T-1 steel, which is currently considered a logical choice of material for the pusher. The test was conducted at the cable stand to allow test-plate recovery. Two different densities of foam were used to obtain the desired impulse. A layer of 2-in.-thick, 2-lb/ft^3-density

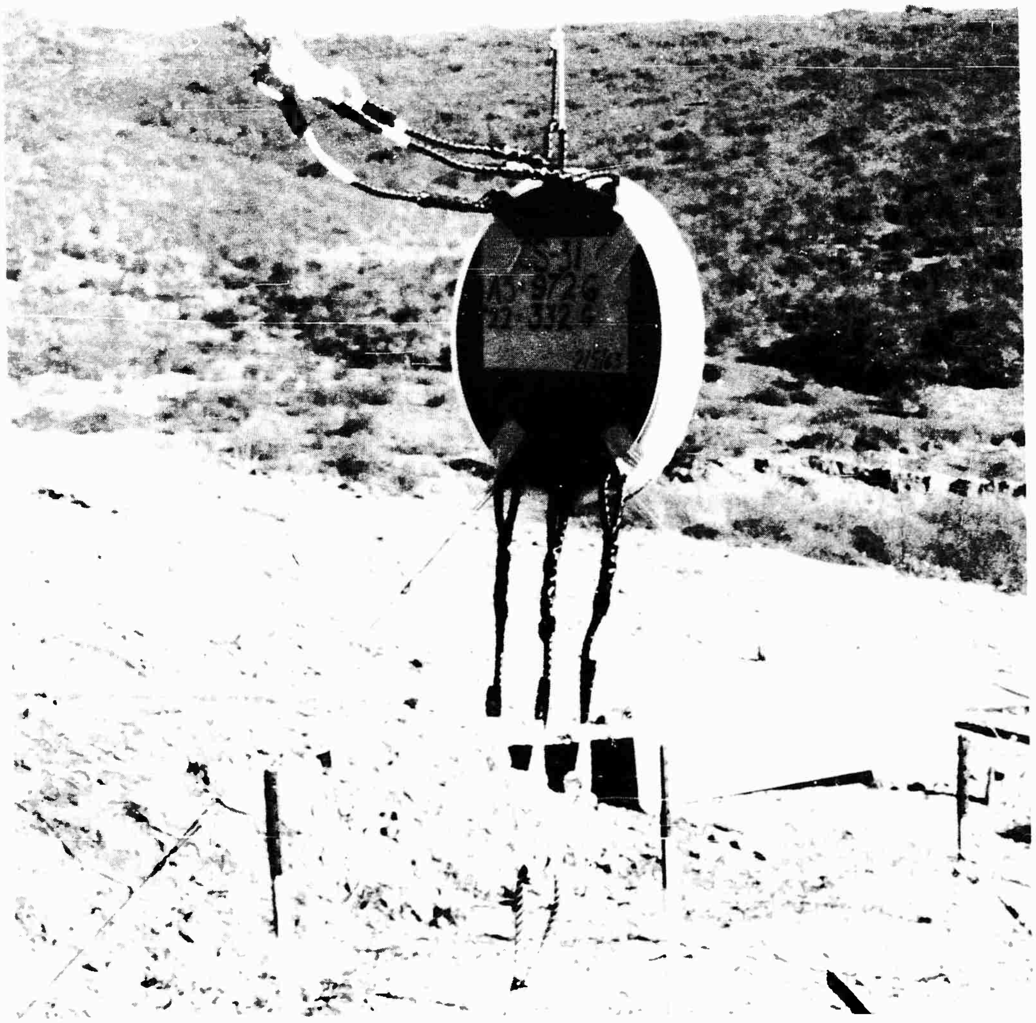

Fig. 3.6--(U) Cable-stand-recovery test setup

foam was used adjacent to the test plate to attenuate the pulse to the desired level. This layer of foam was backed with a layer of 10-lb/ft^3-density foam that was tapered from 2 in. in the center to a knife edge at the periphery. The A-3 sheet HE was then attached to the back of the tapered layer of foam and was center-detonated (see Fig. 3.7). The tapered layer of foam was used to compensate for the radial detonation propagation time of the HE sheet, thus assuring that the impulse arrival time would be essentially uniform over the entire plate surface. The test assembly was attached to the cable stand by threading 1/2-in.-diam nylon lines through eyes welded around the periphery of the test plate and attaching the lines to the cable-stand slide. The bottom eyes on the plate were attached to drag chains. A Wollensak Fastax camera running at 1,000 frames/sec was used to record the plate velocity.

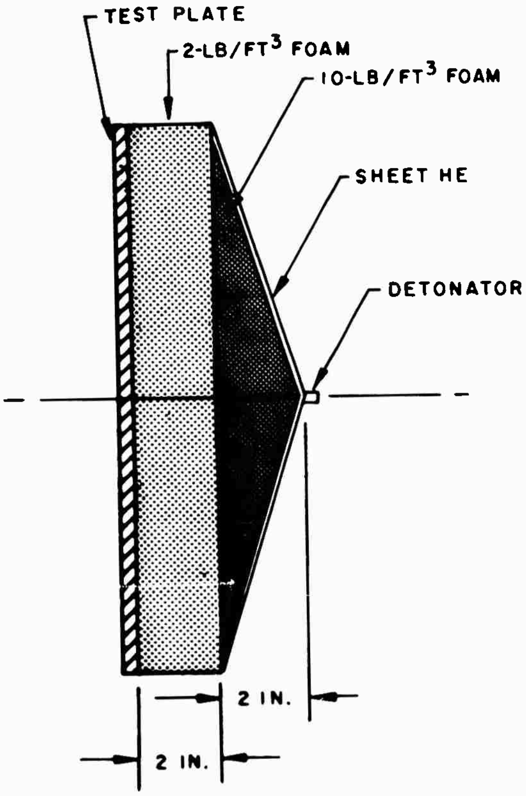

Fig. 3.7--(U) Scaled-plate test configuration

(U) Immediately after the HE was detonated, the test plate broke loose from the recovery harnesses, traveled about 500 ft in free flight, and landed on the side of the hill adjacent to the cable stand. As the fall of the test plate was cushioned by landing in sagebrush and soft earth, the plate was not damaged or deformed.

(C) The reason why the recovery system had failed so completely was not at first apparent. However, after the recording film was analyzed, it was determined that the test plate was traveling at a rate of ~500 ft/sec—about twice the desired velocity. This means that the impulse was high by a factor of two, and thus the energy to be absorbed in the recovery system was a factor of four higher than anticipated.

(C) It is of special interest to note that the test plate, scaled from actual pusher dimensions, remained perfectly flat and was not distorted in any way after being subjected to a scaled impulse of twice the magnitude anticipated for use with the ORION vehicle. The effect of repetitive impulses will be checked on future tests.

(U) One possible cause of the high impulse could have resulted from the use of the 10-lb/ft^3-density foam in series with less dense foam, a condition similar to that discussed in Section 2.1.6. The arrival time of the pulse would have been uniform over the plate surface area; however, the impulse could have varied in intensity as a function of the mass of foam. This, in turn, would have resulted in the center of the test plate receiving a much higher impulse than the edge. One fallacy with this theory, however, is that with the mass distribution of the foam used in this test, the distribution impinging on the test plate should have varied enough to deform the plate. This phenomenon will be analyzed from future tests.

3.3. (U) PLATE-ATTACHMENT TEST

3.3.1. (U) Test Parameters

(C) During the testing of a scaled-down model of a toroidal shock absorber, it was observed that the clamping rings used to attach the shock absorber to the test plate became loose after a few successive explosive impulses. The clamping-ring attachment screws turned or stretched during the test. An analysis was made of this possible stretching phenomenon; however, an idealized geometry was assumed and the elastic and plastic deformation effects were ignored, making the results inadequate and inconclusive. It was therefore decided to test various attachments to determine the cause of screw-loosening, the effects of repeated shock loads, and the safety margin provided by the plastic deformation of the screw. The results of this test are summarized here and are described in detail in Ref. 3.

(C) The steel test plates used were 8 in. in diameter and 5/8 in. thick. In the first test configuration, three 5/16-in.-thick steel bars of 1 in., 1-1/8 in., and 1-1/4 in. width were tested. Each bar was attached to the plate by three 3/8-24 NF high-strength steel screws torqued at the same level per bar but at a different level on each bar. The screws holding the 1-1/8-in. wide bar were drilled to reduce their cross section by half. In the second configuration, only 1-1/8-in.- wide bars were used. The attach screws were modified to provide a smaller cross section, as shown in Figs. 3.8 and 3.9. The third test configuration was a bracket attachment that was envisaged for holding the pusher plate to be tested during the proposed nuclear test.(4) In this application the screws attaching the bracket to the test plate were supposed to fail to facilitate deployment of a recovery system.

(C) All test plates were accelerated to ~250 ft/sec by sheet HE separated from the test plates by 2 in. of light foam (2 lb/ft^3). The HE sheet was 8 in. in diameter and had a thickness corresponding to a weight of 4 g/in.^{2} (A-4). The peak pressure pulse imposed on the test plates was ~100,000 psi and lasted 25 to 30 μsec. This pulse is more severe than the current pulse system design specifies; however, it corresponds to a standard practice of testing structural components to higher than normal operating loads.

(U) For testing the first configuration, the plates were taped in a vertical position on top of a post. After the explosion the plates were stopped when they impacted the ground about 100 ft away. Configurations two and three were tested with a cannon, shown schematically in Fig. 3.10, and the plate recovery system is shown in Fig. 3.11.

3.3.2. (U) Test Results

(U) Measurements were made before and after each test to establish the screw length and height above the test plates, their installation torques, and their angular position. After the test, the screws were retightened to their original torque value and the amount of rotation required was then recorded. The following results were obtained:

1. All screws were loosened by varying degrees. The screws torqued to highest initial values remained the tightest after the test. None of the screws was completely loose. The bar held by the modified screws (half cross section) could be moved freely.

2. The screw rotation caused by the test shot was either very small or nil, but retorquing the screws to the pre-test values required appreciable angular rotation.

3. The change in length of the standard screws was not detectable, but the modified screws (half cross section) had lengthened 0.002 in. to 0.003 in.

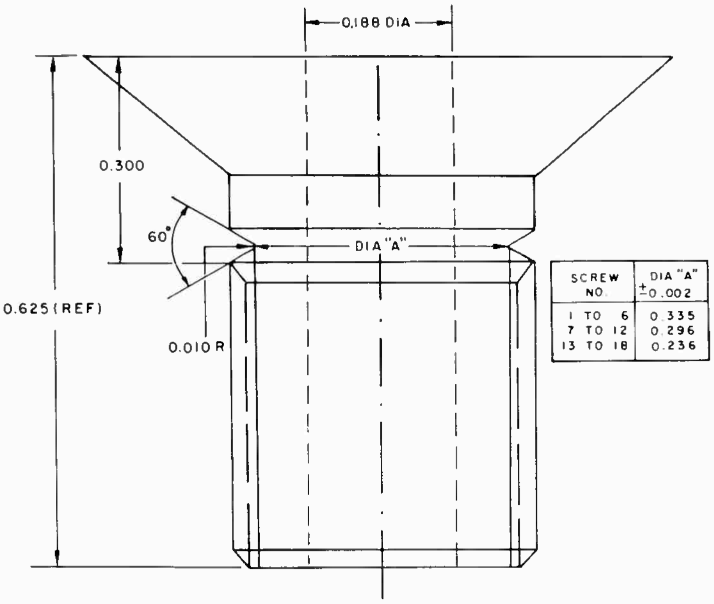

Fig. 3.8--Modified V-notched screw

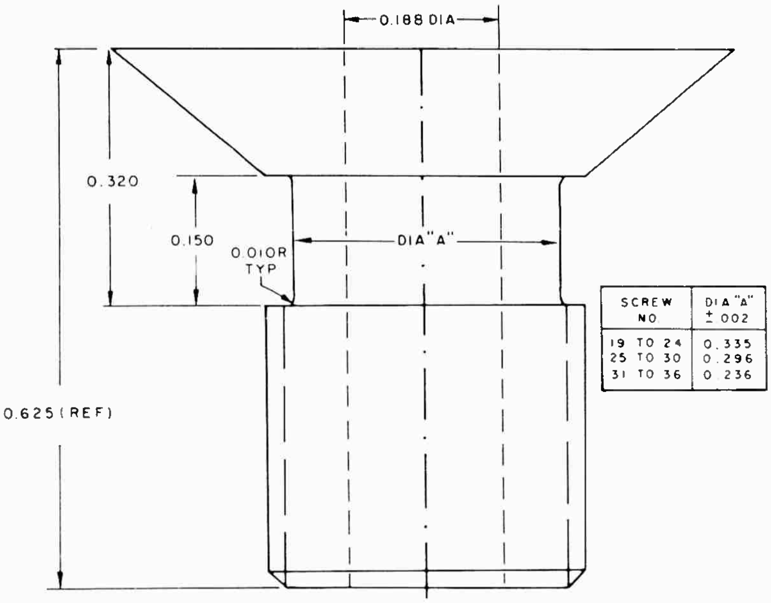

Fig. 3.9--Modified U-notched screw

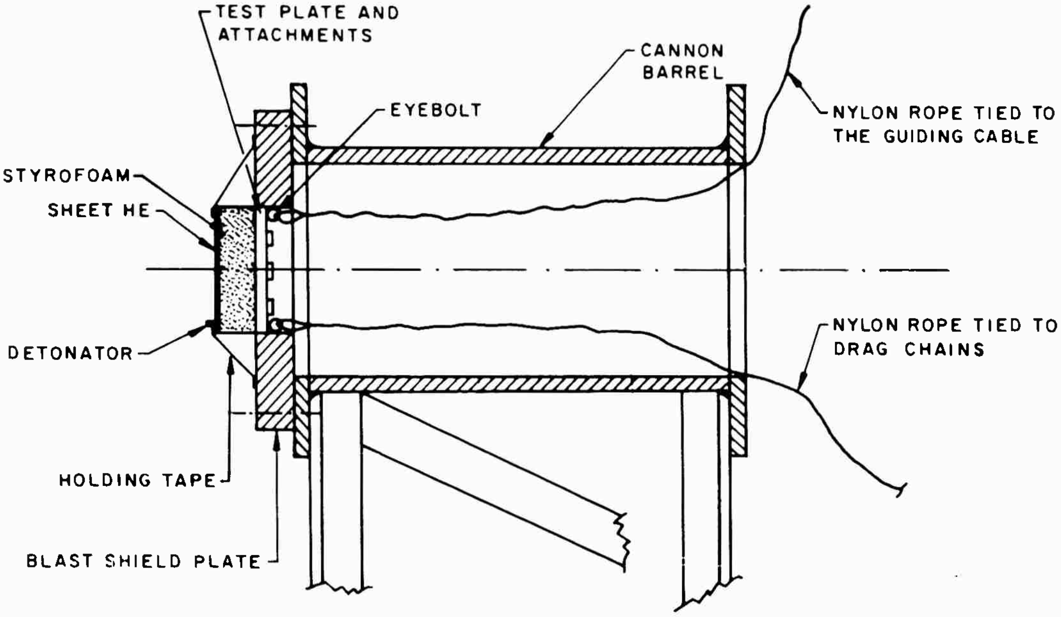
TEST PLATE AND ATTACHMENTS
CANNON BARREL
EYEBOLT
NYLON ROPE TIED TO THE GUIDING CABLE
STYROFOAM
SHEET HE
DETONATOR
NYLON ROPE TIED TO DRAG CHAINS
HOLDING TAPE
BLAST SHIELD PLATE

Fig. 3. 10--Section of test cannon

Fig. 3. 11--Plate recovery system

4. The bar width had no detectable effect.

5. The initial screw torque had an appreciable effect on screw tightness after exposure to the test shot.

6. The modified screws, which should have broken, were intact, but their original torque was completely gone.

The detailed results are tabulated in Table 3.1.

(U) The loading imposed on the screw is apparently a decreasing function of the amount of elastic and/or plastic deformation that the screw can withstand. As this effect appears to be significant, the influence that plastic deformation has on the shock resistance of screws was investigated.

(U) The tested plates underwent significant bowing, or "dishing," as illustrated in Fig. 3.12. This condition is believed to have been caused by lack of flatness of the HE sheet or from the marginal momentum loss at the plate edge. Since the attenuator foam between the steel plate and the HE sheet was not rigid and the HE pancake was taped to the foam which compressed the edge, the center of the HE sheet was farther from the steel plate than the edge. Therefore, the impulse at the test-plate center was different from that at the edge. Another factor is that the steel used for the plate had a relatively low yield strength. Consequently, in the second test series rigid Styrofoam was used for the attenuator and the test plates were made of Type T-1 steel, which has a yield strength of 90,000 to 100,000 psi.

(U) The second series of tests was made to confirm previous data and to obtain additional information on the influence of plastic deformation of the screws. The cross section of the screws was decreased by 1/4, 1/2, and 3/4 in two different ways. All screws were first drilled longitudinally and then notched on the "grip;" half were V-notched (see Fig. 3.8) and half were U-notched (see Fig. 3.9). Two bar-plate assemblies with 1-1/8-in.-wide bars and one bracket-plate assembly, as shown in Figs. 3.13, 3.14, and 3.15, were used in this series. All plates received the same impulse ($\sim$100,000 psi lasting 25 to 30 μsec), with the following results:

1. Only the V-notched screws having 1/4 of their original cross section broke. All other screws remained intact.

2. All screws on the bar plates were loose except the shallowest V- and U-notched screws, which still retained a residual torque.

3. The V-notched screws that had 3/4 and 1/2 of their original cross section and were used to fasten the two brackets were loose but did not break. (It was anticipated that the 1/2 cross-section screws would break.)

Table 3.1

RESULTS OF TESTS ON SCREWS
(One Shot)

Screw No.	Screw Length (in.)		Original Torque (ft-lb)	Residual Torque (ft-lb)	Screw Rotation (degrees)	Total Screw Rotation to Original Torque (degrees)
	Before	After				
Three steel bars 1 in., 1-1/8 in., and 1-1/4 in. wide attached to plate[*]						
A	0.6430	-----	5	2	-3	20
B	0.6474	0.6678	5	0	0	15
C	0.6438	-----	5	2	-4	10
D	0.6426	0.6423	20	0	0	15
E	0.6474	0.6475	20	0	-2	40
F	0.6475	-----	20	6	-6	20
G	0.6460	0.6465	30	6	-4	25
H	0.6459	0.6447	30	8	0	25
I	0.6409	0.6414	30	12	0	25
Three steel bars 1-1/8 in. wide attached to plate[†]						
J	0.6412	-----	5	0	0	10
K	0.6404	0.6400	5	0	0	10
L	0.6447	0.6450	5	0	0	10
α	0.6418	0.6438	18	0	9	40
β	0.6439	0.6453	18	0	Too loose	55
γ	0.6412	0.6420	18	0	Too loose	30
M	0.6431	-----	30	0	4	25
N	0.6393	0.6395	30	0	5	50
O	0.6446	-----	30	2	2	35
Bracket attached to plate[**]						
P	0.6435	-----	5	2	3	10
Q	0.6449	-----	5	0	Too loose	20
R	0.6435	-----	5	2	2	15
S	0.6436	-----	20	5	2	30
T	0.6462	0.6460	20	0	Too loose	40
U	0.6414	-----	20	2	5	30
V	0.6420	-----	30	10	--	--
W	0.6421	-----	30	6	0	35
X	0.6446	-----	30	6	5	40

[*] Dishing deformation of plate was from 0.025 in. to 0.035 in.

[†] Dishing deformation of plate was from 0.050 in. to 0.068 in.

[**] Dishing deformation of plate was from 0.050 in. to 0.065 in.

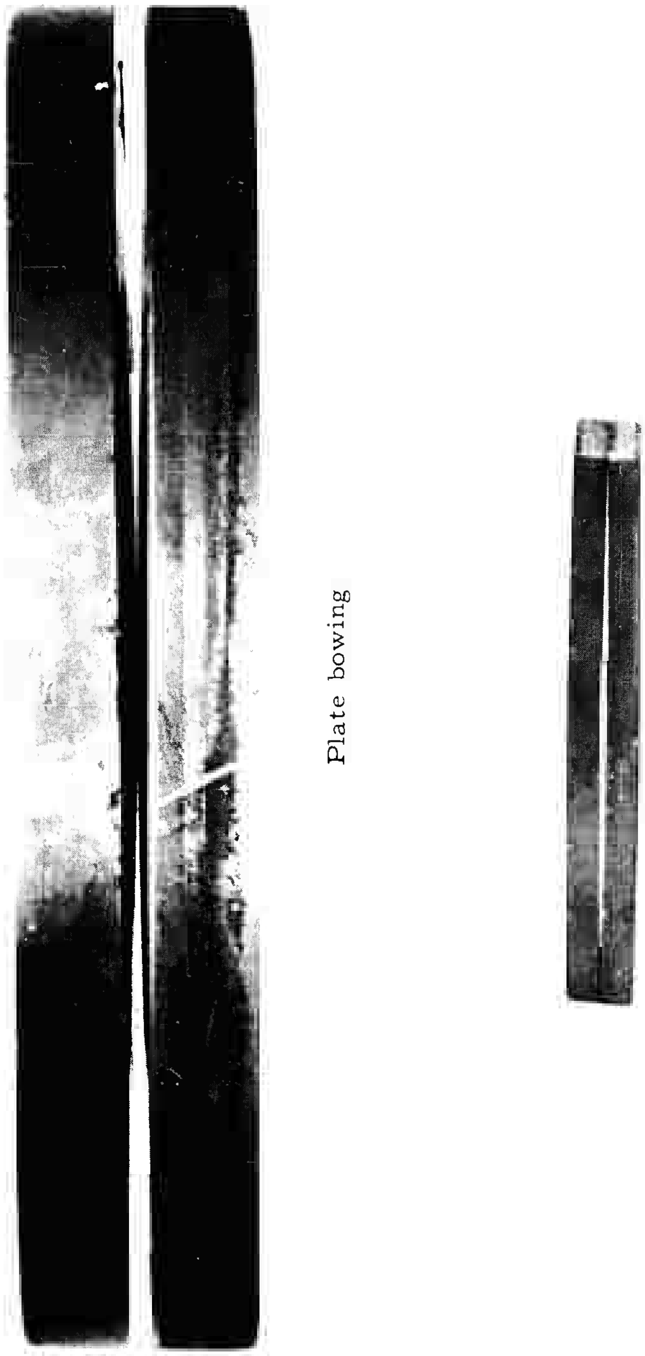

Plate bowing

Bar bending

Fig. 3.12--Plate deformation after first test-series shot

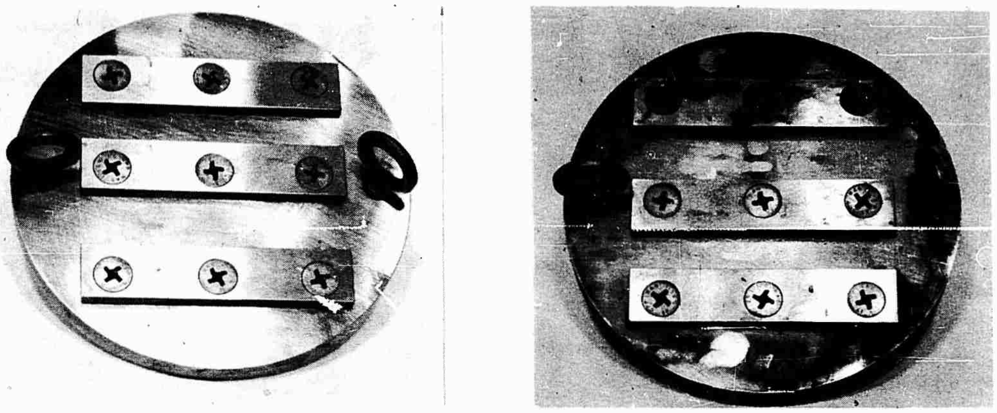

Before After

Fig. 3.13--Bar plate No. 1 before and after the second test series shot

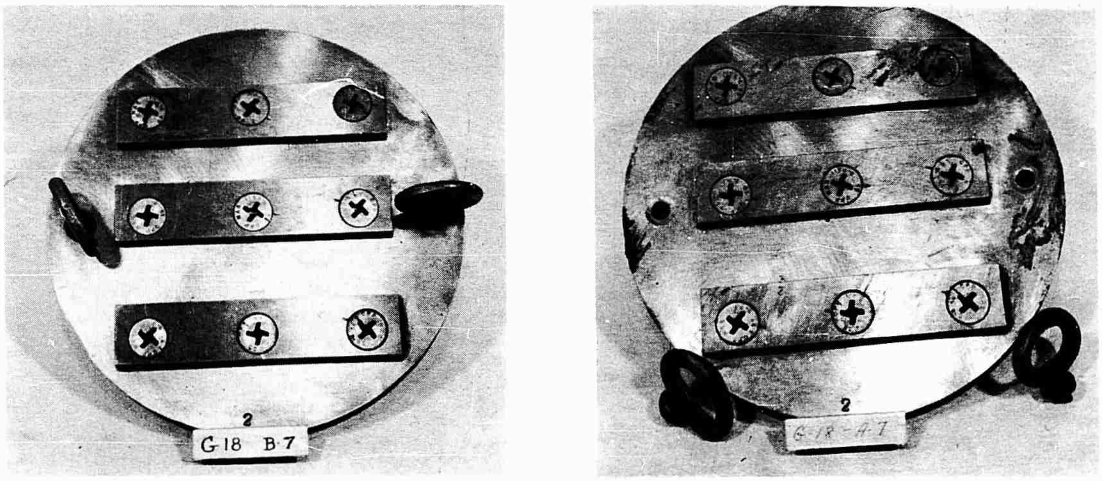

Before After

Fig. 3.14--Bar plate No. 2 before and after the last shot of the third test series

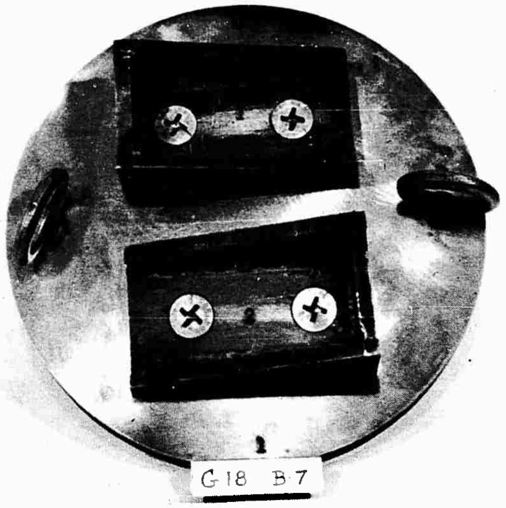

Before

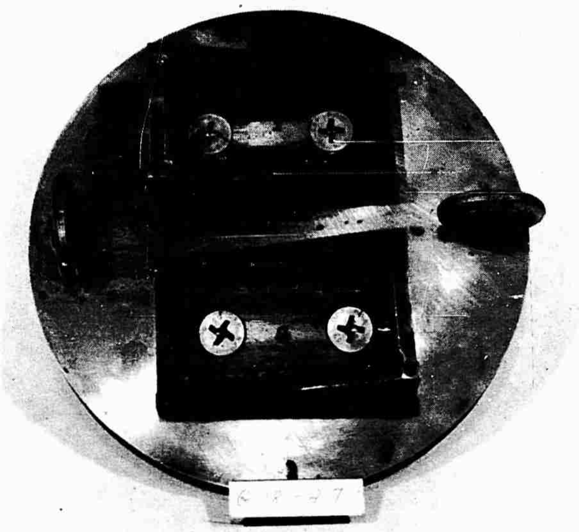

After

Fig. 3.15--Bracket plate before and after the last shot of the third test series

4. The length increase of the V-notched screws was negligible (less than 0.001 in.), but the length increase of the 1/4 cross-section U-notched screws varied between 0.008 and 0.010 in.

5. The screw rotations caused by the test shot were small, but retightening the screws to the original torque required an appreciable rotation.

The tabulated results are given in Table 3.2.

(U) This series of tests indicated that the plastic deformation of the screws relieved the stress on the plate-bar joint.

(U) A third test series was initiated to investigate the behavior of standard screws under repeated shock-loading. The two plate-bar assemblies and the plate-bracket assembly were again used, since the amount of dishing caused by the second test series was negligible. Prior to the test all screws were torqued to fixed values. Half of them were retightened to the original torque after each shot; the other half were retorqued only after they became noticeably loose. The three plates were submitted to impulses of the same magnitude as those used in the previous tests. The torque and angular position of the screws was measured and recorded before and after each shot. No attempt was made to lock the screws since the loosening was not caused by screw rotation. The screws were torqued to three different initial torque levels: 240 in.-lb, 300 in.-lb, and 360 in.-lb.

(U) The results of the seven test shots of this series are summarized here:

1. Only one screw (with a 300 in.-lb torque) was loose after the first shot.

2. All screws not retorqued after the first shot became loose after the second shot.

3. Retorquing the screws that loosened after any one shot did not keep them from loosening after two consecutive shots.

4. The screws holding the brackets, which were heavier than the bars, loosened the most. The amount of loosening is determined by total screw rotation to attain the original torque.

5. The amount of loosening increased with the higher torquing level. This is shown by the curves of Fig. 3.16. The total screw rotation has a tendency to level off after a few shots.

Table 3.2

RESULTS OF TESTS ON SCREWS AFTER MULTIPLE SHOTS

Screw No.	Notch Type	Length (in.)		Original Torque (ft-lb)	Cross Section (in.^{2})	Residual Torque (ft-lb)	Screw Rotation (degrees)	Total Rotation to Original Torque (degrees)
		Before	After					
Bars 1-1/8 in. wide attached to plate with V-notched screws								
1	v	0.6221	0.6222	25	0.0602	4	-4	55
2	v	0.6216	0.6222	25	0.0602	1	-6	55
5	v	0.6220	0.6217	25	0.0602	5	-7	55
7	V	0.6215	0.6220	15	0.0377	0	-10	50
8	V	0.6227	0.6226	15	0.0377	0	-11	50
9	V	0.6214	0.6224	15	0.0377	0	-10	50
13	**V**	0.6224	Broken	10	0.0156	0	Broken	Broken
14	**V**	0.6220	Broken	10	0.0156	0	Broken	Broken
15	**V**	0.6223	Broken	10	0.0156	0	Broken	Broken
Bars 1-1/8 in. wide attached to plate with U-notched screws								
19	u	0.6225	0.6221	25	0.0602	1	-2	55
20	u	0.6221	0.6222	25	0.0602	6	-3	55
21	u	0.6218	0.6216	25	0.0602	12	-3	55
25	U	0.6220	0.6224	15	0.0377	0	-9	50
26	U	0.6224	0.6226	15	0.0377	0	-7	50
27	U	0.6224	0.6228	15	0.0377	0	-2	45
31	**U**	0.6217	0.6305	10	0.0156	0	-4	40
32	**U**	0.6217	0.6297	10	0.0156	0	-6	40
33	**U**	0.6215	0.6296	10	0.0156	0	-6	40
Brackets attached to plate with V-notched screws								
4	v	0.6215	0.6232	30	0.0602	0	-5	55
6	v	0.6215	0.6217	30	0.0602	0	-7	55
10	V	0.6221	0.6227	20	0.0377	0	-10	45
11	V	0.6215	0.6258	20	0.0377	0	-9	45

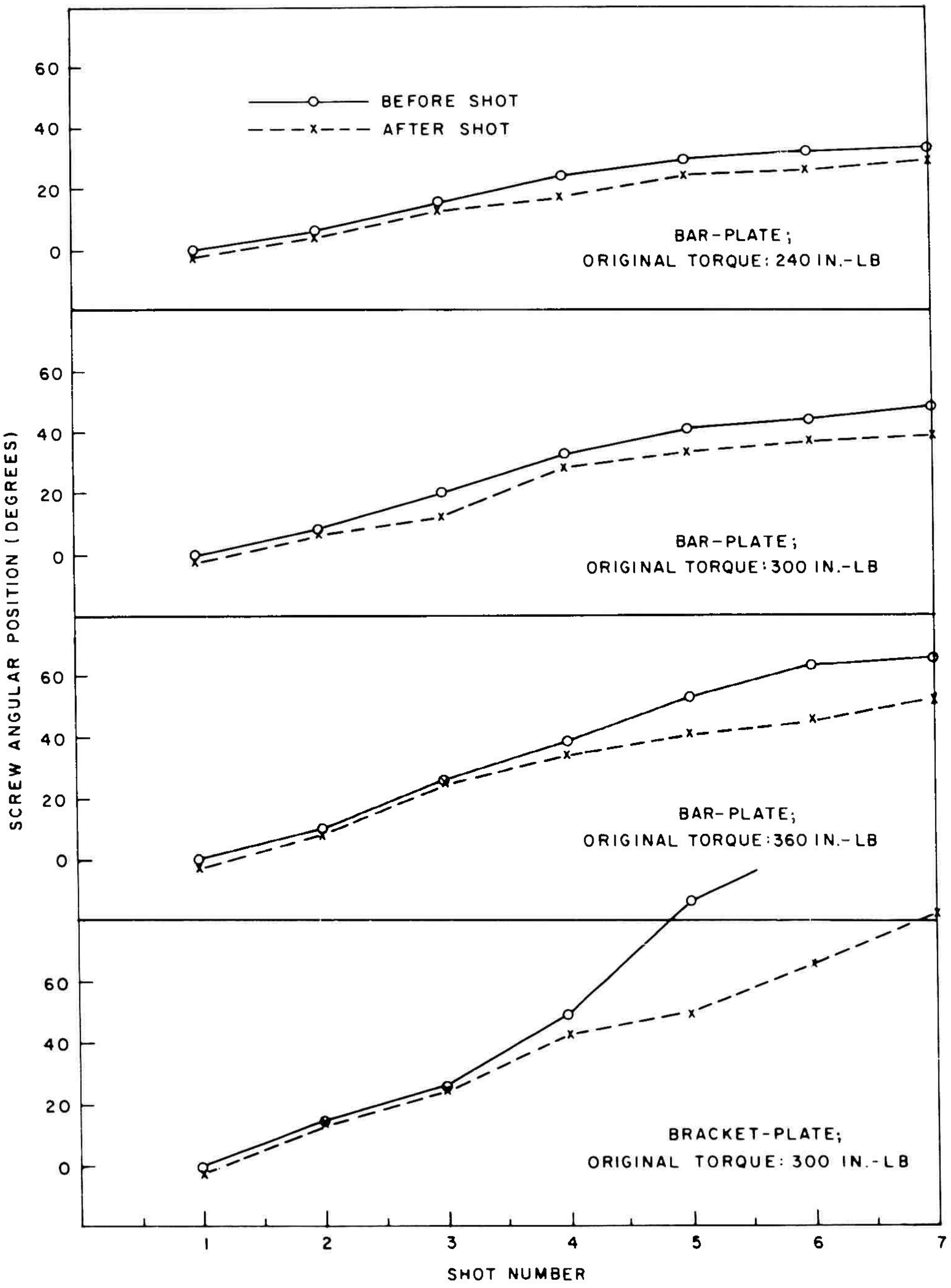

Fig. 3.16--Screw angular position before and after shot (retorqued to original torque)

6. The length increase of the screws varied between 0.003 to 0.005 in. Because of the screw-head deformation, it was not possible to determine where the increase occurred. The screw head was no longer flat and had deformed several thousandths of an inch.

7. Half of the eyebolts were broken after the second shot. These had a 5/16-18 NC thread. They were flattened considerably as shown in Fig. 3.14.

(U) When plates with screw attachments are subjected to dynamic loads, plastic deformation of the screws and the attachment prevents the screws from breaking. Plates subjected to a single impulse do not present attachment problems. However, if the plate and attachments are to be repeatedly shock-loaded, attaching hardware to the plate with screws, bolts, or rivets presents difficulties. Design studies eliminating the use of such parts are being made.

4. (U) STATIC LOADING TEST

(S) Preliminary theoretical work on the pusher for the ORION vehicle has indicated that significant edge compressive stresses may be produced by a mismatch of impulse to pusher mass per unit area. The degree of impulse mismatch is primarily a function of the pulse-system placement and aiming error. The imposition of close tolerances in pulse-system placement, relative to the moving pusher, requires a very complex control system. Therefore, some compromise has to be reached between the complexity of the control system and the weight of the pusher plate. The tendency of the plate edge to buckle under compressive loads (particularly steel with its low thickness-to-diameter ratio) could pose a significant design problem. The problem of edge buckling is further aggravated because arbitrary edge stiffening cannot be incorporated on the plate.* Therefore, a set of very simple tests was conducted to determine the effect of the properties of various structural materials on the modes of edge buckling.

(U) A series of tests was conducted to obtain preliminary data on the bending characteristics of plates of various thicknesses. Three materials were tested: steel (Type 1018), aluminum (6061-T6), and phenolic (paper type). A rather rudimentary setup was used for the test; therefore, no precise measurements were attempted. Only generalized observations and comparisons were made.

(U) The tests were conducted using a Baldwin Universal Testing Machine to supply the required forces. Fourteen 16-in.-diam flat test plates were fabricated for testing: three 0.049-in.-thick steel plates, three 0.074-in.-thick steel plates, three 0.100-in.-thick aluminum plates, three 0.187-in.-thick aluminum plates, and one 0.181-in.-thick phenolic plate. Rubber pads, 2 ft by 2 ft square and totaling 3 in. in thickness, were placed under the specimen tested and 10-in.-diam rubber discs were placed between the test specimen and the compression head of the testing machine. An 8-in.-diam compression head was used for the first series of tests. The test setup is shown in Fig. 4.1.

(U) The tests were performed as follows. The load on the test specimen was slowly increased until peripheral buckling was observed and

---

*(S) The plate is designed so the taper (pusher mass per unit area) varies with radius to match the radial distribution of the expected impulse. The addition of edge stiffening would add mass at large radii and disrupt this design feature.

the applied pressure was recorded. The pressure was then increased and measurements were taken at various pressure increments to record the magnitude of peripheral deflection as a function of the load applied. The pressure was then increased sufficiently to assure that the test specimen was permanently deformed. The amount of permanent deformation was recorded as a function of the total load applied. Two plates of each type were tested. The test data for each type were in such good agreement that it was decided to deform the third plate of each type, but with a smaller-diameter (6.4-in.) compression head. The peripheral buckling pattern that the plate will take is a function of the area subjected to pressure, so the smaller pressure head was used to study a different mode pattern.

(U) All of the plates tested using the 8-in.-diam compression head resulted in the plate edge deforming into five modes of repeated pattern. A typical example is shown in Fig. 4.2. All the plates tested with the 6.4-in.-diam compression head resulted in the plate edge deforming into four full modes except the 0.049-in. steel plate, which went into six full modes. This plate deformed quite differently from the others--from a four full-mode edge-deformation pattern at a 10,000-lb load, it went to a five full-mode pattern at 15,000 lb and ended with a six full-mode pattern at 20,000 lb. No apparent discrepancy was found with the particular test setup. However, it is assumed that some peculiarity existed which masked the anticipated results.

(U) Figure 4.3 shows the magnitude of plate deformation as a function of the load applied. Figure 4.4 shows the amount of permanent plate deformation as a function of the maximum load applied. The phenolic plate seemed to have a certain amount of "memory," as it tended to return to a flat configuration after a few minutes.

(U) Now that some preliminary information has been obtained pertaining to the peripheral buckling of scaled plates, a more sophisticated test series should be performed. These tests should be made with strain gauges installed on the plates to establish the stress levels associated with the onset of and varying degrees of buckling. This would also define points where the yield strength of the material is exceeded. In conjunction with this series, a test setup should be used that closely simulates the loading conditions that the pusher-plate will be subjected to under actual use. The series should also include subjecting the test plates to dynamic mismatch conditions (HE test) so that definite experimental data can be obtained for establishing structural limitation of the plate to edge-buckling. Any further tests should include titanium, as this material has a good thickness-to-diameter ratio for constant plate mass.

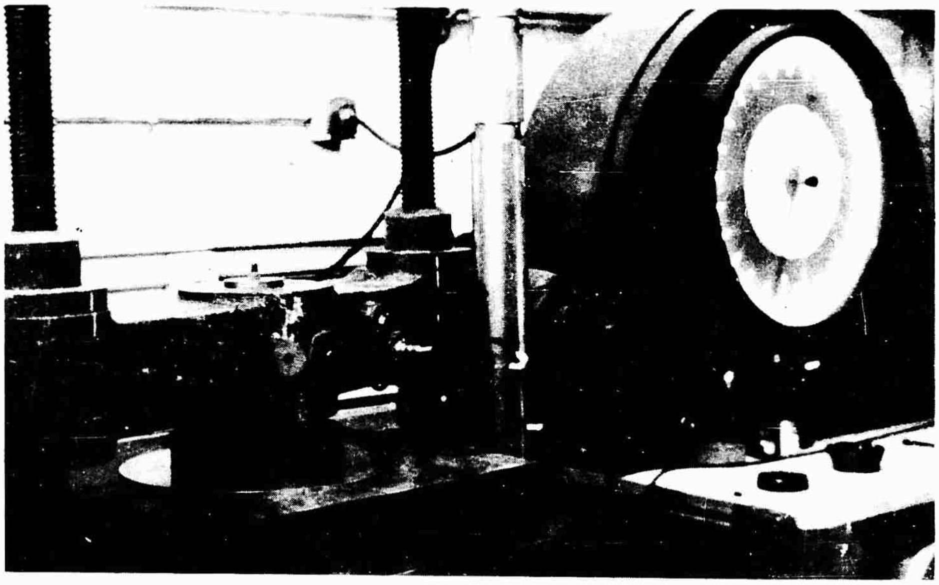

Fig. 4. 1--Static-test plate setup

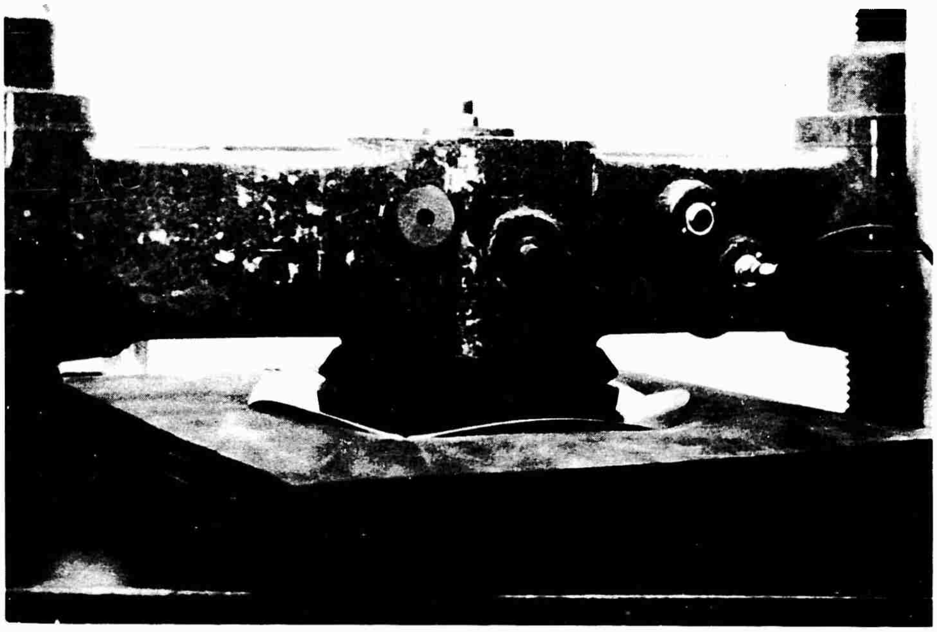

Fig. 4. 2--Static test showing test-plate deformation

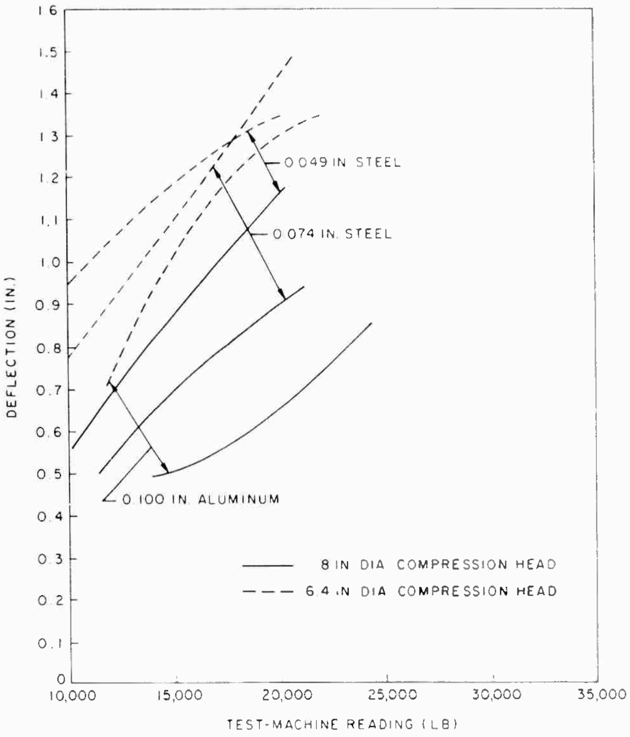

Fig. 4.3--Test-plate deflection

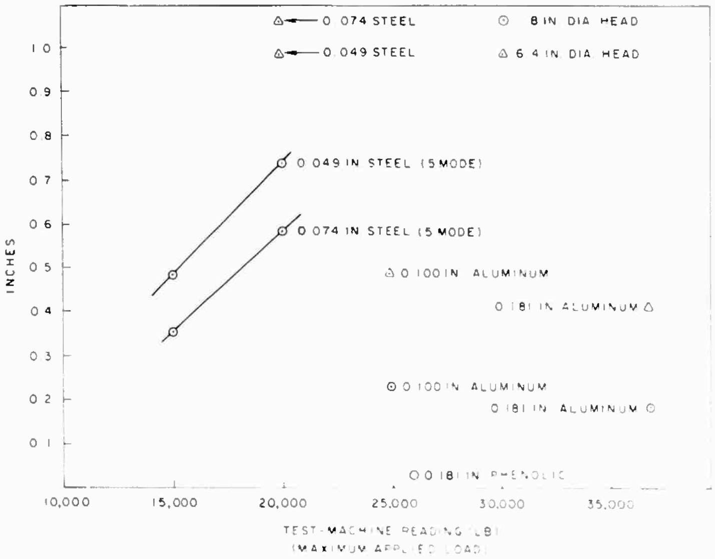

Fig. 4.4--Permanent deformation of test plates

5. (U) A POSSIBLE TECHNIQUE FOR THE RECOVERY OF SAMPLES FROM A NUCLEAR TEST

5.1. (U) TECHNIQUE DESCRIPTION

(S) Considerations for using nuclear tests to conduct experimental investigations of propellant interactions with pusher of ORION vehicles have included a highly instrumented plate tested in a simulated environment (vacuum) in a steel tank. From the nuclear tank tests, it would be desirable to recover for post-test examination the plate samples which have been exposed to only the initial incident propellant. The design of the tank test is such that a finite time period exists between the completion of the propellant-pusher interaction and the arrival at the pusher surface of energy from extraneous sources. This delayed arrival, or "late," energy is two to three orders of magnitude greater than the energy which produces the ablation of direct interest in the test. Therefore, any recovered sample must be protected from the extraneous energy sources.

(C) Several methods have been suggested for exposing and subsequently recovering small samples in tank tests, and two of these appear promising:

1. Protection of the sample area on the plate by covering it with a fluid.
2. Removal of the sample area from the plate and shielding it from the late energy.

Both of these methods would require considerable energy to drive the protective fluid or to remove the sample from the plate surface in the very short time available. Small explosive charges, accurately timed, appear to be the best source of energy for any system requiring auxiliary energy. The first method--the use of a fluid to protect the surface--has not been investigated in detail and hence will not be discussed further. The system discussed here is driven by the momentum of the charge-propellant and is self-timing.

(U) A sketch of the sample recovery assembly installed as a section of a test pusher plate is given in Fig. 5.1. Ten or more strips of width, d, and thickness, h, can be positioned as indicated. A slight taper in the strip thickness, which makes h a bit thicker on the right, as shown, will induce differential acceleration at the joints and thus the surface will be

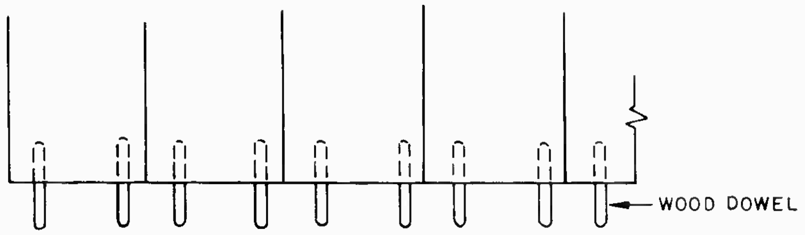

TOP VIEW SHOWING SHEAR DOWELS

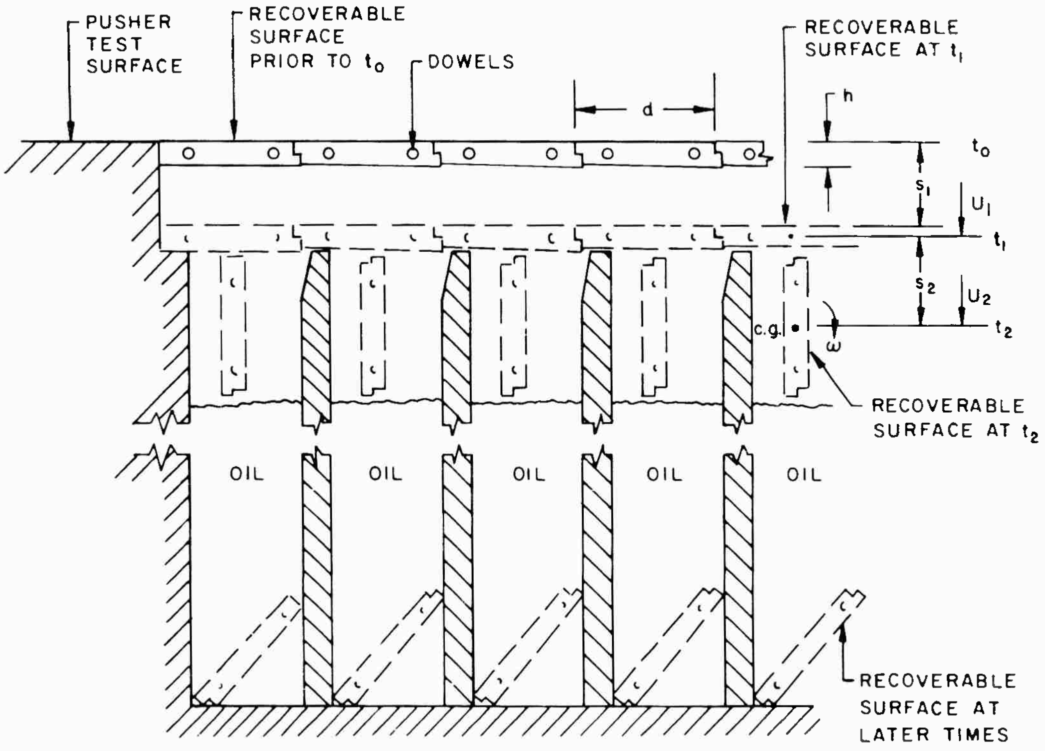
PUSHER TEST SURFACE
RECOVERABLE SURFACE PRIOR TO t_0
DOWELS
d
RECOVERABLE SURFACE AT t_1
h
t_0
s_1
U_1
t_1
s_2
U_2
t_2
c.g.
ω
RECOVERABLE SURFACE AT t_2
OIL
OIL
OIL
OIL
OIL
RECOVERABLE SURFACE AT LATER TIMES

Fig. 5.1--(U) Sample-recovery assembly

held flat during movement. The strips which carry the recoverable test samples are shown in positions they would occupy at four different times relative to the arrival of energy at the test-plate surface.

(C) The samples, which consist of thin metal strips, are accelerated normal to the plane of the pusher and so travel for a period equal to the propellant-pusher interaction time. The travel of the strip is interrupted along one edge to induce rotation. After the strip rotates approximately 90°, it enters a reservoir of liquid. The test surface of the strip is protected by the rotation and by submergence in the fluid.

(S) This system appeared workable from a timing standpoint. There were, however, some questions concerning the entry of the strips into the liquid. For example, would the strip stay straight and not be seriously deformed, thereby preventing it from entering the liquid? Would enough liquid splash from the reservoir to severely reduce the protection? Would the violence of the interruption of the flat movement seriously deform the strip or remove low-strength or brittle ablated or melted material? In other words, would the recovered sample look anything like a section of the pusher plate after one clean propellant-pusher interaction?

(U) To test the theory, a simple fixture with a reservoir was built and three samples were exposed to an impulse simulated by sheet HE. The results were very encouraging. The strips remained relatively flat. Interruption and entrance into the liquid appeared orderly. The violent angular acceleration did not seriously disturb a high-explosive-cratered lead surface. Enough bending occurred to make the successful recovery of brittle or brittle-coated strips highly unlikely. No time-resolved studies of the motion of the strip were attempted. If the test program is reactivated, time-resolution studies should be made, followed by tests of a full-scale assembly of several juxtapositioned strips.

5.2. (U) TANK-TEST PARAMETERS

(U) Any method of specimen recovery requires that certain conditions of the test be accurately predicted. The geometric and material properties that control the dynamic behavior of the specimen strips must be predetermined with reasonable accuracy for this method of self-timing to operate properly.

(S) One possible set of test conditions which constrains the design and operation of this recovery system is the following:

Propellant-pusher interaction time, t_1 . . . . 100 μsec

Time between completion of the propellant-pusher interaction and arrival of late energy from the tank walls, t_2	80 μsec
Average pressure on pusher during interaction time, $\bar{p}$	15, 000 psi

(U) The approximate proportions of these strips can be determined by assuming the value of $\bar{p}$ for the accelerating force per unit area and specifying some travel, s_1, during the interaction time, t_1. That is, if

$$s_1 = \frac{\bar{a} t_1^2}{2} \ ,$$

then the average acceleration, $\bar{a}$, is determined from

$$\bar{a} = \frac{2 s_1}{t_1^2} \ . \tag{1}$$

For the actual conditions of the test, the value of s_1 will be larger because the pressure will be higher than $\bar{p}$ during the early part of t_1, making the average velocity larger than $1/2 \bar{a} t_1$. When the time dependence of p, and consequently of a, is more accurately determined, a more exact value of s_1 can be established.

(S) The average acceleration of a strip of weight per unit area, W/A, when acted upon by $\bar{p}$ is

$$\bar{a} = \frac{\bar{p}}{W/A} g \tag{2}$$

where g is gravity. Substituting Eq. (2) into Eq. (1) gives

$$\frac{\bar{p}}{W/A} g = \frac{2 s_1}{t_1^2} \ ,$$

$$\frac{W}{A} = \frac{g \bar{p} t_1^2}{2 s_1} \ . \tag{3}$$

For the test conditions given above,

$$\frac{W}{A} = \frac{(32.2 \times 12) \times 15,000 \times (10^{-4})^2}{2s_1} ,$$

$$\frac{W}{A} = \frac{0.029}{s_1} \text{ psi}$$

if s_1 is in inches. Assuming elastic action at the interruption and conservation of energy, we have

$$\begin{aligned} 1/2 \frac{m}{\ell} U_1^2 &= 1/2 \frac{m}{\ell} U_2^2 + 1/2 \left(\sum \frac{m}{\ell} r^2 \right) \omega^2 \\ &= 1/2 \frac{m}{\ell} U_2^2 + 1/2 \frac{m}{\ell} \frac{d^2}{12} \omega^2 , \end{aligned}$$

where m/ℓ = mass per unit length of a test strip,
U_1 = velocity of test strip at the end of t_1,
U_2 = velocity of center of gravity of test strip after its interaction with the interrupter strip,
ω = the angular velocity of test strip after its interaction with the interrupter strip,
d = width of strip, and

$$U_1^2 = U_2^2 + \frac{d^2}{12} \omega^2 , \tag{4}$$

$$\omega = \frac{U_2}{d/2} . \tag{5}$$

Substituting Eq. (5) into Eq. (4) gives

$$U_1^2 = U_2^2 + \frac{d^2}{12} \frac{4U_2^2}{d^2} ,$$

$$U_1^2 = U_2^2 + \frac{1}{3} U_2^2 ,$$

then

$$U_2 = \sqrt{3/4}\; U_1 \quad ,$$

$$U_2 = 0.87\; U_1 \quad . \qquad (6)$$

Also,

$$U_1 = \bar{a}\; t_1 \quad .$$

From Eq. (2)

$$U_1 = \frac{\bar{p}}{W/A}\, g\, t_1 \quad ,$$

$$U_2 = 0.87\, \frac{\bar{p}}{W/A}\, g\, t_1 \quad ,$$

and

$$s_2 = U_2 t_2 = 0.87\, \frac{\bar{p}}{W/A}\, g\, t_1\, t_2$$

$$s_2 = \frac{0.87 \times 15,000 \times 32.2 \times 12 \times 10^{-4} \times 0.8 \times 10^{-4}}{W/A} \quad ;$$

$$W/A = \frac{0.04}{s_2} \qquad (7)$$

(S) It is apparent from Fig. 5.1 that s_2 should be greater than d/2 if the test surface of each strip is to be rotated away (>90°) from the incidence of the late energy. By assuming values of 0.8 in. for s_2 and 1 in. for d,

$$W/A = 0.05\ \text{lb/in.}^2$$

and thus

$$h = 0.177\ \text{in. of steel} \quad .$$

By substituting in Eq. (3),

$$W/A = 0.05 = \frac{0.029}{s_1} \quad ,$$

$$s_1 = \frac{0.029}{0.05} \sim 0.6\ \text{in} \ .$$

5. 3. (U) EXPERIMENTS WITH HIGH EXPLOSIVES

(U) To verify the predictions of Section 5. 2., a test fixture was built in which single strips could be accelerated by sheet high explosives. Figure 5. 2 is a sketch of the test arrangement and Fig. 5. 3 is a photograph of the setup just prior to the placement of the impulse-producing assembly of sheet HE and foam plastic.

(U) The steel test strips were purposely made thinner, i. e., h was 0. 150 in. instead of 0. 177 in., as calculated in Section 5. 2., so they would have higher kinetic energy and less resistance to bending. This combination of conditions accentuated the strip deflection, liquid splash, and soft-surface distortion.

(U) Three tests were made at the Green Farm Test Site. The first test was made with a 1-in. by 12-in. by 0. 150-in. low carbon steel strip set in the fixture as shown in Fig. 5. 3. The turbine oil in the reservoir was 4-1/4 in. deep (3-1/4 in. below the top of strip). A diamond-shaped charge of A-2 sheet HE was placed over 8-in. -thick, 2-lb/ft^3-density Styrofoam and detonated from an obtuse corner so that the shock wave reached the center of the strip first and progressed from the center to both ends of the strip.

(U) Examination of the test setup after detonation revealed that the test strip had broken the interrupter strip loose along the center allowing the sample strip to bow in the lengthwise direction. The test strip was lodged in the reservoir and completely covered with oil. The test strip was removed without appreciable further bending. Approximately 1 in. of oil was lost.

(U) For test two, the interrupter strip was replaced by the plate indicated in Fig. 5. 2. This plate was approximately an inch shorter than the test strips. The strip was the same as the one used in the first test. The same types of sheet HE and plastic foam were used except that they were cut into a 20-in. by 10-in. rectangle and detonated along one 20-in. edge by two simultaneously detonated HE line wave generators. Fig. 5. 4 shows the charge arrangement in place prior to the placing of the detonators.

(U) Figure 5. 5. shows the recovered test strip which was successfully interrupted without damage to the interrupter plate. The strip received a concave upward plastic set in its 1-in. direction and compound bending at each end. The test-strip ends were bent because it was longer than the interrupter plate. The test fixture turned over during the test so the oil that remained in the reservoir after the strip entry spilled out. However, the quantity of oil under the overturned fixture indicated that most of the oil remained in the reservoir during the submergence of the strip.

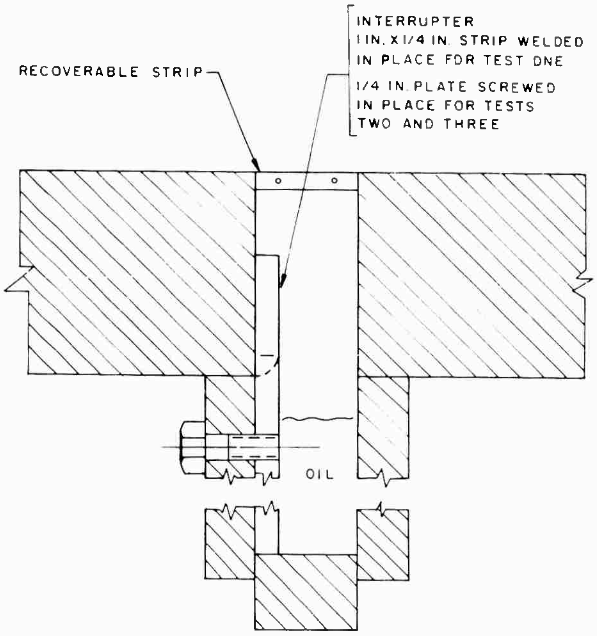
INTERRUPTER
1 IN. X 1/4 IN. STRIP WELDED IN PLACE FOR TEST ONE
1/4 IN. PLATE SCREWED IN PLACE FOR TESTS TWO AND THREE
RECOVERABLE STRIP
OIL

Fig. 5.2--Test fixture

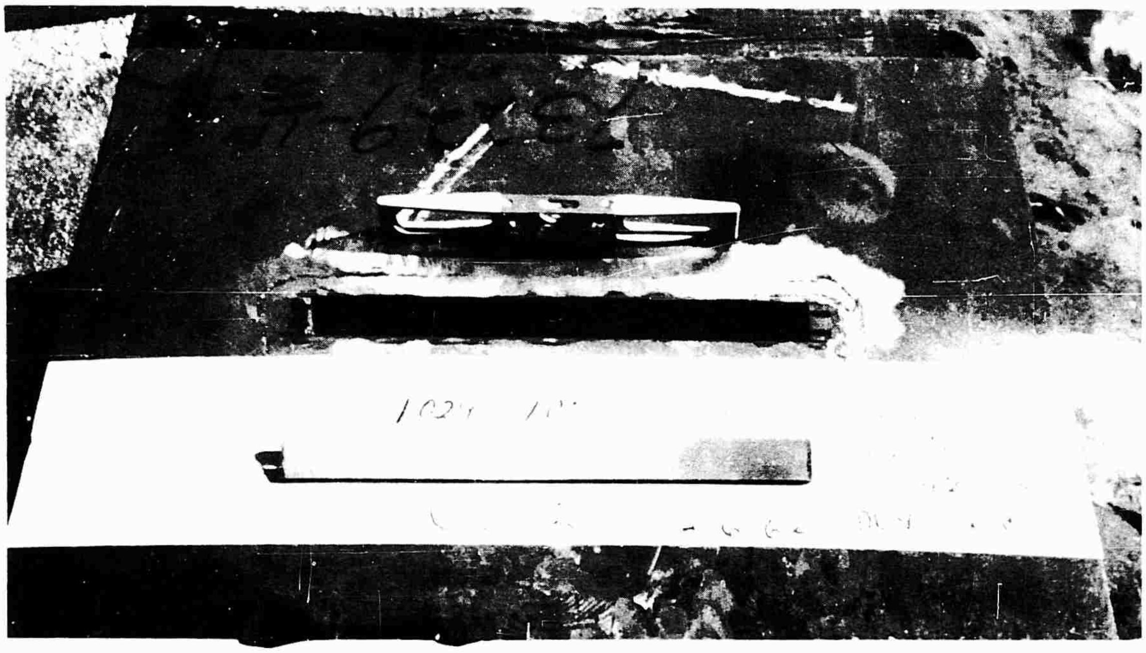

Fig. 5.3--Test fixture with test strip removed from its position over oil reservoir

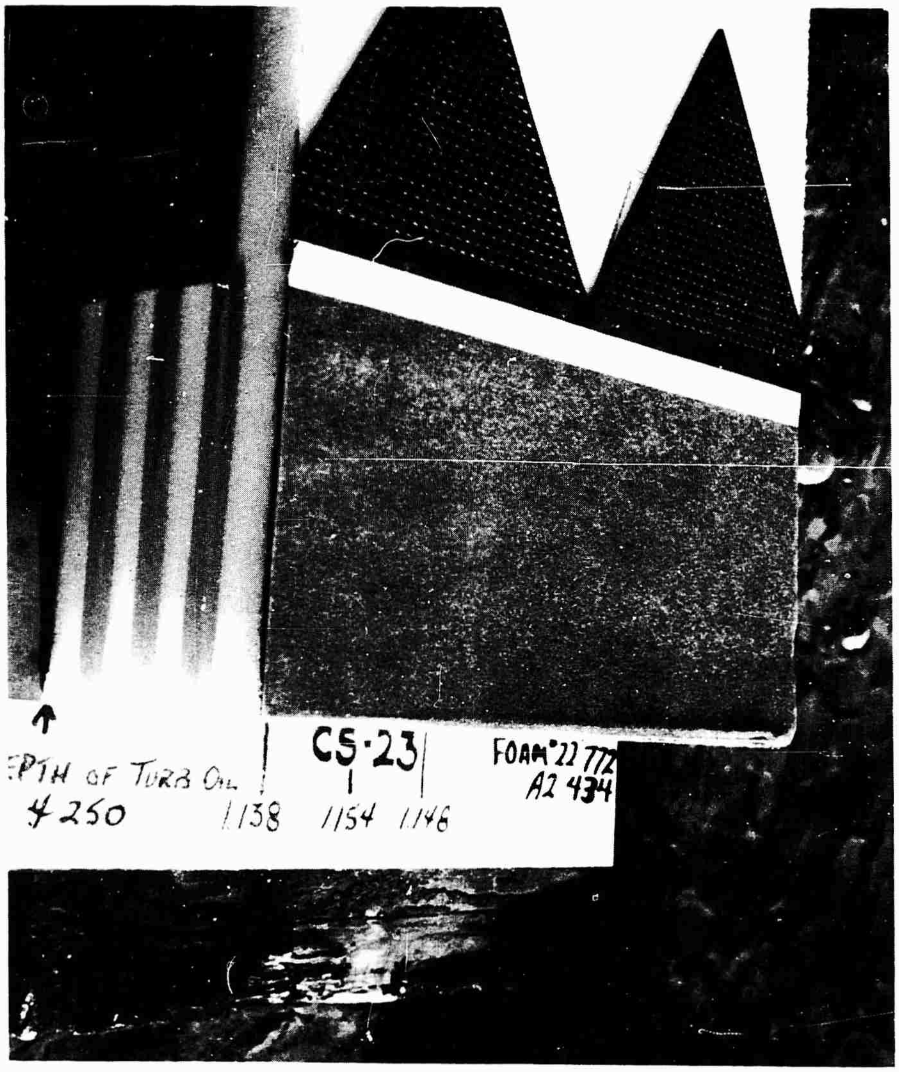

Fig. 5.4--(U) Impulse-producing charge in place (note white foam and dark sheet explosive; HE line wave generators lie to the left)

(U) Test three was identical to the second test except that the test strip was modified. A layer of lead was attached to the top surface of the strips by melting and the resulting lead face was machined to a thickness of 0. 030-in. The added lead weight made the strip equivalent to approximately 0. 190-in. of steel. From previous tests of lead surfaces exposed to this combination of HE and foam, small pock-marked craters with rough edges were expected to appear in the lead.

(U) The fixture again overturned during the test. The recovered strip was somewhat less deformed than the strip used in test two, and the lead surface showed the characteristic craters as expected. There was no evidence of lead movement even at the crater edges, which indicated limited violence during the interrupting and submerging processes. Figure 5. 6 is a photograph of this recovered test strip.

5. 4. (U) CONCLUSIONS

(C) This technique for recovery of test specimens from the vacuum tank nuclear test appears to merit additional consideration. It is very doubtful that brittle or cemented surfaces can be successfully recovered by this technique. However, it is very promising when ductile samples are used. The results of these three tests with HE are most encouraging. Should the nuclear test program be reactivated and tank tests considered, an extension of these simple HE-driven strip tests should be made. Full-size multistrip units could be developed using the sheet HE technique.

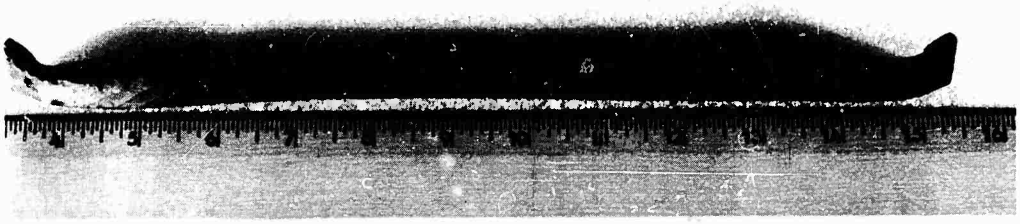

Fig. 5.5--Recovered strip (plain steel)

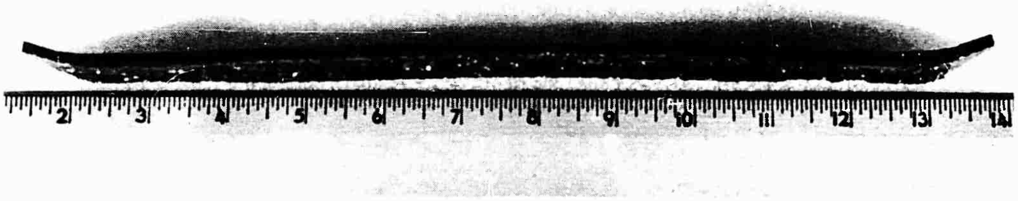

Fig. 5.6--Recovered strip (lead-coated steel)

6. (U) CONCLUSIONS

[redacted]

(S) The technique of using commercial sheet high explosive attenuated with plastic foam has been developed to a point where it is possible to select a set of material parameters that will produce a hydrodynamic pulse with characteristics approximating those predicted for ORION vehicles (see Vol. 1 of this report). The HE-generated pulse is somewhat more "peaked" than that from the pulse system (COSMO-400). Pulse duration for the 4,000-ton reference vehicle is ~ 400 μsec, which is somewhat more than have been produced by this HE technique. However, longer pulse length can be generated by scaling up the generator dimensions. Peak pressures ranging from 1 to 9 kbar and pulse lengths varying from 30 to 300 μsec have been produced. The accuracy of reproducing peak pressures and total impulse are estimated to be ±30 per cent of predicted values for conditions that do not require significant interpolation or extrapolation. Additional testing will be required to improve this accuracy over the range of impulses required for testing ORION engine components.

(S) Large local deviation from a uniform pulse has been detected in the various tests. The nature and resulting response effects of these nonuniformities have been studied. These nonuniformities are sufficiently large to cause concern when testing structures in compression and under dynamic loads near the dynamic elastic limits of the materials. Local surface failures will result, making fatigue testing by this loading technique unattractive. However, for normal design-load conditions, this technique should be quite useful for testing components, such as the pusher, under hydrodynamic pressure loads. Other applications may include, for example, determining the flexural stress of the pusher (due to mismatch of impulse and pusher mass) and attachment quality and ablating-surface bonding strength of laminated-plate designs.

(S) In the pressure and impulse ranges anticipated for the ORION pusher plate, surface damage has been observed only in 6061-T6 aluminum alloy and in lead. Tests up to 9-kbar peak pressure have been made in which the steel plates displayed only minor surface indentations. It should be noted that this pressure is 50% higher than the rated elastic limit of the material.

(C) One advantage in using sheet high explosive for dynamic loading is hat it can be used on both flat or contoured surfaces. Also, the impulse per unit area can be tailored to approximately coincide with the corresponding mass of the test plate. Only a small effort has been expended along these lines experimentally; however, the approach appears to be straightforward within certain limitations. Stepped pulse shapes appear readily attainable, but gradual changes will require very complicated explosive fabrication.

(U) Making significant changes in the detailed shape of the time-dependent pressure pulse will require an extention of the work that has been accomplished up to this time. It appears, however, that a large spectrum of pulse shapes can be obtained by varying the setup combinations used in the impulse-producing system.

(C) The response testing of scaled components of the ORION vehicle has been initiated. Although this experimental program has just started, no structural failures have occurred using properly scaled impulses and, in some cases, from using twice the scaled impulse.

(C) During the development of the impulse-loading technique, considerable experience has been gained and quite a bit of data have been collected on the response of basic plates to dynamic loads. Similar tests have been conducted on attachments connected to the plate by screws(3) or by welding. In general, the attachments using screws withstand only a few impulse loads. Well-designed and fabricated welded joints have been subjected to a series of impulse loads with no failures occurring.

REFERENCES

1. (Uncl. Title) Summary Report for the Period 16 September 1959 through 30 June 1961--The Nuclear/Chemical Pulse Reaction Propulsion Project (Project ORION), General Atomic Report GA-2419, July 28, 1961, Contract AF 29(601)-2207. (S/RD Report)

2. Blackstock, A. W., H. R. Kratz, and M. B. Feeney, Piezoelectric Gauges for Measuring Rapidly Varying Pressures up to Seven Kilobars, General Atomic Report GA-2444 (Rev.), October 3, 1962. (Unclassified Report)

3. (Uncl. Title) David, C. V., Shock-loaded-plate Attachment Tests, General Atomic Informal Report GAMD-3198, June 11, 1962, Contract AF 29(601)-2207. (Conf. Report)

4. (Uncl. Title) Supplement to ORION Annual Report (ORION Staff), General Atomic Report GA-2863, December 31, 1961, Contract AF 29(601)-2207. (S/RD Report)

Dissemination of GAMD documents outside U. S. Government agencies requires the approval of the Contracting Officer at the following address:

AFSWC (SWKRA)
Kirtland AFB, New Mexico

DISTRIBUTION

Copy No.	
	HEADQUARTERS USAF
1	Hq USAF (AFCDA), Wash 25, DC
2	Hq USAF (AFORQ), Wash 25, DC
3-4	Hq USAF (AFRNE, Maj Burke), Wash 25, DC
5	USAF Directorate of Nuclear Safety (AFINS), Kirtland AFB, NM
	MAJOR AIR COMMANDS
6	AFSC (SCT), Andrews AFB, Wash 25, DC
7	TAC (TPL-RQD-M), Langley AFB, Va
	SAC, Offutt AFB, Nebr
8	(OA)
9	(DORQM)
10	(DPLBC, Capt Mixson)
11	AFLC (ADLPD), Wright-Patterson AFB, Ohio
12	ATC (ATTWS), Randolph AFB, Tex
	AUL, Maxwell AFB, Ala
13	(Air University Library)
14	(Research Studies Institute, Col Wilhelm)
15	USAFIT (USAF Institute of Technology), Wright-Patterson AFB, Ohio
	AFSC ORGANIZATIONS
16	AFSC Scientific and Technical Liaison Office, Research and Technology Division, AFUPO, Los Angeles 45, Calif
17	FTD (Library), Wright-Patterson AFB, Ohio
18	ASD (ASNXRR), Wright-Patterson AFB, Ohio
19	RTD (RTNP), Bolling AFB, Wash 25, DC
	SSD, AF Unit Post Office, Los Angeles 45, Calif
20-21	(SSTRP, Maj Baker)
22	(SSPSO, Maj C.C. McMullin)
23	(SSPSS, Maj V.E. Fieker)
24	AF Msl Dev Cen (MDOQ), Holloman AFB, NM
25	6593 Test Group (Development) ATTN: DGLP, Edwards AFB, Calif

DISTRIBUTION (cont'd)

Copy No.	
	KIRTLAND AFB ORGANIZATIONS
	AFSWC, Kirtland AFB, NM
26	(SWKRA)
27	(SWEH)
	AFWL, Kirtland AFB, NM
28	(WLX)
29	(WLRPT (Capt Atkins))
30-31	(WLRPA(Capt Berga))
32	(WLF)
33	(WLDW)
34-83	(WLL)
84	ADC (ADSWO), Special Weapons Office, Kirtland AFB, NM
85	SAC Res Rep (SWL), AFSWC, Kirtland AFB, NM
	OTHER AIR FORCE AGENCIES
	Director, USAF Project RAND, via: Air Force Liaison Office, The RAND Corporation 1700 Main Street, Santa Monica, Calif
86	(RAND Physics Div)
87	(RAND Library)
88	1st Missile Division (OA), Vandenberg AFB, Calif
	ARMY ACTIVITIES
89	Redstone Scientific Information Center, US Army Missile Command (Tech Library), Redstone Arsenal, Ala
90	US Army Air Defense School, ATTN: Modern Weapons Employment Division, Command and Staff Department, Box 9390, Ft Bliss, Tex
	NAVY ACTIVITIES
91	Chief of Naval Research, Department of the Navy, Wash 25, DC
92	Commanding Officer, Naval Weapons Training Center, Pacific, Naval Air Station, ATTN: Director, Weapons Employment and Planning Dept., North Island, San Diego 35, Calif
93	Commander, Naval Ordnance Laboratory, ATTN: Dr. Rudlin, White Oak, Silver Spring, Md

DISTRIBUTION (cont'd)

Copy No.	
	OTHER DOD ACTIVITIES
	Chief, Defense Atomic Support Agency, Wash 25, DC
94	(Document Library)
95	(Radiation Division, Cmdr Charles H. Fugitt)
96	Commander, Field Command, Defense Atomic Support Agency (FCVD), Sandia Base, NM
97	Director, Weapon Systems Evaluation Group, Room 1D-847, The Pentagon, Wash 25, DC
98	Director, Advanced Research Projects Agency, Department of Defense, The Pentagon, Wash 25, DC
	Director, Defense Research & Engineering, The Pentagon, Wash 25, DC
99	(SA(s), Lt Col Lew Allen, Jr.)
100	(Dr. Chalmers Sherwin)
	AEC ACTIVITIES
101	US Atomic Energy Commission (Headquarters Library, Reports Section), Mail Station G-017, Wash 25, DC
102-104	Chief, Division of Technical Information Extension, US Atomic Energy Commission, Box 62, Oak Ridge, Tenn
105-106	University of California Lawrence Radiation Laboratory (Technical Information Division), P.O. Box 808, Livermore, Calif
107-108	Director, Los Alamos Scientific Laboratory (Helen Redman, Report Library), P.O. Box 1663, Los Alamos, NM
109	(T-Div, Dr. Stanislaw Ulam)
	OTHER
110	Administrator, National Aeronautics and Space Administration, 400 Maryland Ave., SW, Wash 25, DC
111	Lewis Research Center (NASA), ATTN: Dr. J.C. Evvard, 21000 Brookpark Road, Cleveland 35, Ohio
112	Goddard Space Flight Center (NASA), ATTN: Dr. R. Jastrow, 8719 Colesville Road, Silver Spring, Md
113	George C. Marshall Space Flight Center (NASA), ATTN: M-P & VE-FE, Mr. W. Y. Jordan, Jr., Huntsville, Ala
114	Central Intelligence Agency (OCR/LY/ILS), Wash 25, DC
115	Arms Control & Disarmament Agency, Chief, Reference Research Bureau, Wash 25, DC

DISTRIBUTION (cont'd)

Copy No.	
116	AEC-NASA Space Nuclear Propulsion Office, National Aeronautical and Space Administration, ATTN: Mr. Harold B. Finger, Manager, Wash 25, DC
117	Battelle Memorial Institute, ATTN: Radiation Effects Information Center, Mr. R. E. Bowman, 505 King Avenue, Columbus, Ohio Contract AF 33(616)-7375
118-119	Technical Data Center, Aerospace Corporation, ATTN: Dr. Vernal Josephson, Laboratory Division, P.O. Box 95085, Los Angeles 45, Calif THRU: SSD (SSTRP, Maj Baker), AF Unit Post Office, Los Angeles 45, Calif
120	California Institute of Technology, Jet Propulsion Laboratory, ATTN: Mr. J.D. Burke, Deputy Lunar Program Director, 4800 Oak Grove Dr., Pasadena, Calif THRU: Administrator, NASA (JPL), 400 Maryland Ave, SW, Wash 25, DC
121	BSD (BSTVK-2), AF Unit Post Office, Los Angeles 45, Calif FOR: Denver Division, Martin-Marietta Corporation, ATTN: Dr. Charles Kober, Director, Advanced Technology, Denver, Colo
122	Rocketdyne, Division of North American Aviation, Inc., ATTN: Librarian, Dept 596-306, 6633 Canoga Avenue, Canoga Park, Calif THRU: AFPR, Rocketdyne Div., North American Aviation, Inc., Canoga Park, Calif
123-137	General Atomic Division, General Dynamics Corporation, ATTN: Mr. John Wild, P.O. Box "S", Old San Diego Station, San Diego 10, Calif Contract AF 29(601)-2207
138	Official Record Copy (WLRPA)

Air Force Weapons Laboratory, Kirtland AF Base, New Mexico
Rpt No. RTD TDR-63-3006, Vol IV. TECHNICAL SUMMARY REPORT, NUCLEAR PULSE PROPULSION PROJECT. Vol IV. Experimental Structural Response. July 1963. 90 p. incl illus, 4 refs.

Secret Report

A simulation technique for producing controlled, high-pressure loading of simple structures has been investigated. The experimental arrangement uses sheet high-explosive and a foam attenuator to produce and control the desired pressure pulse. The technique tested appears to fulfill the simulation requirement over a wide range of the important variables. Experimental investigations have included the determination of the peak

UNCLASSIFIED

1. High explosives
2. Nuclear propulsion
3. Pressure -- simulation
4. Pushers -- effects of blast
5. Putt-Putt
6. Stress and strain
7. Structural materials -- effects of blast

I. AFSC Project 3775, Task 377501
II. Contract AF 29(601)-2207
III. General Dynamics Corp., General Atomic Div., San Diego, Calif.
IV. J.C. Nance, et al.
V. Secondary Rpt No. GA-4205
VI. Not in DDC collection

UNCLASSIFIED

Air Force Weapons Laboratory, Kirtland AF Base, New Mexico
Rpt No. RTD TDR-63-3006, Vol IV. TECHNICAL SUMMARY REPORT, NUCLEAR PULSE PROJECT. Vol IV. Experimental Structural Response. July 1963. 90 p. incl illus, 4 refs.

Secret Report

A simulation technique for producing controlled, high-pressure loading of simple structures has been investigated. The experimental arrangement uses sheet high-explosive and a foam attenuator to produce and control the desired pressure pulse. The technique tested appears to fulfill the simulation requirement over a wide range of the important variables. Experimental investigations have included the determination of the peak

UNCLASSIFIED

1. High explosives
2. Nuclear propulsion
3. Pressure -- simulation
4. Pushers -- effects of blast
5. Putt-Putt
6. Stress and strain
7. Structural materials -- effects of blast

I. AFSC Project 3775, Task 377501
II. Contract AF 29(601)-2207
III. General Dynamics Corp., General Atomic Div., San Diego, Calif.
IV. J.C. Nance, et al.
V. Secondary Rpt No. GA-4205
VI. Not in DDC collection

UNCLASSIFIED

Air Force Weapons Laboratory, Kirtland AF Base, New Mexico
Rpt No. RTD TDR-63-3006, Vol IV. TECHNICAL SUMMARY REPORT, NUCLEAR PULSE PROPULSION PROJECT. Vol IV. Experimental Structural Response. July 1963. 90 p. incl illus, 4 refs.

Secret Report

A simulation technique for producing controlled, high-pressure loading of simple structures has been investigated. The experimental arrangement uses sheet high-explosive and a foam attenuator to produce and control the desired pressure pulse. The technique tested appears to fulfill the simulation requirement over a wide range of the important variables. Experimental investigations have included the determination of the peak

UNCLASSIFIED

1. High explosives
2. Nuclear propulsion
3. Pressure -- simulation
4. Pushers -- effects of blast
5. Putt-Putt
6. Stress and strain
7. Structural materials -- effects of blast

I. AFSC Project 3775, Task 377501
II. Contract AF 29(601)-2207
III. General Dynamics Corp., General Atomic Div., San Diego, Calif.
IV. J.C. Nance, et al.
V. Secondary Rpt No. GA-4205
VI. Not in DDC collection

UNCLASSIFIED

Air Force Weapons Laboratory, Kirtland AF Base, New Mexico
Rpt No. RTD TDR-63-3006, Vol IV. TECHNICAL SUMMARY REPORT, NUCLEAR PULSE PROPULSION PROJECT. Vol IV. Experimental Structural Response. July 1963. 90 p. incl illus, 4 refs.

Secret Report

A simulation technique for producing controlled, high-pressure loading of simple structures has been investigated. The experimental arrangement uses sheet high-explosive and a foam attenuator to produce and control the desired pressure pulse. The technique tested appears to fulfill the simulation requirement over a wide range of the important variables. Experimental investigations have included the determination of the peak

UNCLASSIFIED

1. High explosives
2. Nuclear propulsion
3. Pressure -- simulation
4. Pushers -- effects of blast
5. Putt-Putt
6. Stress and strain
7. Structural materials -- effects of blast

I. AFSC Project 3775, Task 377501
II. Contract AF 29(601)-2207
III. General Dynamics Corp., General Atomic Div., San Diego, Calif.
IV. J.C. Nance, et al.
V. Secondary Rpt No. GA-4205
VI. Not in DDC collection

UNCLASSIFIED

pressures, pressure distributions, pulse duration pulse shape, and total impulse produced as functions of the amount of high-explosives used, the depth and density of the foam attenuator, and partial confinement of the high-explosive. The results of preliminary experiments on simple structures are presented.

Unclassified abstract

UNCLASSIFIED

UNCLASSIFIED

pressures, pressure distributions, pulse duration pulse shape, and total impulse produced as functions of the amount of high-explosives used, the depth and density of the foam attenuator, and partial confinement of the high-explosive. The results of preliminary experiments on simple structures are presented.

Unclassified abstract

UNCLASSIFIED

UNCLASSIFIED

pressures, pressure distributions, pulse duration pulse shape, and total impulse produced as functions of the amount of high-explosives used, the depth and density of the foam attenuator, and partial confinement of the high-explosive. The results of preliminary experiments on simple structures are presented.

Unclassified abstract

UNCLASSIFIED

UNCLASSIFIED

pressures, pressure distributions, pulse duration pulse shape, and total impulse produced as functions of the amount of high-explosives used, the depth and density of the foam attenuator, and partial confinement of the high-explosive. The results of preliminary experiments on simple structures are presented.

Unclassified abstract

UNCLASSIFIED

UNCLASSIFIED

Air Force Weapons Laboratory, Kirtland AF Base, New Mexico
Rpt No. RTD TDR-63-3006, Vol IV. TECHNICAL SUMMARY REPORT, NUCLEAR PULSE PROPULSION PROJECT. Vol IV. Experimental Structural Response. July 1963. 90 p. incl illus, 4 refs.

Secret Report

A simulation technique for producing controlled, high-pressure loading of simple structures has been investigated. The experimental arrangement uses sheet high-explosive and a foam attenuator to produce and control the desired pressure pulse. The technique tested appears to fulfill the simulation requirement over a wide range of the important variables. Experimental investigations have included the determination of the peak

UNCLASSIFIED

1. High explosives
2. Nuclear propulsion
3. Pressure -- simulation
4. Pushers -- effects of blast
5. Putt-Putt
6. Stress and strain
7. Structural materials -- effects of blast

I. AFSC Project 3775, Task 377501
II. Contract AF 29(601)-2207
III. General Dynamics Corp., General Atomic Div., San Diego, Calif.
IV. J.C. Nance, et al.
V. Secondary Rpt No. GA-4205
VI. Not in DDC collection

UNCLASSIFIED

Air Force Weapons Laboratory, Kirtland AF Base, New Mexico
Rpt No. RTD TDR-63-3006, Vol IV. TECHNICAL SUMMARY REPORT, NUCLEAR PULSE PROPULSION PROJECT. Vol IV. Experimental Structural Response. July 1963. 90 p. incl illus, 4 refs.

Secret Report

A simulation technique for producing controlled, high-pressure loading of simple structures has been investigated. The experimental arrangement uses sheet high-explosive and a foam attenuator to produce and control the desired pressure pulse. The technique tested appears to fulfill the simulation requirement over a wide range of the important variables. Experimental investigations have included the determination of the peak

UNCLASSIFIED

1. High explosives
2. Nuclear propulsion
3. Pressure -- simulation
4. Pushers -- effects of blast
5. Putt-Putt
6. Stress and strain
7. Structural materials -- effects of blast

I. AFSC Project 3775, Task 377501
II. Contract AF 29(601)-2207
III. General Dynamics Corp., General Atomic Div., San Diego, Calif.
IV. J.C. Nance, et al.
V. Secondary Rpt No. GA-4205
VI. Not in DDC collection

UNCLASSIFIED

Air Force Weapons Laboratory, Kirtland AF Base, New Mexico
Rpt No. RTD TDR-63-3006, Vol IV. TECHNICAL SUMMARY REPORT, NUCLEAR PULSE PROPULSION PROJECT. Vol IV. Experimental Structural Response. July 1963. 90 p. incl illus, 4 refs.

Secret Report

A simulation technique for producing controlled, high-pressure loading of simple structures has been investigated. The experimental arrangement uses sheet high-explosive and a foam attenuator to produce and control the desired pressure pulse. The technique tested appears to fulfill the simulation requirement over a wide range of the important variables. Experimental investigations have included the determination of the peak

UNCLASSIFIED

1. High explosives
2. Nuclear propulsion
3. Pressure -- simulation
4. Pushers -- effects of blast
5. Putt-Putt
6. Stress and strain
7. Structural materials -- effects of blast

I. AFSC Project 3775, Task 377501
II. Contract AF 29(601)-2207
III. General Dynamics Corp., General Atomic Div., San Diego, Calif.
IV. J.C. Nance, et al.
V. Secondary Rpt No. GA-4205
VI. Not in DDC collection

UNCLASSIFIED

Air Force Weapons Laboratory, Kirtland AF Base, New Mexico
Rpt No. RTD TDR-63-3006, Vol IV. TECHNICAL SUMMARY REPORT, NUCLEAR PULSE PROPULSION PROJECT. Vol IV. Experimental Structural Response. July 1963. 90 p. incl illus, 4 refs.

Secret Report

A simulation technique for producing controlled, high-pressure loading of simple structures has been investigated. The experimental arrangement uses sheet high-explosive and a foam attenuator to produce and control the desired pressure pulse. The technique tested appears to fulfill the simulation requirement over a wide range of the important variables. Experimental investigations have included the determination of the peak

UNCLASSIFIED

1. High explosives
2. Nuclear propulsion
3. Pressure -- simulation
4. Pushers -- effects of blast
5. Putt-Putt
6. Stress and strain
7. Structural materials -- effects of blast

I. AFSC Project 3775, Task 377501
II. Contract AF 29(601)-2207
III. General Dynamics Corp., General Atomic Div., San Diego, Calif.
IV. J.C. Nance, et al.
V. Secondary Rpt No. GA-4205
VI. Not in DDC collection

UNCLASSIFIED

pressures, pressure distributions, pulse duration pulse shape, and total impulse produced as functions of the amount of high-explosives used, the depth and density of the foam attenuator, and partial confinement of the high-explosive. The results of preliminary experiments on simple structures are presented.

Unclassified abstract

UNCLASSIFIED

UNCLASSIFIED

pressures, pressure distributions, pulse duration pulse shape, and total impulse produced as functions of the amount of high-explosives used, the depth and density of the foam attenuator, and partial confinement of the high-explosive. The results of preliminary experiments on simple structures are presented.

Unclassified abstract

UNCLASSIFIED

UNCLASSIFIED

pressures, pressure distributions, pulse duration pulse shape, and total impulse produced as functions of the amount of high-explosives used, the depth and density of the foam attenuator, and partial confinement of the high-explosive. The results of preliminary experiments on simple structures are presented.

Unclassified abstract

UNCLASSIFIED

UNCLASSIFIED

pressures, pressure distributions, pulse duration pulse shape, and total impulse produced as functions of the amount of high-explosives used, the depth and density of the foam attenuator, and partial confinement of the high-explosive. The results of preliminary experiments on simple structures are presented.

Unclassified abstract

UNCLASSIFIED

UNCLASSIFIED